

Electronic Thesis and Dissertation Repository

12-11-2017 10:00 AM

Characterizing the Interaction Between Human Adenovirus E1A and STING

Jessica Hill, *The University of Western Ontario*

Supervisor: Mymryk, Joe, *The University of Western Ontario*

A thesis submitted in partial fulfillment of the requirements for the Master of Science degree in Microbiology and Immunology

© Jessica Hill 2017

Follow this and additional works at: <https://ir.lib.uwo.ca/etd>



Part of the [Immunology of Infectious Disease Commons](#), and the [Virology Commons](#)

Recommended Citation

Hill, Jessica, "Characterizing the Interaction Between Human Adenovirus E1A and STING" (2017).
Electronic Thesis and Dissertation Repository. 5097.
<https://ir.lib.uwo.ca/etd/5097>

This Dissertation/Thesis is brought to you for free and open access by Scholarship@Western. It has been accepted for inclusion in Electronic Thesis and Dissertation Repository by an authorized administrator of Scholarship@Western. For more information, please contact wlsadmin@uwo.ca.

Abstract

When challenged by viral DNA, the cytoplasmic DNA sensor cyclic GMP-AMP synthase (cGAS) signals through the adaptor protein stimulator of interferon genes (STING) to induce a primary type I IFN response. Studies from recent years have also revealed shared architecture between metabolism and innate immunity. Viruses have evolved to counteract these mechanisms. Human adenovirus (HAdV) early region 1A (E1A) protein antagonizes the cGAS-STING pathway to prevent an innate immune response by physically interacting with STING. I hypothesize that the interaction between E1A and STING is mediated through several motifs and involves ribosomal protein S6 kinase beta-1 (S6K1). Using a series of co-immunoprecipitation assays, I determined that the interaction between STING and HAdV E1A is conserved and mediated through the E1A N-terminus region. I also found that E1A physically interacts with S6K1 and ribosomal protein S6 (RPS6). Further studies will reveal the biological function of these interactions.

Keywords

Human Adenovirus, E1A, LXCXE, Interferon, STING, S6K1, RPS6, Co-Immunoprecipitation, Protein-Protein Interaction

Acknowledgments

I would first like to thank my supervisor, Dr. Joe Mymryk, for his guidance and assistance throughout my project. I would like to thank my advisory committee members Dr. Chil-Yong Kang, Dr. Jimmy Dikeakos, and Dr. Greg Dekaban for their unwavering support during the past two years. “Science will prevail!” – J.D. I would like to thank all the members of Dr. Mymryk’s lab for their assistance. Gloria Thomson’s support helped me through midnight working shifts. I would also like to thank Dr. John Barrett and the members of Dr. Nichols’ lab.

Table of Contents

Abstract.....	i
Acknowledgments.....	ii
Table of Contents.....	iii
List of Tables.....	v
List of Figures.....	vi
List of Abbreviations.....	viii
Chapter 1.....	1
1 Introduction.....	1
1.1 Innate Immune Recognition of Pathogens and Trauma: PAMPs, MAMPs, and DAMPs.....	1
1.2 Toll-like Receptors.....	2
1.3 Cytoplasmic Sensing of Nucleic Acids.....	6
1.4 The cGAS-STING Pathway.....	7
1.5 Viral Evasion of the cGAS-STING Pathway.....	11
1.6 Type I IFN Signaling.....	16
1.7 Metabolism and Immune Regulators.....	17
1.8 Human Adenoviruses.....	18
1.9 E1A as a Molecular Hub Protein.....	19
1.10 E1A and Innate Immune Evasion.....	27
1.11 Rationale, Hypothesis, and Objectives.....	28
Chapter 2.....	30
2 Materials and Methods.....	30
2.1 Cell Culture.....	30
2.2 Plasmids.....	30
2.3 Plasmid Transfections.....	32
2.4 Co-Immunoprecipitation.....	32
2.5 Western Blotting Analysis.....	34
2.6 Statistical Analysis.....	34

Chapter 3.....	35
3.1 Mapping the Interaction Between HAdV-5 E1A and STING	35
3.1.1 E1A Isoforms Bind STING.....	35
3.1.2 HAdV-5 E1A N-terminus Region Binds STING.....	38
3.1.3 Assessing the Interaction Between STING and the Extreme N-terminus Region of E1A.....	38
3.1.4 The HAdV-5 LXCXE is Not Necessary for Binding STING.....	42
3.1.5 Analysis of the Conserved Nature Between STING and 13S E1A from Representative Members of HAdV Species A to G.....	47
3.2 Assessment of the Interaction Between E1A, S6K and RPS6.....	52
3.2.1 Verifying the Interaction Between S6K and STING.....	58
3.2.2 E1A Binds Endogenous S6K and RPS6.....	61
3.2.3 Characterizing the Interaction Between Mouse S6K1 and HAdV E1A...61	
3.2.4 Assessing the Effect of Ectopically Expressed S6K2 on Binding Between HAdV- E1A-S6K1 and HAdV-5 E1A-RPS6	66
3.2.5 Assessing the Conserved Nature of the E1A and RPS6 Interaction.....	69
Chapter 4.....	73
4.1 Mapping the Interaction Between E1A and STING.....	73
4.2 Characterizing the Interaction Between E1A, S6K1, and RPS6.....	76
4.3 Significance of Findings and Future Directions.....	78
Chapter 5.....	81
5.1 References	81
Curriculum Vitae.....	92

List of Tables

Table 1.1. Biological properties of the seven human Adenovirus species.....	20
Table 2.1. List of plasmids used in study.....	31
Table 2.2. List of antibodies used in study.....	33

List of Figures

Figure 1.1. Signaling pathways of the toll-like receptors (TLRs)s, RIG-like receptors (RLRs), and DNA sensors.....	3
Figure 1.2. Structure of human STING in complex with c-di-GMP.....	9
Figure 1.3. The cGAS-STING DNA sensing pathway.....	12
Figure 1.4. E1A is a molecular hub protein.....	22
Figure 1.5. Full length sequence alignment of HAdV-3,-4,-5,-9,-12,-40 and -52 E1A protein.....	24
Figure 1.6. Small linear motifs within conserved region 2 of HAdV-5.....	26
Figure 3.1. STING binds the four largest isoforms of HAdV-5 E1A.....	36
Figure 3.2. STING binds to the HAdV-5 E1A N-terminus and CR1.....	39
Figure 3.3. STING binds the Extreme N-terminus of HAdV-5 E1A.....	43
Figure 3.4. STING binds E1A LXCXE deletion mutants.....	48
Figure 3.5. Interaction between STING and E1A conserved across multiple species.....	53
Figure 3.6. E1A extreme N-terminus interaction with STING conservation across multiple species.....	55

Figure 3.7. Endogenous HAdV-5 E1A interacts with mouse S6K1	59
Figure 3.8. HAdV-5 E1A binds endogenous human S6K and RPS6.....	62
Figure 3.9. HAdV-5 interaction with mouse S6K1 conserved across serotypes.....	64
Figure 3.10. Overexpression of RPS6 and S6K2 are required for interaction between ectopically expressed HAdV-5 E1A and p70 S6K.....	67
Figure 3.11. E1A interaction with RPS6 is unique for HAdV-5 serotype.....	70
Figure 3.12. HAdV-5 E1A deletion mutants adjacent to or located at the N-terminus of CR2 abolish binding with RPS6.....	72

List of Abbreviations

AGS	Aicardi-Goutieres Syndrome
Amp	Ampicillin
BMDC	Bone Marrow-Derived Dendritic Cell
BSA	Bovine Serum Albumin
CAR	Coxsackie Adenovirus Receptor
CDN	Cyclic Dinucleotide
cGAMP	Cyclic GMP-AMP
cGAS	GMP-AMP synthase
Co-IP	Co-Immunoprecipitation
CpG	Cytosine-Phosphate-Guanine
CR	Conserved Region
CRISPR	Clustered Regularly Interspaced Short Palindromic Repeats
DAMP	Damage Associated Molecular Patterns
DMEM	Dulbecco's Modified Eagle Medium
dsDNA	Double Stranded DNA
dsRNA	Double Stranded RNA
E1A	Early Region 1A
E2F	E2 Factor
ECL	Enhanced Chemiluminescence
ER	Endoplasmic Reticulum
ERIS	Endoplasmic Reticulum IFN Stimulator
FBS	Fetal Bovine Serum
GFP	Green Fluorescent Protein
HA	Hemagglutinin
HEK293	Human Embryonic Kidney 293
HIV	Human Immunodeficiency Virus
HRP	Horseradish Peroxidase

HSV-1	Human Herpes Simplex Virus-1
IFN	Interferon
IFNAR	Type I IFN receptors
IRF	Interferon Regulatory Factor
ISG	Interferon Stimulatory Genes
Kan	Kanamycin
KSHC	Kaposi's Sarcoma-Associated Herpesvirus
LB	Luria Broth
LANA	Latency Associated Nuclear Antigen
MAVS	Mitochondrial Antiviral-Signaling Pathway
MDA5	Melanoma Differentiation Associated Gene 5
MES	2-[N-morpholino]ethanesulfonic acid
MITA	Mediator of IRF3 Activation
mTOR	Mechanistic Target of Rapamycin
mTORC1	Mechanistic Target of Rapamycin Complex 1
MyD88	Myeloid Differentiation Primary Response Gene 88
NF- κ B	Nuclear Factor - κ B
NP-40	Nonidet-P40
NTase	Nucleotidyl Transferase
ORF	Open Reading Frame
PAMP	Pathogen Associated Molecular Pattern
PBS	Phosphate Buffered Saline
PCR	Polymerase Chain Reaction
PI3K	Phosphatidylinositol 3-Kinase
Pol-III	DNA-Dependent RNA Polymerase III
PONDR	Predictor of Naturally Disordered Regions
pRb	Retinoblastoma Protein
PRR	Pattern recognition Receptor
PVDF	Polyvinylidene Fluoride

qPCR	Quantitative Polymerase Chain Reaction
RCF	Relative Centrifugal Force
RIG-1	Retinoic Acid Inducible Gene 1
RLR	RIG-like-Receptor
RNF5	Ring Finger Protein 5
RPS6	Ribosomal Protein S6
SDS	Sodium Dodecyl Sulfate
S6K	Ribosomal Protein S6 Kinase
SLE	Systemic Lupus Erythematosus
SLiM	Short Linear Interaction Motif
STAT	Signal Transducer and Activator of Transcription
STING	Stimulator of Interferon Gene
SUMO	Small Ubiquitin-like Moiety
TBK-1	Tank Binding Kinase 1
TBS-T 20	Tris Buffered Saline with Tween 20
TIR	Toll/IL-1 Receptor
TLR	Toll-like Receptor
TMEM173	Transmembrane Protein 173
TRAFs	TNF Receptor-Associated Factors
TRIF	TIR-Domain-Containing-Adaptor-Inducing Interferon-Beta
TRIM	Tripartite Motif-Containing Protein
UBC9	Ubiquitin Conjugase 9
ULK1	UNC-51-like Kinase
VSV	Vesicular Stomatitis Virus
vRNA	Viral RNA
WB	western blot
WT	Wild Type

Chapter 1

1.1 Innate Immune Recognition of Pathogens and Trauma: PAMPs, MAMPs, and DAMPs

Innate immunity is acknowledged as the first line of defense against invading foreign microbes and operates as a quick and sensitive counterattack mechanism. As response time post-exposure to an infectious agent can be absolutely paramount, sensors to detect incoming foreign microbial matter are strategically located within the cell. These sensors contain germline-encoded receptors called innate pattern recognition receptors (PRRs), and research over the past decade has shown that these PRRs have extensive breadth in host cell range and ligand specificity (Yoneyama *et al.*, 2004; Kawai & Akira, 2011). Triggering of PRRs subsequently leads to intracellular signalling cascades that ultimately result in the transcriptional expression of inflammatory mediators that eliminate infected cells and pathogens (Takeuchi & Akira, 2010).

Pathogen-associated molecular patterns (PAMPs) and microbe-associated molecular patterns (MAMPs) are conserved molecular structures found in microbial pathogens, such as flagellins, peptidoglycans, and lipopolysaccharides (Wu & Chen, 2014). However, nucleic acids can also act as PAMPs/MAMPs because DNA is an essential genetic material across all organisms (with the exception of RNA viruses). Nucleic acids themselves are not regarded as the ‘problem’, but rather the mislocalization of nucleic acids in the cytoplasm triggers specific PRRs, and detection of anomalous nucleic acids serves as a fundamental mechanism of host defense. Nucleic acids can also act as damage-associated molecular patterns (DAMPs), which are biomolecules derived from the host that trigger innate immunity in response to trauma, cellular stress, tissue damage, and necrotic cell death (Tang *et al.*, 2013).

However, there exists no perfect biological system, and the detection of DNA, particularly double-stranded DNA, by innate immune sensors can lead to autoimmune diseases such as Aicardi-Goutieres Syndrome (AGS) and Systemic Lupus Erythematosus (SLE)(Ablasser *et al.*, 2013). Therefore, the host has evolved a range of distinct PRRs to identify different PAMPs and activate appropriate and specific cellular responses to combat infection

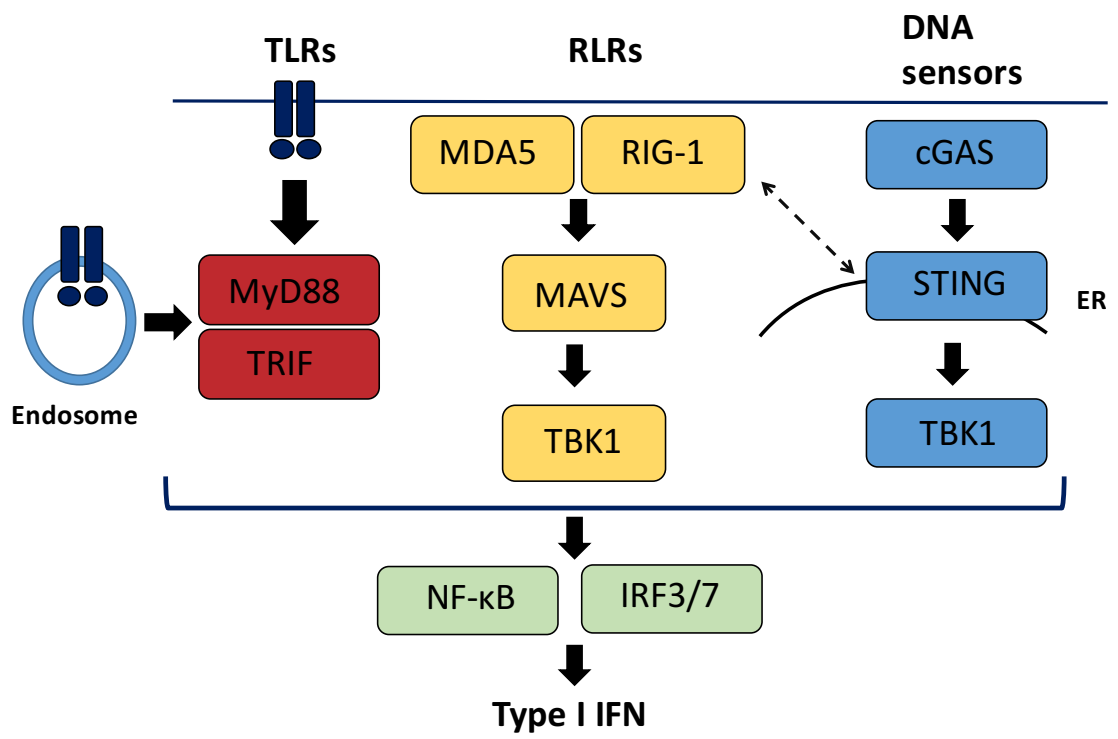
(Yoneyama *et al.*, 2005; Ablasser *et al.*, 2013). The innate immune sensors involved in sensing nucleic acids can be subdivided into multiple groups depending on where they are located within the cell, the cell type, and their targets of recognition (Kawai & Akira, 2011). To date, the Toll-like receptor (TLR) family is the most extensively studied of these groups and has provided new insights into the mechanisms by which PRRs operate.

1.2 Toll-like Receptors

Toll-like receptors are often cited as the prototypical PRRs that recognize PAMPs or damage-associated molecular patterns (DAMPs). These single transmembrane proteins contain leucine-rich domains designed to recognize PAMPs. Structurally, TLRs also contain a transmembrane domain, situated upstream of the cytosolic Toll/IL-1 receptor (TIR) domain, which is highly effective at transducing signals to the downstream adaptor proteins TIR-domain-containing adapter-inducing interferon- β (TRIF) and myeloid differentiation primary response gene 88 (MyD88)(Figure 1.1)(Bell *et al.*, 2003; Bell *et al.*, 2005; Ishii *et al.*, 2005; Kawai & Akira, 2010). TLRs undergo dimerization, which is initiated by the binding of extracellular ligands. This triggers the interaction of the TIR domain with adapter molecules to initiate downstream signaling. The adaptor proteins TRIF and MyD88 both activate nuclear factor- κ B (NF- κ B), but the MyD88 pathway results in the activation of interferon regulatory factor 7 (IRF7), while the TRIF pathway leads to the activation of interferon regulatory factor 3 (IRF3)(Xu *et al.*, 2000; Tao *et al.*, 2002 Khan *et al.*, 2004; Kawai & Akira, 2010). These IRFs are integral members of the interferon regulatory factor family of transcription factors. Activated IRF3 and IRF7 translocate to the nucleus and play a role in transcriptional activation of type I interferon (IFN) genes. IRF3 induces interferon-beta (IFN- β) expression, while IRF7 induces IFN- β and interferon-alpha (IFN- α) expression to activate innate immune cell responses (Colonna, 2007). The type I IFN response is described in detail in section 1.6.

The genetic family of TLRs has expanded relatively quickly over the last decade. To date, five (of ten) TLRs in humans have been characterized for their ability to recognize nucleic acids, and these include: TLR3, TLR4, TLR7, TLR8 and TLR9 (O'Neill *et al.*, 2013; Tao *et al.*, 2016). Several groups took it upon themselves to identify the ligand specificities of

Figure 1.1 Signaling pathways of the toll-like receptors (TLRs)s, RIG-like receptors (RLRs), and DNA sensors. Diagram depicting a general outline of the three most studied PRRs and their signaling pathways. TLRs are found within endosomal compartments and anchored to the cell surface membrane. TLRs activate the downstream adaptor proteins MyD88 or TRIF, which recruit downstream molecules to trigger the secretion of pro-inflammatory cytokines and type I IFN. RLRs RIG-1 and MDA5 activate and recruit the adaptor protein MAVS to trigger NF- κ B and type I IFN. The cytoplasmic DNA sensor cGAS binds DNA and triggers the formation of a second messenger (cGAMP) (not shown) to activate STING, which in turn traffics from the ER and recruits TBK1 and IRF3, leading to the secretion of type I IFN. Dashed arrow represents signaling between STING and RIG-1 (Wu *et al.*, 2017). Adapted from Ma & Damania, 2016.



nucleic acid-sensing TLRs. Both synthetically generated ligands together with pathogen-derived nucleic acids, such as genetic viral fragments, were used to challenge TLRs. For example, TLR3 was determined to be a double-stranded RNA (dsRNA) sensor using the synthetic analog polyinosinic-polycytidylic acid (Marshall-Clarke *et al.*, 2007), and then subsequently shown to restrict several RNA viruses, including West Nile Virus, and Respiratory Syncytial Virus (Negishi *et al.*, 2008; Wu & Chen, 2014). It was also discovered that TLR3 could recognize a select number of dsRNA replicative intermediates from various single-stranded (ssRNA) viruses (Bell *et al.*, 2006).

With the exception of TLR3 and TLR4, many TLRs are expressed on the cell surface. TLR3 and 4 are located within the endoplasmic reticulum, endosomes, and endolysosome. TLR7 recognizes ssRNA sequences rich in guanosine and uridine, and thus operates to restrict Influenza A Virus, Vesicular Stomatitis Virus (VSV) and Sendai Virus. Additionally, TLR7 and the functionally similar TLR8 have gained attention for their recognition of Human Immunodeficiency Virus (HIV) (Diebold *et al.*, 2004; Heil *et al.*, 2004; Hofmann *et al.*, 2016).

The notable discovery of the first DNA sensor TLR9 was made in the year 2000 by Hemmi and colleagues. TLR9 is located within the endosomal lumen and monitors for microbial unmethylated cytosine-phosphate-guanine (CpG) dinucleotides (Krieg, 2004). Monitoring for unmethylated CpG DNA allows for the vital distinction between host and foreign DNA, as host genomes generally have methylated cytosines at CpG sites. Up to 90% of the vertebrate genomic CpGs are believed to be in a methylated state (Kass *et al.*, 1997; Ng & Bird, 1999; Hoelzer *et al.*, 2008). The evolutionary pressures placed upon host cells from microbes drives innate immunity into a diversification of the levels of nucleic acid-sensing TLRs. Many of the TLRs are structured such that their ligand binding domains face inwards toward the endosomal lumen of immune cells. This effectively prevents them from detecting any incoming pathogens traveling through the cytoplasm. The role of TLRs, or lack thereof, in innate immunity was questioned with the observation that several different nonimmune cells, such as fibroblasts, do not have TLRs yet are capable of mounting innate immune responses to infection (O'Neill *et al.*, 2013). This led to the subsequent discovery of pathways involved in cytoplasmic nucleic acid sensing (Wu & Chen, 2014).

1.3 Cytoplasmic Sensing of Nucleic Acids

As a foreward to the topic of cytoplasmic sensing of nucleic acids, it should be mentioned that pre-2017, researchers categorized cytoplasmic sensing pathways into two main families, each characterized by their mode of ligand recognition; DNA or RNA. However, new research is beginning to reveal signaling events between cytoplasmic sensors and downstream adaptor proteins across these families, thus categorizing whole pathways under groups of strictly DNA-detecting or RNA-detecting would appear too general. Therefore, the following summary of cytoplasmic sensing pathways should be viewed, keeping in mind, that some studies will be reanalyzed to accommodate these new insights.

Viral RNA (vRNA) is a very strong TLR-independent activator of type I IFNs (Diebold *et al.*, 2003) and detection within the cytoplasm of vRNA occurs through RIG-1-like receptors (RLRs)(Yoneyama *et al.*, 2004). The first RLR to be described was the cytoplasmic sensor retinoic acid-inducible gene 1 (RIG-1), which was required for dsRNA-induced IFN induction. The second most notable RLR is the cytoplasmic RNA sensor melanoma differentiation associated gene 5 (MDA5) (Figure 1.1)(Yoneyama *et al.*, 2005; Kolakofsky *et al.*, 2012). Sensors that constitute an RLR have a highly conserved domain structure; a DExD/H-box helicase core composed of two helicase domains. The C-terminal domain of RLRs is the area where ligand specificity has evolved (Kolakofsky *et al.*, 2012; Luo *et al.*, 2013). MDA5 and RIG-1 also have two caspase activation and recruitment domains (CARDs), which mediate the downstream signaling to adaptor protein mitochondrial antiviral-signaling pathway (MAVS)(Figure 1.1)(Jiang *et al.*, 2012; Kowalinski *et al.*, 2011). The ligand specificities between RIG-1 and MDA5 are dissimilar, with the length of the RNA being the critical distinction factor. MDA5 recognizes long synthetic RNA fragments (>3.9Kb), while RIG-I is activated by shorter synthetic RNA fragments (~300bp) (Kato *et al.*, 2008). The structure of the RNA cap is also used by RIG-1 as a method of detecting vRNA. Pathogenic RNA carries a 5'-triphosphate (5' ppp) group (Hornung *et al.*, 2006; Pichlmair *et al.*, 2006) while eukaryotic mRNA evades RIG-1 detection because of post-translational modifications that result in 5'-end capping with 7-methyl guanosine (m7G0) and 2'-O-methylation of 5'-end nucleotides (Devarkar *et al.*,

2016). RNA derived from viruses can either be recognized by MDA5 or RIG-1, or both. Detection of RNA by MDA5 sensors is less understood compared to RIG-1, but one study demonstrated that high molecular weight RNA can form web-like structures because of an inclusion of both ssRNA and dsRNA, and this induces IFN activity in a MDA5-dependent manner (Pichlmair *et al.*, 2009). Looking further downstream at the adaptor protein MAVS, Sun and colleagues (2006) demonstrated through mouse knockout studies that viral induction of type I IFN was abolished in MAVS $^{-/-}$ mice, leaving the mice highly susceptible to lethal Vesicular Stomatitis Virus infection. The induction of type I IFNs and cytokines by MDA5/RLRs and MAVS also acts through two cytosolic kinases, κ B kinase (IKK) and tank-binding kinase 1 (TBK1), which activate IRF3 and IRF7 via phosphorylation (Seth *et al.*, 2005).

Intriguingly, Ishii and colleagues (2006) discovered that B-form double-stranded DNA poly(dA:dT) could activate type I IFNs in a RIG-I/MAVS dependent manner in certain cell types. There was much confusion over this phenomenon, but that was subsequently diminished when two independent studies were conducted demonstrating that poly(dA:dT) could be converted to RNA that bore a 5'triphosphate group and had double-stranded secondary structures, much like the ligands for RIG-1. DNA-dependent RNA Polymerase III (Pol-III) was the enzyme responsible for synthesizing 5'triphosphate RNA from the poly(dA:dT) template (Ablasser *et al.*, 2009; Chiu *et al.*, 2009). The plasticity of Pol-III acting as a DNA sensor allows the RIG-1/MAVS pathway to defend against pathogens by an alternative mechanism. However, the strict dependence that Pol-III has for AT-rich sequence, and the fact that Type I IFN production could occur through sequence-independent mechanisms hinted that another DNA-sensing pathway was yet to be found (Wu & Chen, 2014).

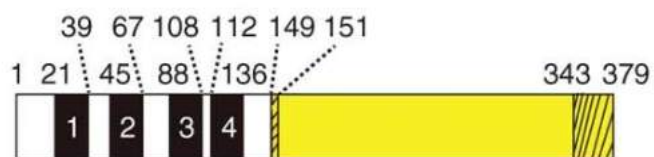
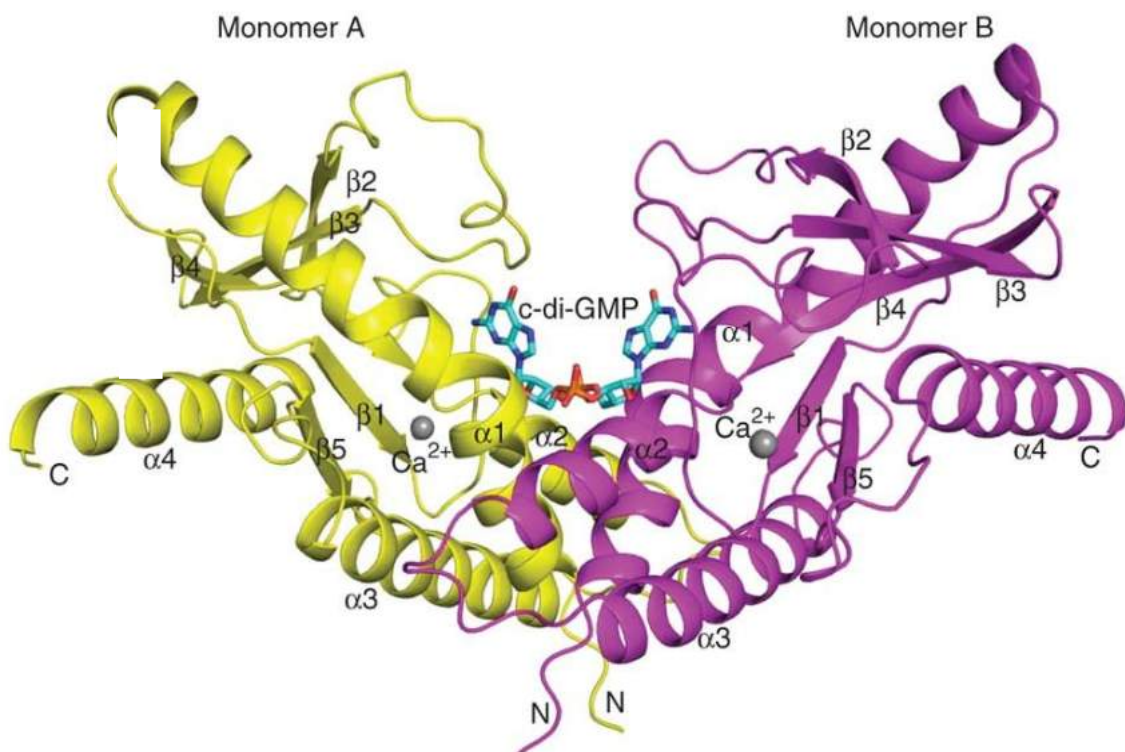
1.4 The cGAS-STING Pathway

In 1908, Mechnikov spoke of the immunostimulatory abilities of nucleic acids, long before the structure of DNA was established in 1953 (Mechnikov, 1908). The main cytosolic DNA sensor that could lead to such a robust type I IFN response remained elusive until 2012, when the breakthrough by Dr. Zhijian Chen's group led to the identification of cyclic GMP-

AMP synthase (cGAS) using quantitative mass spectrometry and biochemical fractionation (Sun *et al.*, 2013). cGAS is a nucleotidyl transferase (NTase) and as such, possesses the structurally conserved NTase core domain. cGAS provides surveillance within the cytoplasm and upon recognizing and binding target sequence-independent DNA, cGAS catalyzes the synthesis of the cyclic dinucleotide (CDN) cyclic GMP-AMP (cGAMP) from ATP and GTP (Sun *et al.*, 2013; Wu *et al.*, 2013). Extensive work by multiple groups went into describing the phosphodiester linkages between GMP and AMP, predominantly to show that a mix of phosphodiester products could be produced. Both an endogenous mammalian form and bacterial form of cGAMP have been structurally analyzed. The metazoan 2'3'-cGAMP and bacterial second messengers c-di-GMP, c-di-AMP, and 3'3'-cGAMP can all bind and activate the adaptor molecule stimulator of interferon genes (STING), triggering innate immune defense (Gao *et al.*, 2013). The secretory mechanisms of these CDNs continues to be studied (Civril *et al.*, 2013; Zhang *et al.*, 2013; Ablasser *et al.*, 2013; Diner *et al.*, 2013).

STING (also known as MITA, MPYS, ERIS and TMEM173) was discovered between 2008 and 2009 by four independent groups through the use of cDNA expression library screens (Jin *et al.*, 2008; Zhong *et al.*, 2008; Ishikawa *et al.*, 2009; Sun *et al.*, 2009). STING is a direct sensor of CDNs and has a broad tissue distribution (Zhong *et al.*, 2008). STING is anchored to the endoplasmic reticulum through its N-terminal domain, and is comprised of four transmembrane domains (Ishikawa *et al.*, 2008). The use of crystallography has also revealed that the carboxyl-terminal domain of STING extends into the cytosol. The native, unliganded state of STING is a symmetrical dimer in which two monomers of the C-terminal domain form a cleft. This cleft is the binding site of cGAMP, and each STING dimer can bind one cGAMP (Shang *et al.*, 2012; Ouyang *et al.*, 2012). Dimerized STING binds cGAMP (Figure 1.2) which triggers relocalization of STING from the ER to the Golgi complex (Ishikawa *et al.*, 2009; Shang *et al.*, 2012). STING is phosphorylated by TBK1 at Serine 366, while the carboxyl-terminal region of STING activates TBK1, which in turn stimulates the phosphorylation of IRF3 (Tanaka & Chen, 2012). STING is often described as a 'scaffold protein' because of its interaction with both TBK1 and IRF3 to promote phosphorylation of IRF3. The study by Tanaka and Chen (2012) demonstrated that selective mutations in STING that disrupted its binding to IRF3 abolished

Figure 1.2 Structure of human STING in complex with c-di-GMP. (A) Schematic representation of human STING where black and yellow boxes represent the transmembrane domain and cytoplasmic C-terminal domain, respectively. Disordered regions are represented with dashed lines. (B) Ribbon diagram of STING C-terminal domain in complex with c-di-GMP. Monomer A is yellow and monomer B is purple. The c-di-GMP is in stick representation. Taken from Shang *et al.*, 2016. Image reproduced with permission of the rights holder, *Nature*.

A**B**

phosphorylation of IRF3 without impacting activation of TBK1. Phosphorylated IRF3 translocates to the nucleus to induce the transcription of IFN genes (Figure 1.3). Signal transducer and activator of transcription 6 (STAT6) has also been similarly identified as being recruited by STING for subsequent phosphorylation by TBK1 and translocation to the nucleus. This leads to the induction of genes responsible for immune cell homing, namely expression of the STAT6-dependant chemokines CCL2, CCL20, and CCL26 (Chen *et al.*, 2011).

Optimal signaling of STING can enhance the antiviral response, but chronic activation of STING leads to an excessive and harmful type I IFN and pro-inflammatory cytokine response. Therefore, STING undergoes several different post-translational modifications for optimal signaling, including ubiquitination, phosphorylation, sumoylation and proteasome-mediated degradation. The ubiquitin ligase tripartite motif-containing protein 56 (TRIM56) was demonstrated to bind STING and mediate ubiquitination of STING at lysine 150, which can facilitate STING dimerization and binding to TBK1 (Tsuchida *et al.*, 2010). The TRIM32 ubiquitin ligase was also shown to interact with STING and is important for STING-TBKI interaction upon Sendai Virus and Herpes Simplex Virus 1 infection (HSV-1) (Zhang *et al.*, 2012). STING can also be negatively regulated through several mechanisms. Recently, a study by Hu and colleagues (2016) revealed how STING can be stabilized by sumoylation and the SUMO protease SENP2 can mediate degradation of STING after desumoylation. Ubiquitin ligase ring finger protein 5 (RNF5)-mediated lysine 48-linked ubiquitination can also control degradation of STING (Zhong *et al.*, 2009). Within human diploid cells, a negative feedback system has been put in place to avoid excessive STING response whereby RIG-1 and IL-6 promote STING degradation by activating/dephosphorylating UNC-51-like kinase (ULK1). Interestingly, this negative feedback mechanism is not present in HEK293 cells (Wu *et al.*, 2017).

1.5 Viral Evasion of the cGAS-STING Pathway

The Red Queen Hypothesis (L.M. Van Valen, 1973) proposes that organisms must constantly evolve to survive against evolving opposing organisms. Viruses have adapted

Figure 1.3 The cGAS-STING DNA sensing pathway. The DNA sensor cGAS binds DNA and catalyzes the formation of the second messenger 2'3'-cGAMP. 2'3'-cGAMP binds to the ER bound adaptor protein STING and activates IKK and TBK1. STING and IRF3 are phosphorylated by TBK1 to form a STING-TBK1-IRF3 complex. Phosphorylated IRF3 dimerizes and enters the nucleus, where it functions with NF- κ B to induce the expression of type I IFN and pro-inflammatory cytokines (Adapted from Chen *et al.*, 2016).

many different methods of evading detection within the cytoplasm through antagonizing the cGAS-STING DNA sensing pathway. Being the first DNA virus reported to activate STING *in vivo* and *in vitro*, human HSV-1 is widely used in experimental systems as a viral activator of the cGAS-STING pathway. In one study, knockout of STING in mice resulted in lethal susceptibility to HSV-1 infection (Kalamvoki & Roizman, 2014). However, it should be noted that Kalamvoki & Roizman (2014) reported that STING, while critical for cellular restriction of HSV-1, could also be necessary for HSV-1 replication in certain cell types.

Continuing with the Herpes Viral family, Kaposi's Sarcoma-Associated Herpesvirus (KSHV) can also activate the cGAS-STING pathway. The KSHV viral interferon regulatory factor 1 (vIRF1) inhibits cGAS-STING dependent IFN- β induction by preventing STING from binding TBK1, disallowing phosphorylation of STING (Ma *et al.*, 2015). ORF52, an abundant KSHV tegument protein, was also shown to directly inhibit cGAS enzymatic activity through a mechanism involving both cGAS binding and DNA binding. A conserved mechanism is likely at play as the ORF52 homologs in related Herpesviruses also demonstrate this inhibitory effect (Wu *et al.*, 2015). Finally, the N-terminally truncated cytoplasmic isoforms of KSHV latency associated nuclear antigen (LANA) can antagonize the cGAS-STING sensing pathway through direct binding with cGAS, effectively allowing reactivation of latent KSHV (Zhang *et al.*, 2016).

Within the family Hepadnaviridae, Hepatitis B Virus polymerase inhibits STING-triggered IFN- β promoter activation and can bind STING to attenuate lysine 63-linked polyubiquitination and functional activation, without modulating STING protein levels. The RNase H domain is believed to be the interacting partner that effectively suppresses STING (Liu *et al.*, 2015).

Initial studies involving human Adenovirus by Falck-Pedersen's group (2014) concluded that the cGAS/STING pathway was vital for type I IFN induction in response to Adenovirus. In addition, they did not find evidence of suppression of cGAS/STING-dependent TBK1/IRF3 activation, at least up to 6 hours post-infection. However, these

experiments were undertaken with recombinant Adenoviruses that omitted the Adenoviral early genes (*i.e.* E1A) that regulate antiviral strategies. Lau and colleagues (2015) investigated previous observations that most immortalized and tumor cell lines (*e.g.* HEK293, HeLa, HEK293T) fail to respond to intracellular DNA, whereas primary cell lines mount a vigorous DNA-activated antiviral response through activation of type I IFN. Their study tested for type I IFN presence in HEK293 and HeLa cells after transfection with DNA. Compared to primary human fibroblasts, HEK293 and HeLa cells did not mount robust responses to transfected DNA. An understanding of how these cells were immortalized by viral oncogenes (HEK293 cells with the human Adenovirus type 5 E1A oncogene, and HeLa cells derived from a cervical tumor and positive for HPV18) led to the hypothesis that a common Leu-X-Cys-X-Glu protein motif sequence present within E1A and HPV18 E7 may be the point of interaction with STING. Other studies looking at Adenovirus and IFN production include one by Look and colleagues in 1998, which reported that E1A blocked STAT1 activation after IFN- β was produced (Look *et al.*, 1998; Ma & Damania, 2017). Collectively, these studies on Adenovirus suggest that upstream cGAS/STING-dependent signaling may not affect Adenoviral replication while E1A is expressed, but further study is required.

The question of whether STING is sufficient to act as a direct sensor for DNA has been debated within the literature. While the C-terminal domain of STING can independently associate with dsDNA, it occurs at a significantly lower binding affinity to that of cGAS (Kd of 200 μ M vs. Kd of 88 nM)(Abe *et al.*, 2013). Zhang and colleagues (2014) demonstrated that adding STING back into HEK293T cells, which do not express endogenous STING or cGAS, could restore an IFN- β response to cyclic di-nucleotides. However, this IFN- β response could not be restored upon challenge with dsDNA. As mentioned earlier, HEK293 cells are also unable to produce a type I IFN response when challenged with DNA, despite the presence of endogenous STING. When Lau and colleagues (2015) put cGAMP (5 μ M) into HEK293 cells to stimulate STING, they could not induce a type I IFN response. However, when Zhang and colleagues (2014) put cGAMP into HEK293 cells to stimulate STING, they reported an almost 30-fold increase in IFN- β mRNA response. They also reported a very low increase in endogenous IFN- β

expression in response to immunostimulatory DNA. This puts forward the question of whether STING expression alone, can stimulate a biologically relevant IFN- β response in HEK293 cells.

1.6 Type I IFN Signaling

The secretion of type I IFNs is a pivotal antiviral mechanism found in almost all cells that operates to restrict viral growth and spread. The type I IFN family encodes multiple IFN- α gene products and a single IFN- β gene. Generally, type I IFN responses are divided into two mechanisms, a primary response where the host cell can activate IFN gene expression, and a secondary response whereby IFN from the primary response binds to type I IFN (IFNARs) receptors on neighboring cells, leading to the activation and expression of hundreds of interferon stimulatory genes (ISGs) that ultimately promote further production of IFN- β and IFN- α (McNab *et al.*, 2015).

Cells that express TLRs or have intracellular nucleic acid sensing pathways can initiate the primary type I IFN response. Through TLR signaling, TLRs engage with the adaptor proteins previously mentioned, TRIF and MyD88, which recruit the kinases TBK1 and IKK for IRF3 activation and translocation to the nucleus for transcription of IFN- β or $-\alpha$ genes. Some TLR-adaptor protein complexes recruit the IL-1R-associated kinases (IRAKs) and TNF receptor-associated factors (TRAFs) to interact with IKK α and activate IRF7 (Liu *et al.*, 2015).

Both the adaptor proteins STING and MAVS have a conserved C-terminal pLxIS (p-hydrophilic residue, S-phosphorylation site) motif. The phosphorylation of this site occurs at the time of ligand binding and a mutation within this motif abolishes recruitment of IRF3. After STING and MAVS are activated by the adaptor proteins TBK1 and TBK1/IKK respectively, a conserved positively-charged patch on the IRF3 molecule binds STING and MAVS. This triggers recruitment of a second IRF3 molecule, which upon phosphorylation, binds with the first monomer to form a dimer. The activated IRF3 dimer translocates to the nucleus to induce expression of IFN- β or $-\alpha$ (Liu *et al.*, 2015; Lau *et al.*, 2015; McNab *et al.* 2015).

1.7 Metabolism and Immune Regulators

The intricate relationship between metabolism and immune regulators is gradually being elucidated. This is generating much interest, as the innate immune regulation of metabolic pathways remains poorly understood because the systemic inflammation seen in chronic diseases can often overshadow direct underlying molecular causes. Recently, Hasan *et al.* (2016) established TBK1-mTORC1 (mechanistic target of rapamycin complex 1) as a key regulatory axis between cell-intrinsic immune signaling and metabolism. mTORC1 is one of two distinct complexes formed by the interaction of several proteins with mTOR. mTOR is a serine/threonine protein kinase and a member of the phosphoinositide 3-kinase (PI3K)-related kinase family. The mTORC1 pathway controls major processes such as autophagy and lipid and protein synthesis by responding to inputs from cellular cues such as stress, growth factors, amino acids, and oxygen (Laplante & Sabatini, 2012). Hasan *et al.* (2016) put forward the concept that chronic TBK1-STING activation and trafficking can lead not only to the recruitment of TBK1 and IRF3 signaling, but also bring TBK1 within close proximity to mTORC1 on the lysosomes. TBK1 was found to suppress mTORC1, leading to the dysregulation of cellular metabolism.

Wang *et al.* (2016) later demonstrated that the mTORC1 substrate S6K is recruited to the STING-TBK1-IRF3 complex to promote IFN signaling during DNA stimulation. The two forms of ribosomal protein S6 kinase (S6K), S6K1 and S6K2, are effector serine-threonine kinases downstream of mTOR (Wang *et al.*, 2016). To characterize the profile of adenovirus-induced IRF3 phosphorylation in mouse bone marrow– derived dendritic cells (BMDCs), they transduced wild-type BMDCs with recombinant human adenovirus serotype 5 (rHAdV-5) vector carrying deletions of E1 and E3, which are involved in mediating adenovirus replication and host immunomodulation. They determined that S6Ks, especially S6K1, were required for rHAdV-induced activation of IRF3. The phosphorylation of IRF3 was profoundly impaired in S6K1^{-/-}S6K2^{-/-} BMDCs. Immunoblotting analysis showed that recombinant rHAdV promoted translocation of IRF3 to the nucleus in wild-type BMDCs but not in S6K1^{-/-} S6K2^{-/-} BMDCs. As previously discussed, STING has a scaffold function and binds both TBK1 and IRF3, but the binding of IRF3 to STING was abolished in S6K1^{-/-} S6K2^{-/-} BMDCs. Finally, through a series of

co-immunoprecipitation experiments, Wang and colleagues demonstrated that S6K binds STING to promote IRF3 phosphorylation.

1.8 Human Adenoviruses

The work in this thesis investigates the interplay between human Adenovirus and the STING pathway. As such, I will briefly introduce human Adenoviruses, which are well characterized genera in the Adenovirus family of DNA viruses. Infection by Adenoviruses affects human populations worldwide. While many infections present as asymptomatic, these viruses are able to infect multiple organ systems, generally causing mild self-limiting illnesses including gastroenteritis, conjunctivitis, and pharyngitis. However, for children and immunocompromised individuals, infection can lead to more serious complications (Krilov, 2005; Walls *et al.*, 2003).

The type and severity of disease can also be dependent on the infectious Adenoviral species, with Adenovirus F and G generally causing gastroenteritis, whereas Adenovirus D can cause conjunctivitis (Table.1.1) (Chang *et al.*, 2008; Sambursky *et al.*, 2007; Walls *et al.*, 2003). A select number of Adenoviruses can be linked with specific historical outbreaks. For example, Adenovirus 14 is considered responsible for a fatal pneumonia outbreak in the United States of America in 2005 (Lewis *et al.*, 2009).

Adenoviruses are used to study cell cycle control, DNA replication, transcription mRNA processing, apoptosis and immunological responses. Identified in 1953, they are small non-enveloped viruses with a linear double-stranded DNA genome of approximately 35 kbp. There are 100 members within the Adenovirus family, which infect a wide range of species covering reptiles, avian, and mammals. There are currently 57 members of human Adenovirus, which are separated into 7 species categorized A through G and characterized by their biological properties (Table 1.1)(Jones *et al.*, 2007; Walsh *et al.*, 2011). They are labelled as oncogenic viruses, but do not actually cause cancer in humans (Mackey *et al.*, 1976; Green *et al.*, 1980). In 1962, human Adenovirus 12 was found to cause tumours in baby hamsters, which was the first example of a human virus inducing cancers. However, not all Adenoviruses cause tumours in rodents, but within tissue culture, they can transform rodent cells. The differences in tumourgenicity can be traced to immune response strategies

(Trentin *et al.*, 1962; Gallimore, 1972).

Human Adenovirus 5 (HAdV-5) interacts with the host coxsackie-adenovirus receptor (CAR)(Bewley *et al.*, 1999). The virions enter the cell through receptor-mediated endocytosis, and are released into the cytoplasm via acidification of the endosome (Wickham *et al.*, 1993). The genome undergoes uncoating and travels to the nucleus via the cellular microtubule network. Upon reaching the nucleus, the first gene transcribed is the early region 1A gene (E1A). E1A performs many functions in the infected cell, including the rapid induction of transcription of the other early genes: E1B, E2, E3 and E4 (Fessler & Young, 1998; Tollefson *et al.*, 2007). In addition to its role as a potent viral transactivator, the E1A protein abolishes the activity of the retinoblastoma protein (pRB) and its family members p107 and p130, which repress the E2F family of transcription factors. Cell cycle control and progression from the G₁ to S phase is largely controlled by the E2F family (Berk, 1986; DeCaprio, 2009). Abolishing the control of E2F through the interaction of E1A with pRB promotes cell cycle progression, a well known trait of E1A function. It is hypothesized that the activation of cell cycle progression in the infected cell increases the availability of substrates for efficient viral progeny production (Pelka *et al.*, 2008). E1A also functions to modulate innate immunity, which is described in detail in section 1.9.

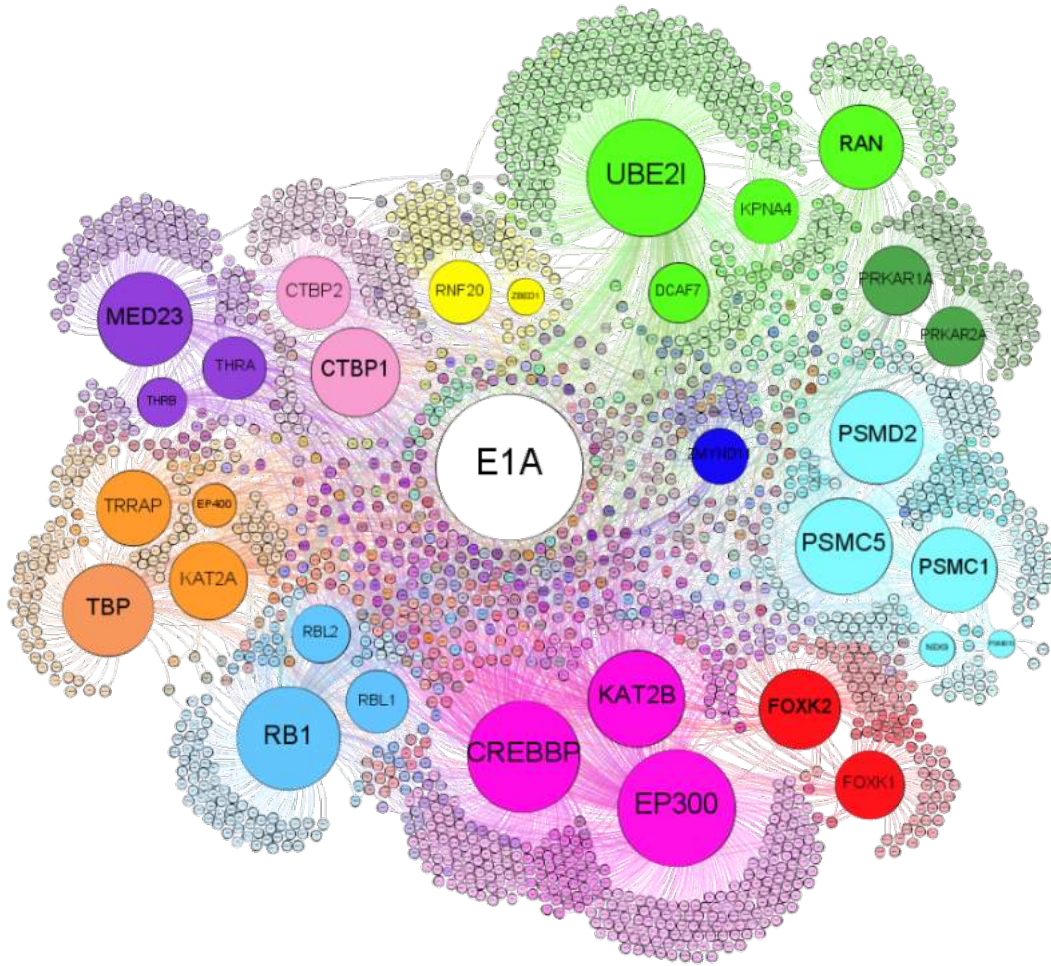
1.9 E1A as a Molecular Hub Protein

The E1A oncoprotein is a classic example of an intrinsically disordered protein that can operate as a molecular hub (Pelka *et al.*, 2008). E1A displays nuclear and nucleocytoplasmic localization and can interact with a large number of different cellular proteins to regulate a wide range of biological processes, including the transcription of viral and cellular genes, cell cycle, apoptosis, differentiation, transformation, and immune responses (Figure 1.4). E1A is differentially spliced to produce five isoforms, which have mRNA sedimentation rates of 13S, 12S, 11S, 10S, and 9S. The two largest of these products are 13S and 12S, which encode proteins of 289 and 243 amino acids in length, respectively (Perricaudet *et al.*, 1979; Stephens & Harlow, 1987). Comparing the largest sequences of E1A proteins across species identifies four highly conserved regions, referred

Table 1.1 Biological properties of the seven human adenovirus species. Human Adenovirus species A through G, their hemagglutination group, serotypes, tumorigenicity in animals, transformation in tissue culture, sequence GC percentage, and linked clinical infection/disease. Adapted from Berk (2007), Ghebremedhin (2014), and Jones *et al.*, (2007).

Species	Hemagglutination Group	Adenovirus Types	Tumours in Animals	Transformation in Tissue Culture	Percentage of GC in DNA	Type of Infection/Disease
A	IV (little or no agglutination)	12, 18, 31	High	+	48-49	Gastrointestinal respiratory, urinary
B	I (complete agglutination of monkey erythrocytes)	3,7,11,14,16,21,34,35,50	Moderate	+	50-52	Keratoconjunctivitis, gastrointestinal, respiratory, urinary
C	III (partial agglutination of rat erythrocytes)	1,2,5,6	Low or none	+	57-59	Gastrointestinal, respiratory, urinary
D	II (complete agglutination of rat erythrocytes)	8,9,10,13,15,17,19,20,22-30,32,33,36-39,42-49,51	Low or none	+	57-61	Gastrointestinal, keratoconjunctivitis
E	III	4	Low or none	+	57-59	Respiratory, keratoconjunctivitis
F	III	40,41	Unknown	Unknown	Unknown	Gastrointestinal
G	Unknown	52	Unknown	Unknown	55	Gastrointestinal

Figure 1.4 E1A is a molecular hub protein. Graphic demonstrating the primary and secondary interactors of E1A. Modeled with the Gephi 0.9.1 software with data from BioGRID build 3.4.144. E1A is shown as the center molecule, with the primary interactors represented in the larger coloured circles. Relative sizes are correlated with number of binding partners. The secondary interactors are represented by the smaller coloured circles. This diagram represents 31 primary interactors and 2125 unique secondary interactors. Created by and reproduced with permission from Dr. Joe Mymryk (Western University, unpublished, 2017).



to as CR1, CR2, CR3 and CR4 (Figure 1.5). These would indicate regions that are essential for adenoviral E1A function (Avvakumov *et al.*, 2002). The N-terminus of E1A of most adenovirus types is predicted to form an α -helix, while the CR regions 1, 2 and 4 are intrinsically disordered. This allows E1A to form numerous interactions with cellular proteins through short linear interaction motifs (SLIMs). E1A mediates its effects on cellular processes through protein-protein interactions, as E1A does not directly bind DNA and has no enzymatic activity (Ferguson *et al.*, 1985). SLIMs can be 3 to 10 residues in length and are typically found within intrinsically disordered regions of a protein, but also can be found on surfaces of solvent-exposed alpha helices. Interactions that are of low affinity or transient, are mediated by SLIMs, so stable binding between some protein-protein interactions requires multiple SLIMs mediating the interaction (Davey *et al.*, 2001; Pelka *et al.*, 2013; Van Roey *et al.*, 2014). There exist a number of HAdV-5 E1A SLIMs found in the CR2 region, within close proximity to each other (Figure 1.6). The LxCxE motif within CR2 is used to interact with pRB, in addition to being recently proposed to interact with STING (Dyson *et al.*, 1992; Fattaey *et al.*, 1993; Lau *et al.*, 2015). The neighboring PxLxP and EVIDLT motifs are used to interact with BS69 and small ubiquitin-like moiety (SUMO) conjugase ubiquitin conjugase 9 (UBC9), respectively (Ansieau & Leutz, 2002; Avvakumov *et al.*, 2004; Lau *et al.*, 2015; Yousef *et al.*, 2010). The potential ability of E1A to interact with multiple partners suggests that, in addition to its ability to sequester or re-localize individual targets, it may perform a “scaffold” like function to bring various targets into virally-mediated protein complexes not present in uninfected cells.

HAaV-3 MRHLRFI~~POEVI~~SSETC~~TEIL~~EFV~~NTIM~~-GD-L~~DEPP~~VQ~~PFDP~~SL~~LDL~~Y~~DLE~~LDGP-EDPNE~~EAVNGFT~~DS~~MLAA~~EGL~~D~~INP-----P-PETIV~~EGVV~~VESG~~CGKK~~IPDL
 HAaV-4 MRHLRDI~~PDEE~~I~~IAS~~SE~~ILL~~V~~NATM~~-GD~~DE~~HE~~PP~~-T~~PEGT~~PS~~LDL~~Y~~DLE~~V~~DE~~EDPNE~~KAVND~~LS~~DA~~LA~~AA~~E~~AS~~SPSS-----DSDSSLH~~HT~~-----FRH~~DR~~CE~~KE~~TE~~PC~~I
 HAaV-9 MRHLRL~~LP~~-----S~~TV~~ES~~ML~~IA~~AI~~AN~~STP~~-----I~~HL~~FT-----LSP~~PE~~L
 HAaV-5 MRH~~I~~CHGG-V~~ITE~~M~~A~~S~~ILL~~QL~~HE~~EV~~I~~-AD-N~~L~~PP-S~~HE~~PP~~PL~~HE~~LY~~DL~~LV~~TAP-EDPNE~~EAV~~S~~QI~~EP~~D~~SV~~LA~~Q~~EG~~L~~L~~TP~~PA~~FG~~SP~~PP~~HL~~SR~~Q~~EQ~~PE~~QR~~A~~CG~~PV~~SP~~NI~~
 HAaV-10 MRTEM-T~~FL~~-V~~LS~~Y~~QEA~~D~~ILL~~HL~~MD~~N~~FF~~-NE-V~~F~~S~~DD~~--D~~LY~~V~~PS~~Y~~EL~~L~~D~~V~~ES~~AG~~DN~~NE~~QAV~~NE~~FP~~ES~~LL~~LA~~SE~~GL~~FL~~PE-----P-P~~V~~L--S~~P~~-----V~~CE~~P~~T~~GG~~EC~~MP~~QL~~
 HAaV-12 MRMI~~P~~DF~~F~~-----H~~GN~~W-D~~DM~~F~~OGL~~HE~~Y~~V~~ED~~-H~~ERS~~-E~~ASE~~EM~~S~~H~~DL~~DE~~V~~D~~GD~~ED~~AN~~Q~~EAV~~DM~~GP~~ER~~LI~~SE~~AS~~AE~~SGS~~-----G~~D~~SG~~CG~~-----E~~EL~~
 HAaV-52 MRL~~V~~PE~~Y~~CG-V~~F~~C~~SE~~T-V~~R~~NS~~EL~~NTD~~L~~-L~~D~~-V~~NS~~E--V~~T~~SP~~F~~SL~~H~~DL~~D~~EV~~D~~PF-Q~~D~~NE~~D~~AV~~NS~~MP~~PE~~CF~~FEA~~EG~~SH~~SS~~E~~-----E~~SK~~

CR1

HAaV-3 G-AAEM~~IL~~LC~~YE~~GF~~PP~~SD~~DE~~GE~~TE~~QS-I~~H~~T---A~~N~~NE~~G~~K~~AA~~AS~~V~~FK~~D~~CP~~EL~~PG~~H~~CK~~SC~~F~~H~~R~~N~~NT~~G~~M~~K~~EL~~L~~CS~~L~~C~~Y~~M~~R~~M~~H~~CH~~E~~TI~~S~~PS~~V~~SD~~DE~~S---P
 HAaV-4 K-WE~~K~~IL~~LC~~YE~~CL~~PP~~SD~~DE~~DE~~Q~~AI~~Q---N--A~~S~~H~~G~~V~~Q~~AV~~S~~SE~~AD~~CP~~EL~~PG~~H~~CK~~SC~~F~~H~~R~~N~~NT~~G~~K~~A~~V~~I~~CA~~L~~C~~Y~~M~~R~~AY~~N~~HC~~V~~Y~~S~~V~~S~~DA~~D~~ET~~P~~-----
 HAaV-9 EEE~~DE~~IL~~LC~~YE~~GF~~PP~~SD~~SE~~DE~~R-----C~~P~~V~~SE~~DE~~LS~~-P
 HAaV-5 V-PE~~V~~IL~~LC~~HE~~GF~~PP~~SD~~DE~~DE~~EG-----H~~E~~F~~V~~D~~Y~~V~~H~~PG~~H~~GC~~R~~S~~CH~~Y~~H~~R~~N~~T~~G~~PD~~I~~M~~C~~S~~L~~C~~Y~~M~~R~~TC~~G~~E~~V~~Y~~S~~V~~S~~EP~~PE~~PE~~PE~~PE~~PE~~PAR~~TR~~PK~~MA~~FA~~IL~~
 HAaV-12 H-PE~~D~~MI~~IL~~LC~~YE~~GF~~PS~~LS~~DE~~Q~~D~~EN~~G~~MA~~H~~VS~~AS~~AAAA~~A~~DR~~ER~~EE~~F~~LD~~HP~~ED~~FG~~LN~~CK~~S~~CH~~H~~R~~N~~ST~~GN~~T~~DL~~M~~CS~~L~~C~~Y~~I~~RAY~~NE~~I~~Y~~S~~V~~S~~DM~~NE~~PE~~NS~~T
 HAaV-40 L-P~~V~~DL~~IL~~LC~~YE~~CL~~PP~~SD~~PE~~DE~~AE~~AE~~EE~~A---A~~M~~PT~~Y~~M~~N~~EN~~E~~NL~~V~~LD~~CP~~EN~~PG~~CR~~AC~~F~~H~~R~~G~~T~~S~~GN~~PE~~AM~~CAL~~C~~Y~~M~~R~~L~~T~~G~~H~~C~~I~~Y~~S~~E~~T~~S~~D~~A~~E~~GE~~SES~~-----
 HAaV-52 R-GE~~B~~LL~~LC~~YE~~CL~~PS~~LS~~DE~~TE~~QT~~CG~~-----D---C~~T~~EP~~V~~--V~~K~~NE~~P~~V~~L~~DR~~FP~~Q~~G~~H~~GC~~R~~A~~F~~F~~H~~R~~N~~AS~~GN~~PE~~TC~~AL~~C~~Y~~I~~R~~L~~T~~S~~D~~E~~V~~Y~~S~~V~~S~~DA~~D~~CG~~D~~-----

CR2

HAaV-3 ---S~~P~~S~~T~~TS~~P~~PE~~Q~~AP~~A~~AN~~G~~K~~P~~EV~~K~~PK~~PC~~RP~~AV~~K~~IED~~LEG---G~~Q~~PL~~D~~LS-TR~~K~~J~~R~~-Q
 HAaV-4 ---T~~S~~TS~~P~~PE~~IC~~T~~S~~PS~~D~~N~~I~~VR~~P~~V~~R~~AT~~G~~-R~~RA~~AV~~E~~LD~~DL~~L~~Q~~GG---D~~E~~PL~~D~~L~~C~~TR~~R~~-R~~R~~-H
 HAaV-9 ---S~~E~~D~~H~~PS~~P~~PE~~S~~GE~~T~~L~~Q~~RF~~P~~T~~Q~~RR~~AV~~K~~IED~~L~~Q~~MG--G~~E~~PD~~L~~LS-~~I~~K-R~~R~~-N
 HAaV-5 RR~~P~~T~~S~~V~~S~~REC~~N~~S~~T~~SD~~C~~S~~G~~F~~S~~N~~PP~~PE~~HP~~V~~LC~~PK~~PA~~VR~~CG~~-R~~CA~~AV~~E~~I~~E~~DL~~L~~EP---G~~Q~~PL~~D~~LS-~~C~~K-R~~R~~-P
 HAaV-12 ---L~~D~~G~~E~~R~~P~~SP~~P~~K~~I~~GS~~AV~~EG~~V~~IK~~P~~V~~Q~~RV~~I~~G~~R~~RR~~CA~~V~~ES~~I~~DL~~Q~~E~~ERE~~Q~~T~~V~~P~~D~~LS-~~V~~K-R~~R~~PC~~N~~
 HAaV-40 ---S~~P~~D~~DE~~HP~~HT~~AT~~PH~~IV~~BT~~Q~~R~~V~~C~~RR~~PA~~V~~E~~I~~E~~DL~~L~~EPDP--T~~E~~PE~~N~~LS-~~I~~K-R~~P~~K~~C~~S
 HAaV-52 ---R~~S~~G~~S~~AN~~S~~E~~CT~~LC~~AV~~V~~E~~GL~~IK~~PA~~VR~~V~~SG~~-R~~CA~~V~~E~~K~~I~~E~~D~~LL~~Q~~EE--Q~~T~~E~~P~~LD~~L~~S-~~M~~K-R~~R~~K~~L~~T

CR3

CR4

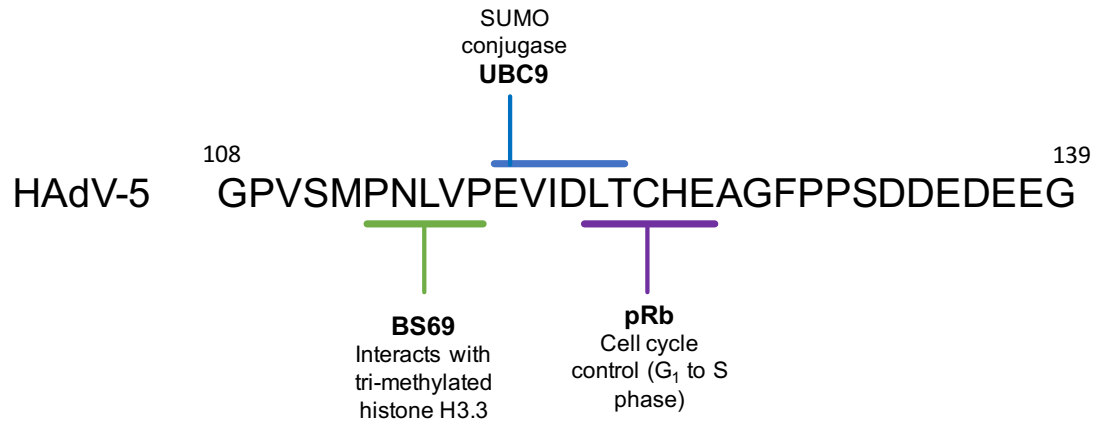


Figure 1.6 Small linear motifs within conserved region 2 of HAdV-5. Amino acid residues 108-139 of HAdV-5 E1A. The PXLXP, EVIDLT and LXCXE motifs are highlighted with their reported binding partners BS69, UBC9, and pRB.

1.10 E1A and Innate Immune evasion

With respect to immune evasion strategies, the first indication that E1A could block IFN signaling was in 1988 when Reich and colleagues used E1A-deletion mutagenesis experiments to demonstrate that E1A blocks interferon signaling in infected HeLa cells. This was followed up with mapping studies that indicated the N-terminus was responsible for modulating transcriptional activation of IFN target genes (Kalvakolanu et al., 1991; Anderson and Fennie, 1987). In 2012, Fonseca and colleagues showed how E1A disrupts the transcription of interferon stimulatory genes (ISGs) by antagonizing chromatin remodeling complexes. How E1A antagonizes the primary type I IFN response is less well understood. As mentioned previously, Lau and colleagues (2015) proposed that E1A can antagonize the STING pathway. A detailed mechanism of this antagonism has not been elucidated and many questions regarding the consequences of this interaction remain.

1.11 Rationale, Hypothesis, and Objectives

Since the discovery of the cytoplasmic DNA sensor cGAS in 2012, extensive research has been undertaken to elucidate how the cGAS-STING pathway limits viral replication. In equal measure, the vast array of evasion strategies employed by viruses to prevent a primary interferon response has also been studied. The ability of a virus to escape innate immune detection is paramount to its survival. HAdV-5 E1A was identified as an antagonist of the cGAS-STING DNA sensing pathway by the group of Stetson in 2015 (Lau *et al.*, 2015). They proposed that a small linear LXCXE motif encoded by HAdV-5 E1A could mediate an interaction with STING in the cytoplasm. However, the nature of this protein-protein interaction is poorly understood and its conservation across Adenoviral species is unknown. This LXCXE motif was previously identified for its role in mediating the interaction between E1A and pRb in the nucleus. The potential for this motif to have dual function requires further investigation and multiple motifs are likely required for stable binding between E1A and STING. Therefore, and I set out to characterize the interaction between E1A and STING.

In 2016, the group of Lichty (Wang *et al.*, 2016) identified S6K1 as an additional binding partner of the STING-TBK1-IRF3 complex. S6K1 is a mTORC1 substrate and their study supports work by Hasan *et al.* (2016) that established a TBK1-mTORC1 regulatory axis between cell intrinsic immunity and metabolism. The suppression of mTORC1 activity by TBK1 during chronic STING activation, and the known interaction between S6K1 and STING led me to question if E1A targets S6K1 function. The nature of the relationship between E1A and S6K1 is currently unknown. Therefore, I set out to determine if E1A interacts with S6K1, and potentially the S6K1-STING-TBK1-IRF3 complex.

Based on the rationale, I hypothesize that antagonism of the STING-pathway by adenovirus E1A requires the LXCXE motif, in conjunction with additional E1A motifs that also mediate binding with S6K1. To test my hypothesis, I have formed two objectives:

1. Characterize the interaction between E1A and STING and determine the conservation of this interaction in different human Adenoviral species.

2. Determine if E1A interacts with S6K1 in complex with STING.

Chapter 2

2 Materials and Methods

2.1 Cell Culture

Human Embryonic Kidney 293 (HEK293) cells, HT1080 human fibrosarcoma cells, IMR-90 primary human lung fibroblast cells, and A549 human alveolar basal epithelia cells were all derived from frozen laboratory stocks and cultured in Dulbecco's Modified Eagle's Medium (Multicell) supplemented with 10% calf serum (Gibco) and 1% PenStrep (100U/ml Penicillin and 100µg/mL Streptomycin, Multicell). Cells were cultured at 37°C with 5% CO₂.

2.2 Plasmids

HAdV E1A plasmids were prepared and constructed by myself, and other (past and present) members of the laboratory (Table 2.1) (* indicates plasmids I modified, sub-cloned, or constructed myself). E1A mutants were generated by PCR-based mutagenesis or sub-cloned into the appropriate vectors. E1A mutants were either tagged with GFP or contained no tag and cloned into pcDNA3.1 vectors. The human STING open reading frame was synthesized by Integrated DNA Technologies (gBlocks Gene Fragments) and generated with a C-terminal haemagglutinin (HA) epitope tag. The STING-HA fragment was subsequently cloned into a pcDNA3.1 vector. The mouse S6K1-HA plasmid was kindly gifted from Brian Lichty (McMaster University). S6K2 and RPS6 open reading frames were synthesized by ThermoFisher (GeneArt Cloning Service) and cloned into pcDNA3.1 vectors.

Transformation of all plasmids were conducted using competent DH5α *E.coli* grown in Luria Broth (LB) supplemented with ampicillin (50µg/ml, BioShop) or kanamycin (20µg/ml, Bioshop). Large scale plasmid purification was conducted using the PureLink HiPure Plasmid Midiprep kit (Invitrogen).

Table 2.1 List of plasmids used in this study.

#	Name	Parent Vector	Characteristics
1	GFP-13S Ad3	pGFP	Full length 13S E1A of Ad3
2	GFP-13S Ad4	pGFP	Full length 13S E1A of Ad4
3	GFP-13S Ad5	pGFP	Full length 13S E1A of Ad5
4	GFP-13S Ad9	pGFP	Full length 13S E1A of Ad9
5	GFP-13S Ad12	pGFP	Full length 13S E1A of Ad12
6	GFP-13S Ad40	pGFP	Full length 13S E1A of Ad40
7	GFP-13S Ad52	pGFP	Full length 13S E1A of Ad52
8	GFP-12S	pGFP	12S E1A of Ad5
9	GFP-11S	pGFP	11S E1A of Ad5
10	GFP-10S *	pGFP	10S E1A of Ad5
11	GFP-N-terminus *	pGFP	AA 1-80 of Ad5 E1A
12	GFP-CR2	pGFP	AA 93-139 of Ad5 E1A
13	GFP-CR3 *	pGFP	AA 139-204 of Ad5 E1A
14	GFP-C-terminus *	pGFP	AA 187-289 of Ad5 E1A
15	GFP- N-terminus	pGFP	AA 1-14 of Ad5 E1A
16	GFP- N-terminus	pGFP	AA 14-22 of Ad5 E1A
17	GFP- N-terminus	pGFP	AA 16-22 of Ad5 E1A
18	GFP- N-terminus	pGFP	AA 29-49 of Ad5 E1A
19	GFP-N-terminus (Δ 4-25) *	pGFP	Plasmid #11 with Δ 4-25
20	GFP-N-terminus (Δ 26-35)	pGFP	Plasmid #11 with Δ 26-35
21	GFP-N-terminus (Δ 30-49)	pGFP	Plasmid #11 with Δ 30-49
22	GFP- Δ N-terminus *	pGFP	Plasmid #3 with Δ 1-80
23	GFP-dl1105	pGFP	Plasmid #3 with Δ 70-81
24	GFP-dl1106	pGFP	Plasmid #3 with Δ 90-105
25	GFP-dl1107	pGFP	Plasmid #3 with Δ 111-123
26	GFP-dl1108	pGFP	Plasmid #3 with Δ 124-127
27	GFP-dl1109	pGFP	Plasmid #3 with Δ 128-138
28	13S Ad5 *	pcDNA3.1	Full length 13S E1A of Ad5
29	dl1106	pcDNA3.1	Plasmid #28 with Δ 90-105
30	dl1107 *	pcDNA3.1	Plasmid #28 with Δ 111-123
31	dl1108 *	pcDNA3.1	Plasmid #28 with Δ 30-49
32	GFP- Ad3 N-terminus	pGFP	AA 1-14 of Ad3
33	GFP- Ad5 N-terminus	pGFP	AA 1-14 of Ad5
34	GFP- Ad9 N-terminus	pGFP	AA 1-14 of Ad9
35	GFP- Ad12 N-terminus	pGFP	AA 1-14 of Ad12
36	GFP- Ad40 N-terminus	pGFP	AA 1-14 of Ad40
37	GFP- Ad52 N-terminus	pGFP	AA 1-14 of Ad52
38	Human HA-STING *	pcDNA3.1	Full length STING
39	Mouse HA-S6K1	pcDNA3.1	Full length mS6K1
40	S6K2 *	pcDNA3.1	Full length S6K2
41	RPS6 *	pcDNA3.1	Full length RPS6

2.3 Plasmid Transfections

All transfections and co-immunoprecipitation assays were conducted in 10cm dishes (Sarstedt). HT1080 cells were seeded at 2×10^6 cells prior to transfection the following day with 5 μ g of STING-HA expression constructs, 5 μ g of full length E1A-GFP, 5 μ g of E1A deletion mutants (Table 2.1), 5 μ g of mouse S6K1-HA, 5 μ g of human S6K2, 5 μ g of human RPS6, 5 μ g GFP, or 5 μ g pcDNA3.

Transfections were conducted using X-tremeGene HP DNA Transfection Reagent (Roche, 6366244001) according to the manufacturer's protocol. HEK293 cells were seeded at 2.5×10^6 cells prior to transfection the following day with 5 μ g STING-HA, 5 μ g full length E1A, 5 μ g E1A deletion mutants, or 5 μ g E1A-GFP. The pRb-GFP plasmid was used as a positive technical control, the 13S-GFP and 13S-pcDNA3.1 plasmids were used as positive controls, and the GFP and pcDNA3.1 plasmids were used as negative controls.

2.4 Co-Immunoprecipitation

Cells were harvested 24 hr post-transfection and pelleted by centrifugation at 500 RCF for 3 minutes at 4°C. The cells were then washed with phosphate buffered saline (PBS) (4.2mM Na₂HPO₄, 2.7mM KCl, 173mM NaCl, and 1.5mM KH₂PO₄ (BioShop)). Cellular pellets were lysed at 4°C with 0.8mL NP-40 lysis buffer (0.5% NP-40, 150mM NaCl, and 50mM Tris-HCl, pH 7.8 (BioShop) supplemented with 0.6% Mammalian Tissue Protease Inhibitor Cocktail (Sigma). The lysate was then centrifuged and 2% of the supernatant was aliquoted for sample input control. Sepharose-Protein A beads were transferred to the cell lysate in addition to either anti-HA antibody, anti-GFP antibody, anti-STING antibody, anti-E1A (M73 and M58) antibody, or anti-RPS6 antibody (Table 2.2). The samples were then rotated at 4°C for either 4 hr or overnight. Samples were then washed 3 to 5 times with NP-40 lysis buffer. The samples were then re-suspended in LDS sample buffer (2X, NuPage; Thermo Fisher) and 0.2M DTT (BioShop) before being denatured at 98°C for 10 min.

Table 2.2 List of antibodies used in this study.

Specificity	Description	Usage	Company	Catalogue #
GFP	Rabbit polyclonal	Primary	Clontech	632592
HA	Rat monoclonal	Primary/IP	Roche	11867423001
E1A (M58) Epitope: 1-120 AA	Mouse monoclonal	Primary/IP	In house hybridoma	N/A
E1A (M73) Epitope: 271-289 AA	Mouse monoclonal	Primary/IP	In house hybridoma	N/A
STING D2P2F	Rabbit monoclonal	Primary/IP	Cell Signaling	13647
S6K	Rabbit polyclonal	Primary/IP	Cell Signaling	2708
RPS6 5G10	Rabbit monoclonal	Primary/IP	Cell Signaling	2217
Actin	Rabbit polyclonal	Primary	Sigma	M-7023
Rat IgG	Goat	Secondary	Thermo Scientific	31470
Rabbit IgG	Goat	Secondary	Santa Cruz	Sc-2004
Mouse IgG	Rabbit	Secondary	Santa Cruz	Sc-358923
HA 12CA5	Mouse monoclonal	IP	In house hybridoma	N/A

Note: Antibodies used for immunoprecipitations were added directly to the cell lysate. Primary and secondary antibodies are diluted in 5% w/v Skim Milk with TBS-T or 3% BSA with TBS-T.

2.5 Western Blotting Analysis

Samples were prepared and loaded into NuPAGE 10% or 4-12% Bis-Tris polyacrylamide gels (Invitrogen). Resolution by electrophoresis was at 200V with MES running buffer (50mM MES, 50mM Tris, 3.47mM SDS, and 1.03mM EDTA (BioShop)) and samples were transferred to polyvinylidene fluoride (PVDF) membrane (Amersham Hybond, GE Healthcare Life Science) with transfer buffer (25mM Bicine, 25mM Bis-Tris, 1.03mM EDTA, 20mM Chlorobutanol, and 10% Methanol (BioBasic)). The membrane was blocked for 1hr at room temperature with 5% w/v Skim Milk Powder (BioShop) in TBS-T (20mM Tris, 136mM NaCl (BioShop)), and 0.1% Tween-20 (Sigma). Primary antibodies (Table 2.2) were diluted in either 5% w/v Skim Milk in TBS-T, or 3% Bovine Serum Albumin (Sigma) in TBS-T. Membranes were washed with TBS-T before appropriately diluted secondary antibodies (Table 2.2) were applied for 1hr at room temperature. Luminanta Crescendo Western horseradish peroxidase (HRP) Substrate or Forte Crescendo Western HRP Substrate (Millipore) were used to detect protein according to the manufacturer's protocol. Images were developed on the Amersham Hyperfilm Enhanced Chemiluminescence (ECL) membrane (GE Healthcare) with the Konica Minolta SRX-101A automated film processor according to the manufacturer's protocol.

2.6 Statistical Analysis

Each co-immunoprecipitation experiment was replicated either two or three times.

Chapter 3

3.1 Mapping the Interaction Between HAdV-5 E1A and STING

Identifying and defining the regions of HAdV E1A that mediate interaction with STING can provide insight into the nature of this protein-protein interaction. Lau *et al.* (2015) suggested that the E1A LXCXE motif is necessary and sufficient for this interaction, but by drawing comparisons to the functional importance of the E1A LXCXE-mediated interaction with pRb, the possibility of a multi-region interaction cannot be dismissed. The LXCXE motif can be found in several viral and cellular proteins, with several of the latter showing mixed capacity and transient binding for pRb. Structural analysis of LXCXE motifs from multiple proteins revealed the importance of the side chain residues in making strong hydrophobic interactions with the target domains. Structural analysis has shown that the highly positive surface of the pRb domain LXCXE binding cleft repels the positive residues in the LXCXE motif and flanking residues (Singh *et al.*, 2005). Therefore, analysis of the interaction between E1A and STING should be extended beyond the 5 amino acid residue LXCXE motif.

3.1.1 HAdV-5 E1A Major Isoforms Bind STING

Differential splicing of E1A produces multiple isoforms of varying length, which form at certain stages of infection. The 5 major isoforms (Figure 3.1A) have mRNA sedimentation rates of 13S, 12S, 11S, 10S, and 9S and consist of 289 residues (R), 243R, 217R, 171R, and 55R respectively (Figure 3.1A). The 13S and 12S major isoforms are expressed in the early phases of infection, while the 11S, 10S, and 9s follow later in infection (Perricaudet *et al.*, 1979; Stephens & Harlow, 1987). Analyzing the interaction between STING and the E1A isoforms allows for a general mapping of the interaction, revealing key deductions. For example, the 12S isoform does not contain the CR3 region. Four isoforms of E1A, namely 13S, 12S, 11S and 10S were prepared in GFP-tagged constructs for co-transfection with the HA-tagged STING construct. HT1080 cells were co-transfected with HA-tagged

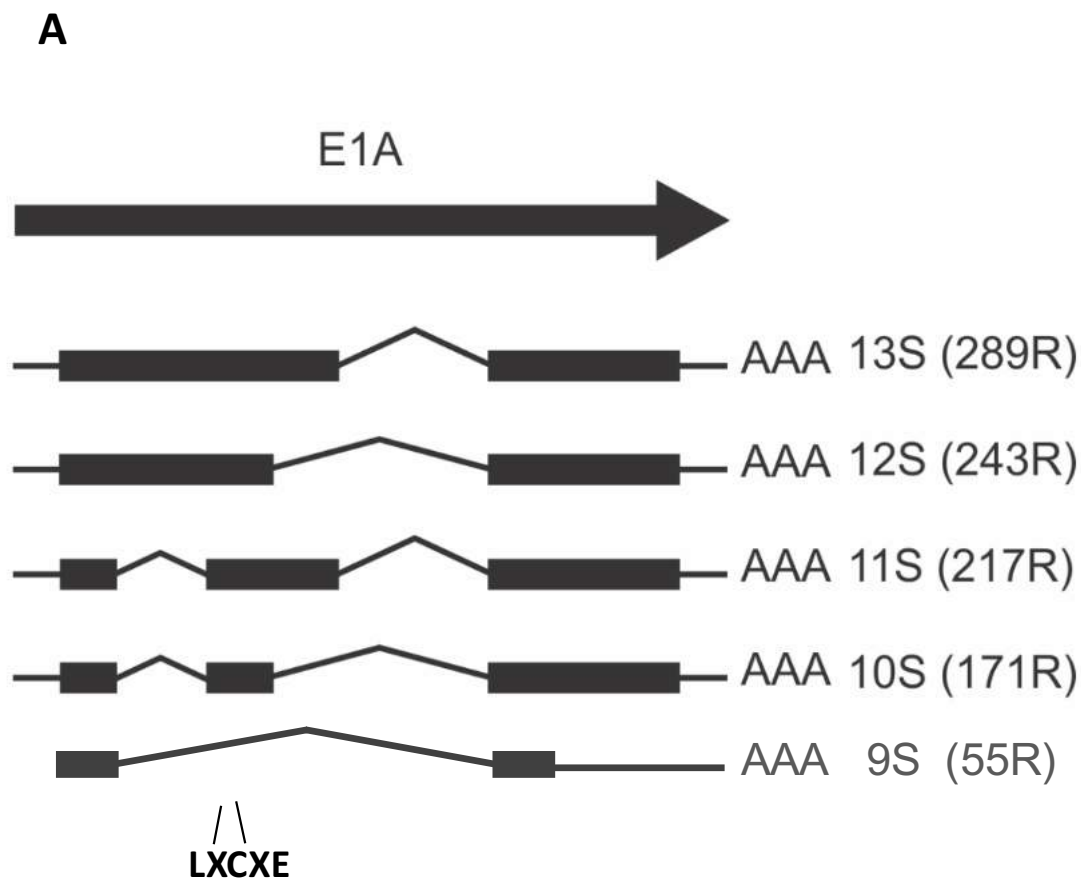
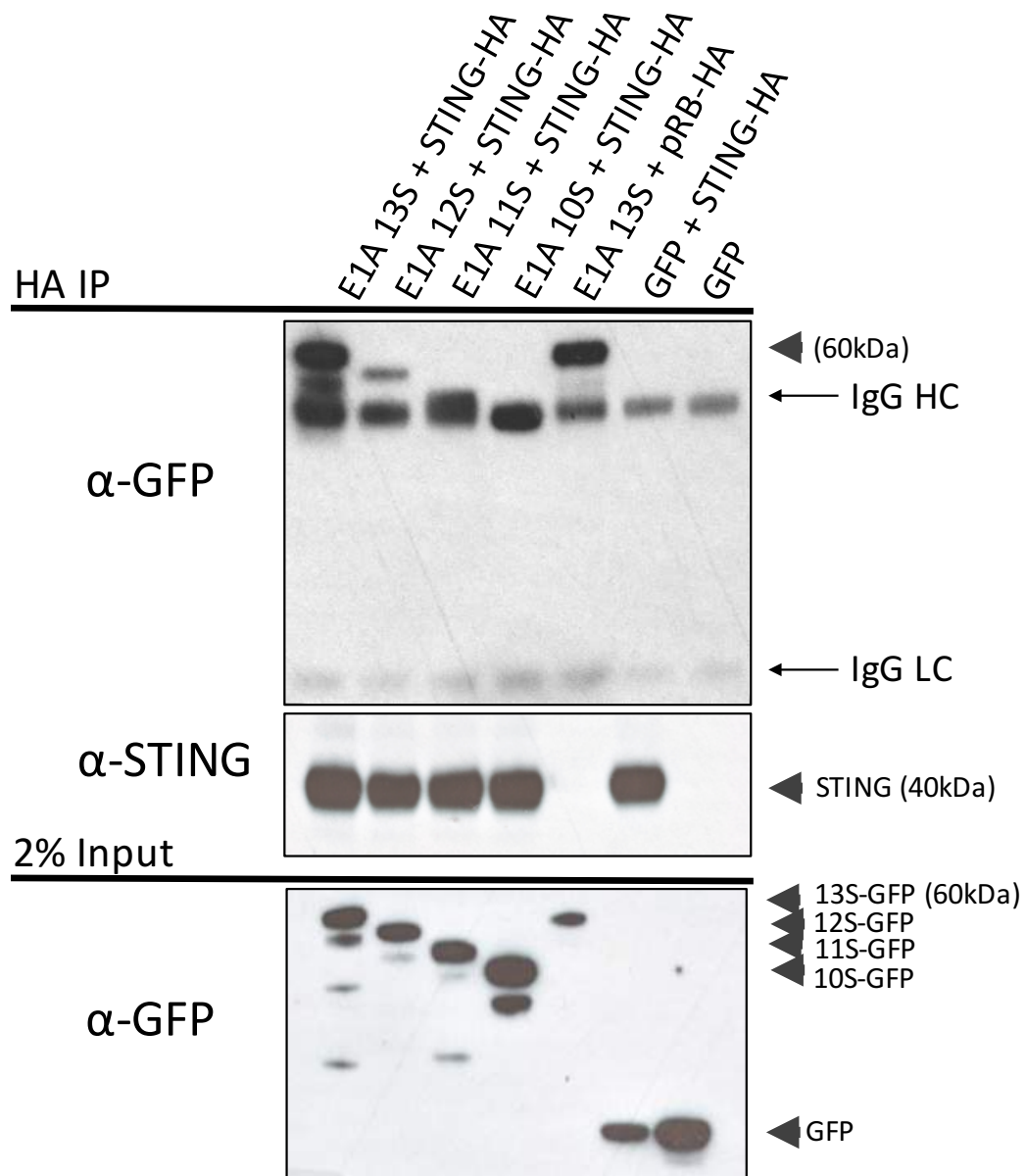


Figure 3.1. STING binds the four largest isoforms of HAdV-5 E1A. (A) Diagram depicting the structure of E1A mRNA transcripts. Boxes represent the coding regions, which are all read in the same frame, with the exception of 9S (Figure adapted with permission from Dr. Joe Mymryk, Western University, unpublished data) (B) HT1080 cells were transfected with 5 μ g human STING-HA expression vector and 5 μ g of either 13S-GFP, 12S-GFP, 11S-GFP, or 10S-GFP E1A expression vector. After 24 hr, cells were harvested and lysed, followed by immunoprecipitation of HA and western blotting for GFP-tagged E1A proteins. GFP was used as a control and pRb-HA was used as a technical positive. IgG HC denotes the heavy chain. IgG LC denotes the light chain. Inputs shown in the bottom panel. Results representative of three independent experiments.

B

STING and GFP-tagged 13S, 12S, 11S, 10S, E1A from HAdV-5. A plasmid encoding HA tagged pRb was used as a technical positive control for interaction with E1A.

Our laboratory has previously demonstrated that an E1A CR2 construct possessing the LXCXE motif forms a strong interaction with pRb in co-immunoprecipitation experiments (unpublished data). After 24 hr, cells were harvested and lysed, followed by immunoprecipitation of HA. Western blotting using anti-GFP polyclonal antibody demonstrated that all four HAdV-5 E1A isoforms tested could interact with STING *in vitro* (Figure 3.1B). All four isoforms contain the LXCXE motif, so this result is within agreement with the prediction made by Lau and colleagues (2015). However, these E1A isoforms also share common regions within the N-terminus and CR4 region.

3.1.2 HAdV-5 E1A N-terminus Region Binds STING

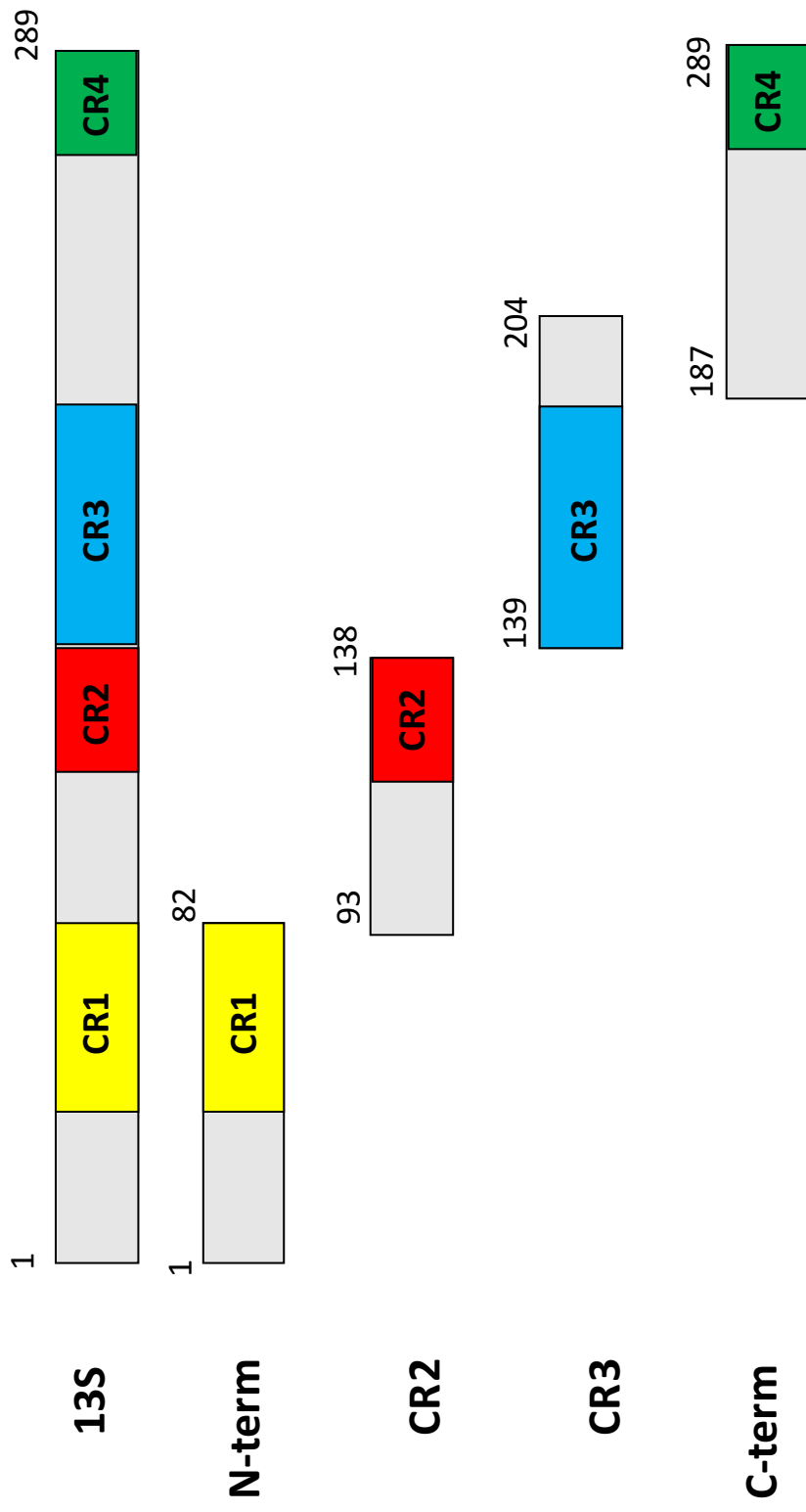
To better map the region of interaction on HAdV-5 E1A, I performed a series of co-immunoprecipitation experiments using mutants encompassing the conserved regions of HAdV-5 E1A (Figure 3.2A). HT1080 cells were co-transfected with STING-HA and the following GFP-tagged 13S E1A mutants: 1-82 AA, which contains the N-terminal region and CR1 residues (42-72AA); 93-139AA which spans CR2 (116-139); 187-289AA which spans CR3 (144-191); and 187-289AA which spans CR4 (240-288AA). Immunoprecipitation of STING was followed by western blotting with polyclonal anti-GFP antibody (Figure 3.2B). Consistent with Figure 3.1B, STING-HA binds to the N-terminal region of HAdV-5. However, this contradicts the notion that the LXCXE motif is necessary and sufficient for E1A-STING binding as the LXCXE motif is located within the CR2 region.

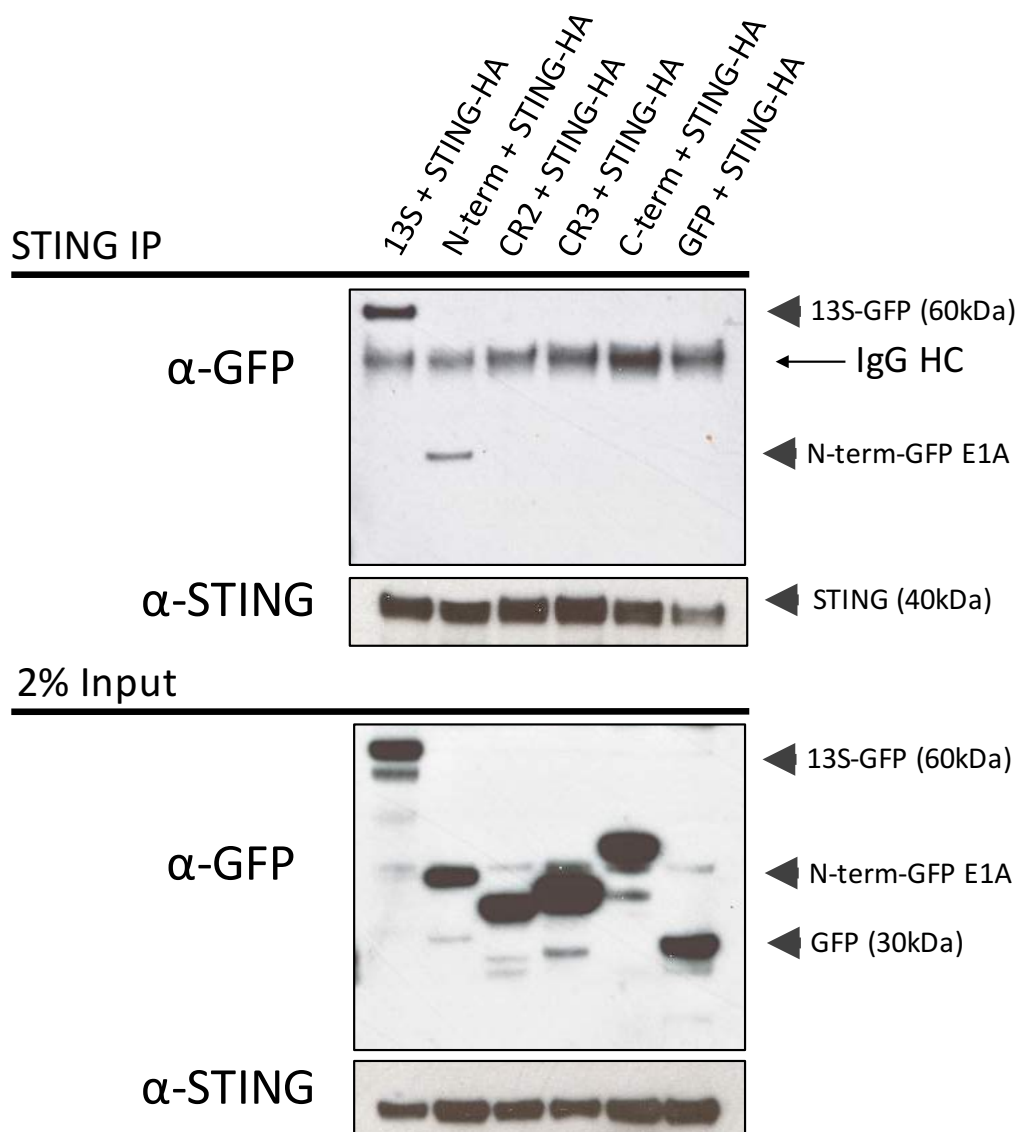
3.1.3 Assessing the Interaction Between STING and the Extreme N-terminus Region of E1A

To further analyze and map the region of HAdV-5 E1A required for interaction with STING, multiple E1A constructs were generated that spanned the N-terminus. E1A constructs consisted of amino acid residues 1-14AA, 14-22AA, 16-22AA, and 19-49AA.

Figure 3.2. STING binds to the HAdV-5 E1A N-terminus and CR1. (A) Diagram depicting the conserved amino acid regions (CRs) of human adenovirus E1A. (B) HT1080 cells were transfected with 5 μ g of human STING-HA expression vector and 5 μ g of either N terminus-GFP, CR2-GFP, CR3-GFP, or C terminus-GFP E1A expression vector. After 24 hr, cells were harvested and lysed, followed by immunoprecipitation of STING and western blotting for GFP-tagged E1A proteins. GFP was used as a control with STING-HA. IgG HC denotes the heavy chain. Inputs shown in the bottom panel. Results representative of three independent experiments.

A



B

Co-immunoprecipitation experiments were conducted in HT1080 cells using anti-STING antibody, followed by western blotting with anti- GFP antibody. The first 14 amino acid residues of E1A were found to bind STING, while E1A amino acid residues 29-49 were found to mediate a much weaker binding, as indicated by a faint signal (Figure 3.3A). However, this 29-49AA mutant was present at a much higher concentration within the lysate (as shown by the input), potentially producing a false-positive result. This finding was consistent with earlier results indicating that the N-terminus was an important region of interaction between E1A and STING.

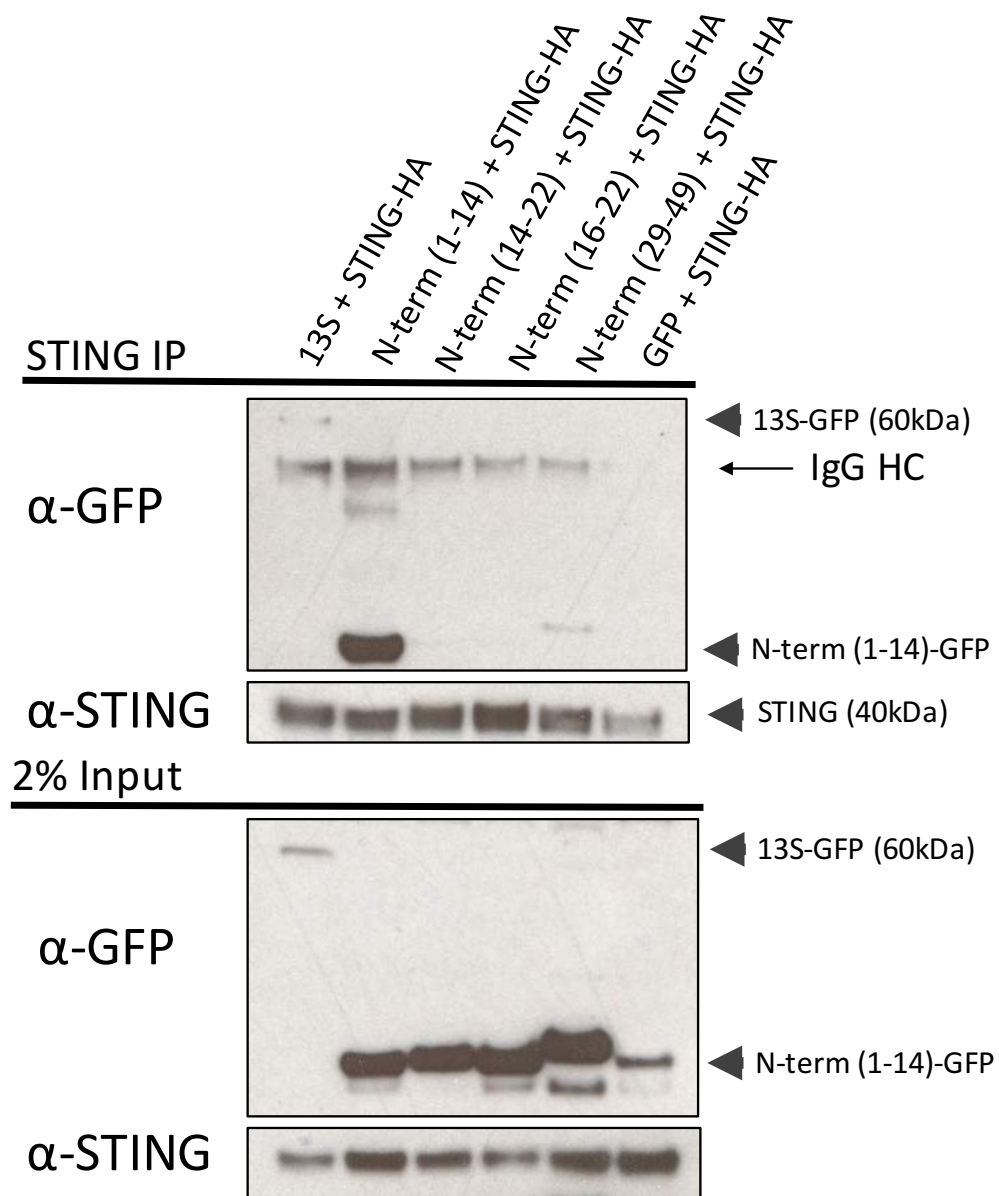
To further verify that the region of HAdV-5 E1A was required for binding STING *in vitro*, deletion mutants were prepared by removing stretches of amino acids within the N-terminal backbone (Figure 3.3B). These small deletion mutants of E1A are well characterized and the biological effects of these mutations have been studied in different models (Jelsma *et al.*, 1988). The dl1101 mutant contains deletion of amino acid residues 4-25, the dl1102 mutant contains deletion of amino acid residues 26-35, and the dl1103 mutant contains the deletion of amino acid residues 30-49. As Figure 3.3C indicates, the WT N-terminus and dl1103 E1A mutants were found to bind STING, while dl1101 and dl1102 had significantly reduced/non-detectable binding. This is consistent with the previous finding that the first 14 amino acid residues were of particular importance for interaction. This also supports the hypothesis that the LXCXE motif is not sufficient for interaction. As the dl1103 mutant was also found to bind STING, it supports the earlier suggestion that the N-terminal amino acid residues 29-49 do not play significant roles in mediating the interaction.

3.1.4 The HAdV-5 LXCXE Motif is Not Necessary for Binding STING

The suggestion by Lau *et al.* (2015) that the LXCXE motif was the point of interaction between HAdV-5 E1A and STING in HEK293 cells requires further investigation. HEK293 cells were immortalized by HAdV-5 E1A, and therefore express the E1A protein (Thomas & Smart, 2005). Despite the presence of endogenous E1A, Lau and colleagues co-transfected HEK293 cells with STING and an E1A construct containing mutations that disabled the LXCXE motif. They reported that these mutations within the LXCXE motif

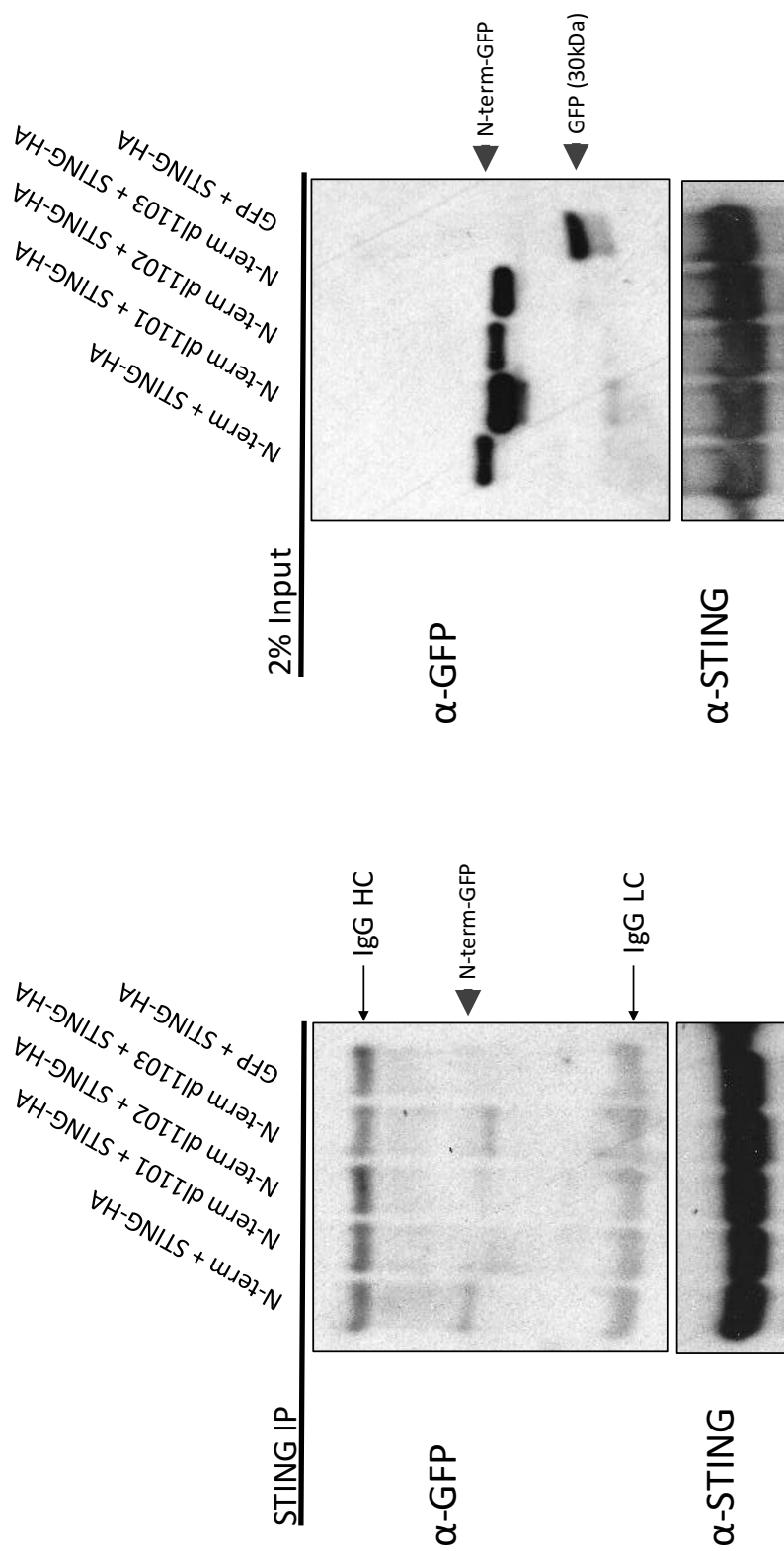
Figure 3.3. STING binds the Extreme N-terminus of HAdV-5 E1A. (A) HT1080 cells were transfected with 5 μ g of human STING-HA expression vector and 5 μ g of N terminus-GFP E1A expression vector mutants; 1-14AA, 14-22AA, 16-22AA, and 29-49AA. After 24 hr, cells were harvested and lysed, followed by immunoprecipitation of STING and western blotting for GFP-tagged E1A mutants with anti-GFP antibody. GFP was used as a control with STING-HA. Inputs shown in the bottom panel. IgG HC denotes the heavy chain. (B) Diagram depicting the E1A N-terminus deletion mutants; dl1101 (Δ 4-25), dl1102 (Δ 26-35), dl1103 (Δ 30-49). (C) HT1080 cells were transfected with 5 μ g of human STING-HA expression vector and 5 μ g of N terminus-GFP and N-terminus-GFP deletion mutants dl1101 (Δ 4-25), dl1102 (Δ 26-35) and dl1103 (Δ 30-49). IgG HC denotes the heavy chain. IgG LC denotes the light chain. Inputs shown in right panel. Results representative of three independent experiments.

A



B**HAdV-5 E1A**

C



abolished binding with STING, as compared to WT full length E1A. To verify and explore further, I co-transfected HEK293 cells with GFP-tagged HAdV-5 13S E1A and a GFP-tagged dl1108 E1A construct. The dl1108 E1A mutant construct contains a deletion of amino acids 122-126, which removes the CXE of the LXCXE motif to effectively abolish the motif (Figure 3.4A). This mutant has previously been documented to be transformation defective and does not bind pRb or p130 (Egan *et al.*, 1988; Jelsma *et al.*, 1988). Immunoprecipitation with anti-STING was followed by western blotting for anti-GFP and anti-E1A (anti-M73 antibody)(Figure 3.4B). In agreement with Lau and colleagues, transfection and immunoprecipitation with anti-STING was found to be sufficient for binding between ectopically expressed STING and endogenous 13S, but contrary to their findings, the LXCXE mutant dl1108 was still capable of binding STING. There is a slight spillover in the empty lane because of partial well collapse.

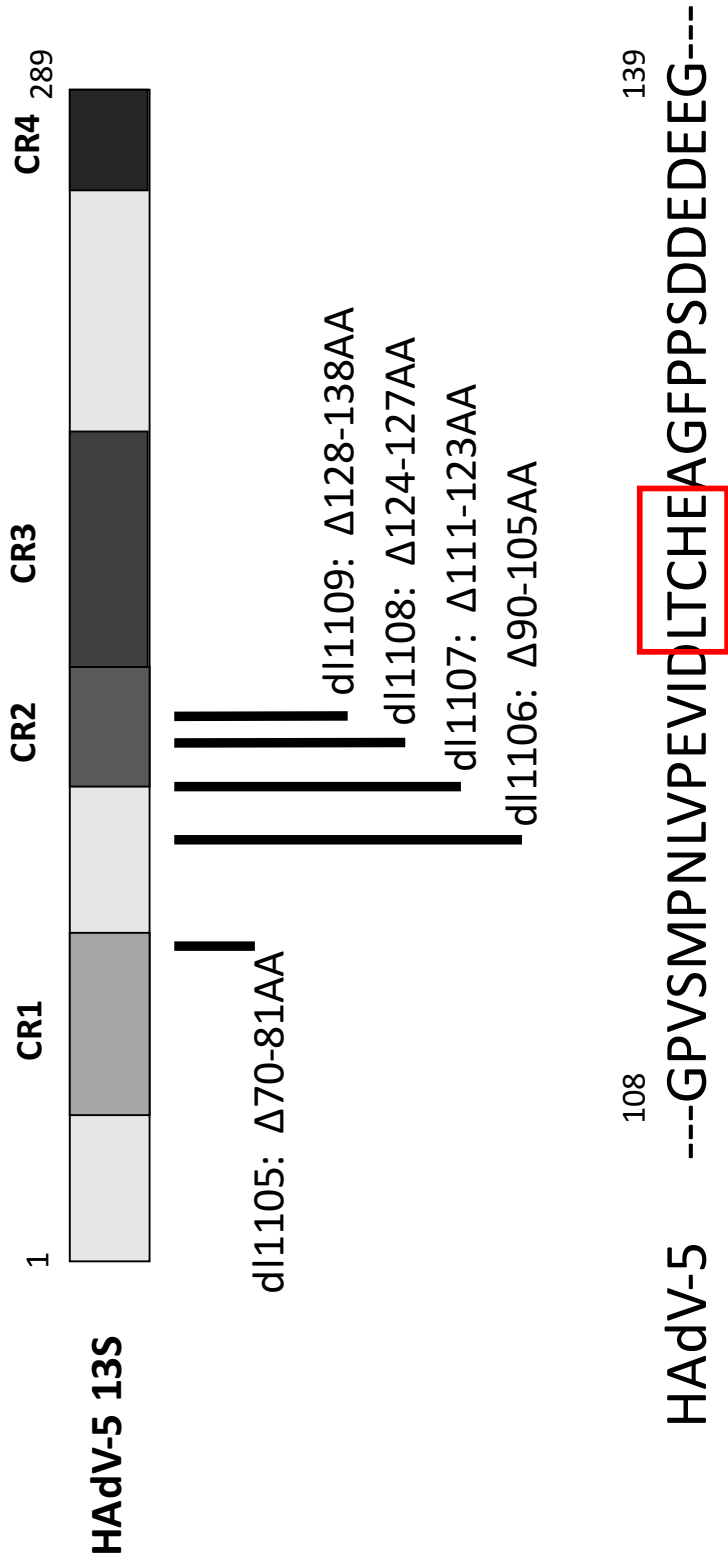
To further my analysis, I chose a different cellular model. HT1080 cells were prepared and a series of deletion mutants spanning the CR2 region of HAdV-5 (including the LXCXE motif), were constructed. Deletion mutant dl1107, which deletes amino acids 111-123, and dl1108, which deletes amino acids 124-127, both disrupt the LXCXE motif. Either of the two deletion mutants should theoretically inhibit binding with STING if the LXCXE motif is necessary for the interaction with STING. Additional deletion mutants were constructed that flanked both sides of the LXCXE motif, or removed part of CR1 (see Figure 3.4A). Immunoprecipitation with STING was followed by western blotting with anti-GFP. As shown in figure 3.4C, all of the deletion mutants displayed binding affinity with STING. There was a noticeable reduction in expression between dl1107 and dl1108 with STING, which could potentially indicate that the LXCXE motif may play a secondary role in the interaction with STING.

3.1.5 Analysis of the Conserved Interaction Between STING and 13S E1A from Representative Members of HAdV Species A to G

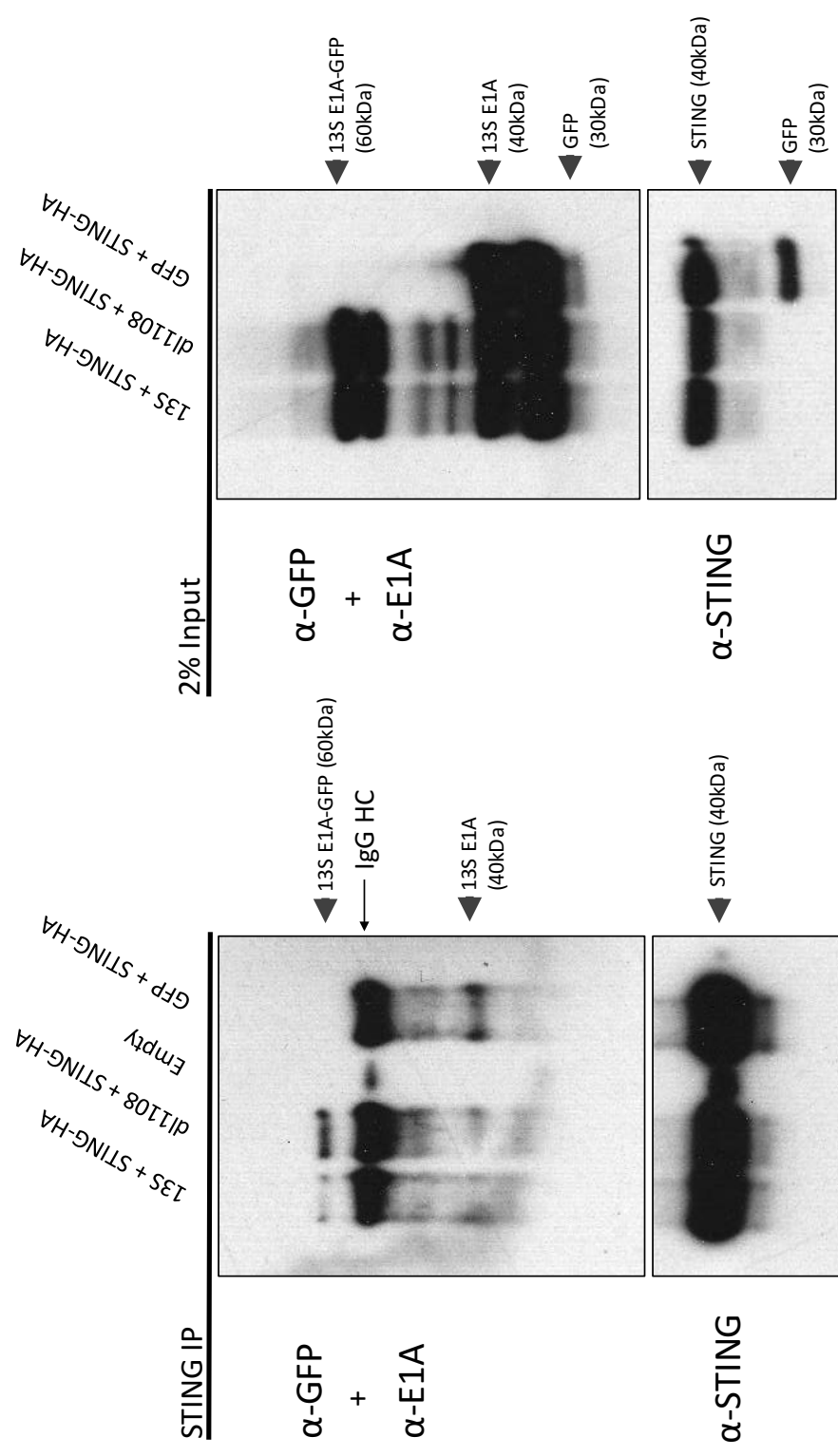
Across the various distinct species and serotypes of Adenovirus, there are multiple

Figure 3.4. STING binds E1A LXCXE deletion mutants. (A) Diagram depicting characterized E1A deletion mutants that span CR1, CR2 and the region preceding CR2. The red box indicates the LXCXE motif. Deletion mutants dl1107 and dl1108 disable the LXCXE motif. (B) HEK293 cells were transfected with 5 μ g of STING-HA and 5 μ g of E1A-GFP deletion mutant dl1108. After 24 hr, cell were harvested and lysed, followed by immunoprecipitation of STING and western blotting for E1A or GFP-tagged protein using anti-E1A (anti-M73) and anti-GFP antibodies. 13S E1A at 40kDa represents endogenous E1A. Inputs shown in the right panel. (C) HT1080 cells were transfected with 5 μ g of human STING-HA expression vector and 5 μ g of E1A-GFP deletion mutants; dl1105, dl1106, dl1107, dl1108, and dl1109. After 24 hr, cells were harvested and lysed, followed by immunoprecipitation of STING and western blotting for GFP-tagged E1A mutants with anti-GFP antibody. Inputs shown in right panel. IgG HC denotes the heavy chain. Results representative of two (B) or three independent experiments (C).

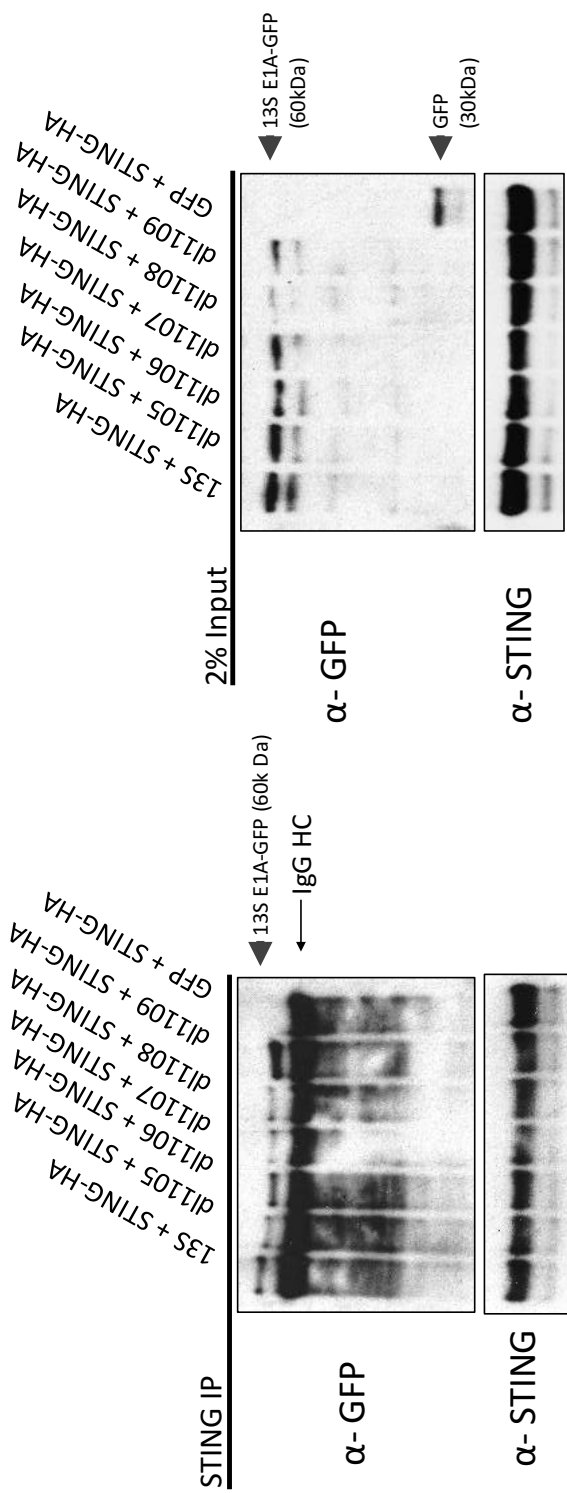
A



B



C



conserved motifs that interact with important cellular proteins such as GCN5, CtBP, p300 and pRb (Avvakumov *et al.*, 2004; Pelka *et al.*, 2008). The identification of new proteins that demonstrate conserved interactions with multiple species of E1A may indicate new important roles for those proteins during the Adenoviral lifecycle. To determine if STING could bind multiple species of Adenoviral E1A protein, we utilized a series of 13S E1A constructs representing the major species groups of Adenovirus A through G (Figure 3.5A). The constructs represented were HAdV-3,-4,-5,-9,-12,-40, and -52. 13S E1A constructs were co-transfected with STING into HT1080 cells and immunoprecipitation with STING was followed by western blotting with anti-GFP. The binding between HAdV-52 and STING was almost non-detectable (Figure 3.5B), but an interaction was detected for all other serotypes.

The next investigation was to look at the extreme N-terminus of each species as shown in Figure 3.6A. There is a considerable level of conservation between species within this region of the N-terminus. Each GFP-tagged E1A mutant construct was co-transfected with STING into HT1080 cells and immunoprecipitation with STING was followed by western blotting with anti-GFP. As demonstrated in Figure 3.6B, the N-terminus 1-15AA mutants of HAdV-5,-3,-9,-12, and -40 interacted with STING, whilst HAdV-52 did not.

3.2 Assessment of the Interaction Between E1A, S6K and RPS6

Wang and colleagues (2016) demonstrated a novel interaction between mouse p70 S6K1 and mouse STING. The p70 S6 kinase is a mitogen activated serine/threonine kinase necessary for cell growth and survival. Studies have demonstrated that S6K regulates protein synthesis (Thomas, 2000), cell cycle progression (Lane *et al.*, 1993), and cell size (Montagne *et al.*, 1999). Through an *in vitro* model of chronic activation of the cGAS-STING pathway *via* transduction of cells with recombinant virus, Wang and colleagues showed that S6K1 associates with the STING-TBK1 IRF3 complex, leading to IRF3 phosphorylation and translocation to the nucleus. Disruption of this S6K1-STING interaction resulted in the abolition of IRF3 phosphorylation and translocation. I posed the

Figure 3.5. Interaction between STING and E1A conserved across multiple species. (A) Diagram depicting the seven (A-G) HAdV species and respective serotypes. Serotypes highlighted in red were expressed at full length (13S) in GFP constructs. (B) HT1080 cells were co-transfected with 5 μ g of human STING-HA expression vector and 5 μ g of 13S E1A-GFP expression vectors representing the seven HAdV species; HAdV-3,-4,-5,-9,-12,-40, and -52. After 24 hr, cells were harvested and lysed, followed by immunoprecipitation of STING and western blotting for GFP-tagged 13S E1A serotypes with anti-GFP antibody. Inputs shown in bottom panel. IgG HC denotes the heavy chain, IgG LC denotes the light chain. Results representative of three independent experiments.

A

HAdV Species	Serotype
A	12 , 18, 31
B	3 , 7, 11, 14, 16, 21, 34, 35, 50
C	1, 2, 5 , 6
D	8, 9 , 10, 13, 15, 17, 19, 20, 22-30, 32, 33, 36-39, 42-49, 51
E	4
F	40 , 41
G	52

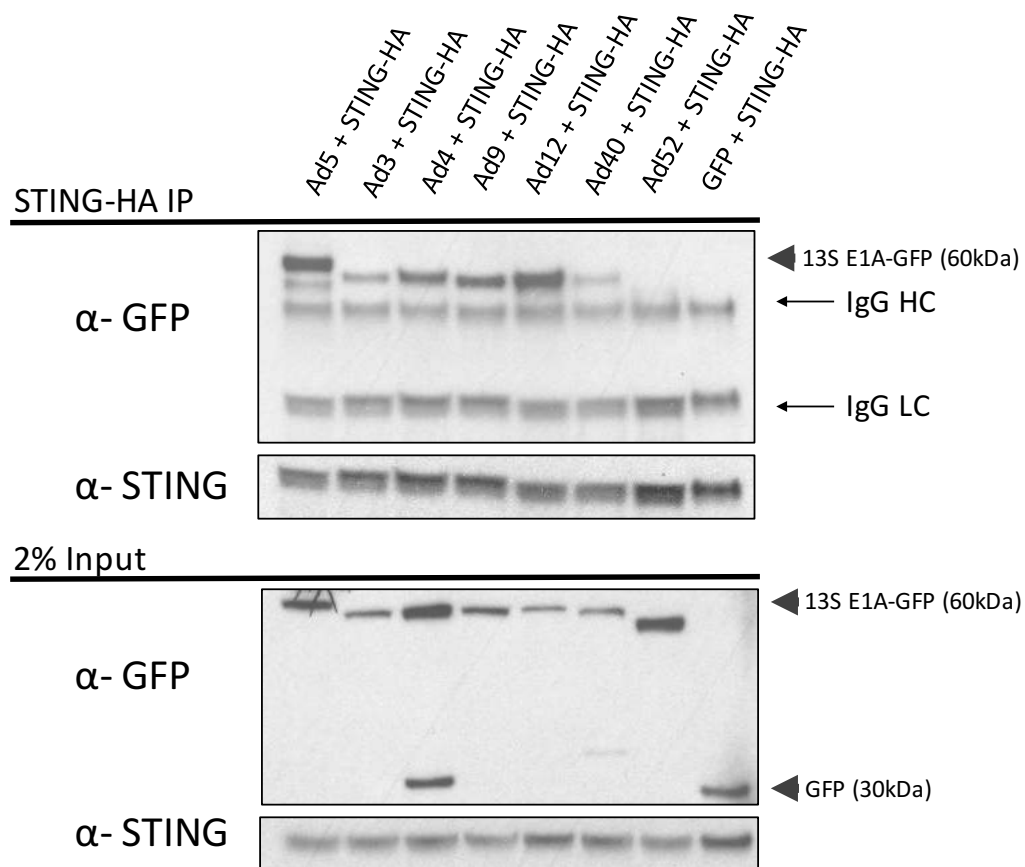
B

Figure 3.6. E1A extreme N-terminus interaction with STING conservation across multiple species. (A) Diagram depicting the sequence alignment of amino acids 1-80 across multiple serotypes representing homology across seven HAdV species. Shaded areas represent conservation in sequence across serotypes. (B) HT1080 cells were transfected with 5 μ g of human STING-HA expression vector and 5 μ g of 13S E1A-GFP expression vectors representing amino acids 1-14 across seven HAdV species; HAdV-3,-4,-5,-9,-12,-40, and -52. After 24 hr, cells were harvested and lysed, followed by immunoprecipitation of STING and western blotting for GFP-tagged E1A serotypes with anti-GFP antibody. Inputs shown in right panel. IgG HC denotes the heavy chain. Results representative of three independent experiments.

A

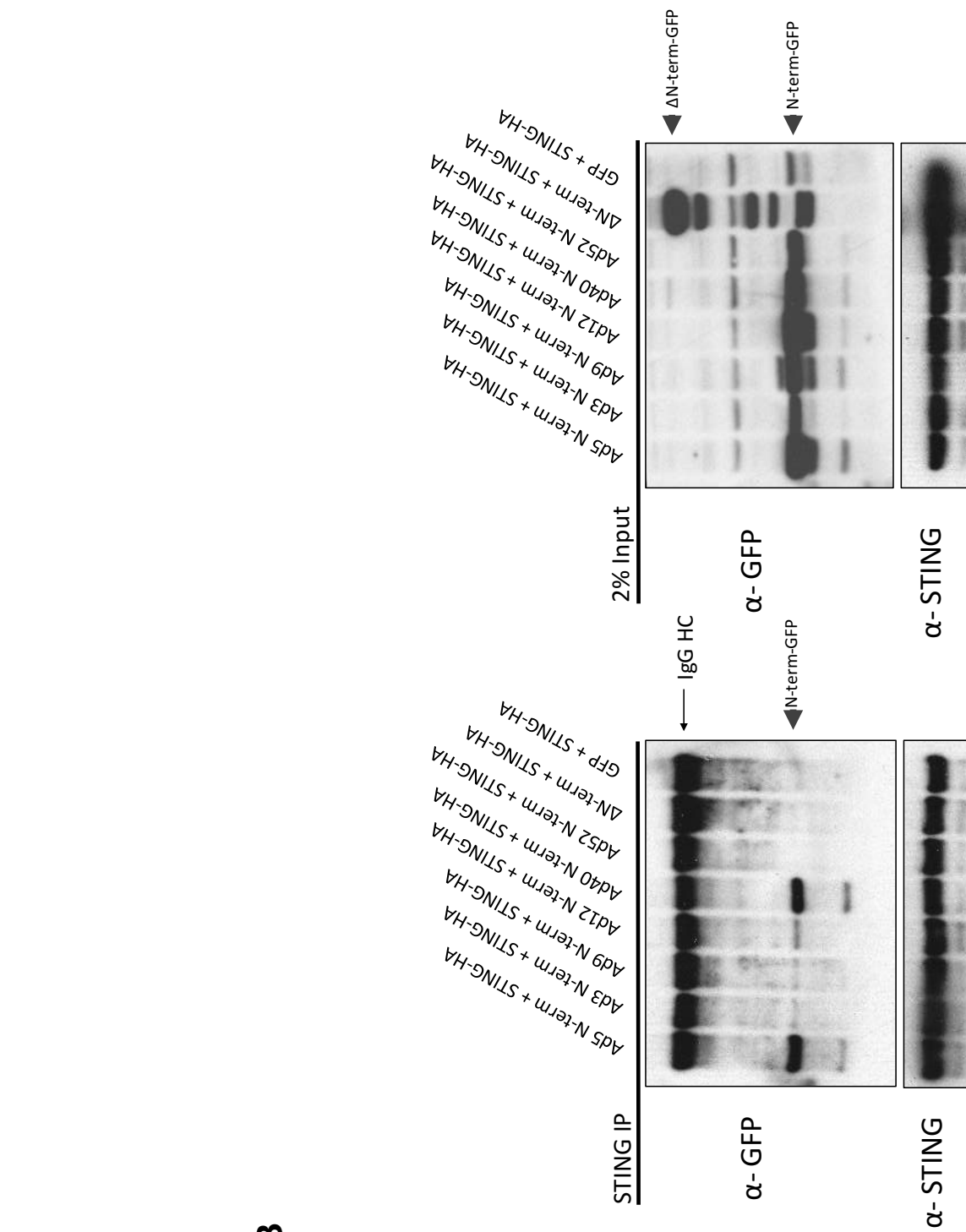
80

1

HAdV-3 MRHLRFIPQEVISSETGIEILEFVVNTLM-GD-DPEPPVQPFDPPTLHLDLYDLEIDGP-EDPNEEAVNGFFTDSMILAADEG
HAdV-4 MRHLRDLPEDEEIIIASGSEILELVVNTM-GDDHPEPP-TFFGTPLSLHLDLYDLEVDVPEDDPNEKAVNDIFSAAIAAEEFA
HAdV-9 MRHLRLIP-----STVPESMIQADIA
HAdV-5 MRHICHGG-VITEEMAASILDQLIEEVL-AD-NLPPP-SHFEPPILHFLYDLDVTAP-EDPNEEAVSQIFPDSVMLAVQEG
HAdV-12 MRTEM-TPL-VLSYQEAADDILEHLVDNFF-NE-VPD--DLYVPSIYELYDLDVESAGEDNNEQAVNEFFPESLJLAASEG
HAdV-40 MRMLPDPFF---TGNW-DDMFQGLIETEYVFD-FPEPS-EASEEMSLHDLFDVEVDGFEEDANQEAVDGMPFPRLLSEAEESA
HAdV52 MRLVPEMYG-VFCSET-VRNSDELINTDIL-ID-VPNSP--VTSPPSLHDLFDVEVDPP-QDPNEDAVNSMFFPECFFAAEEG

CR1

B

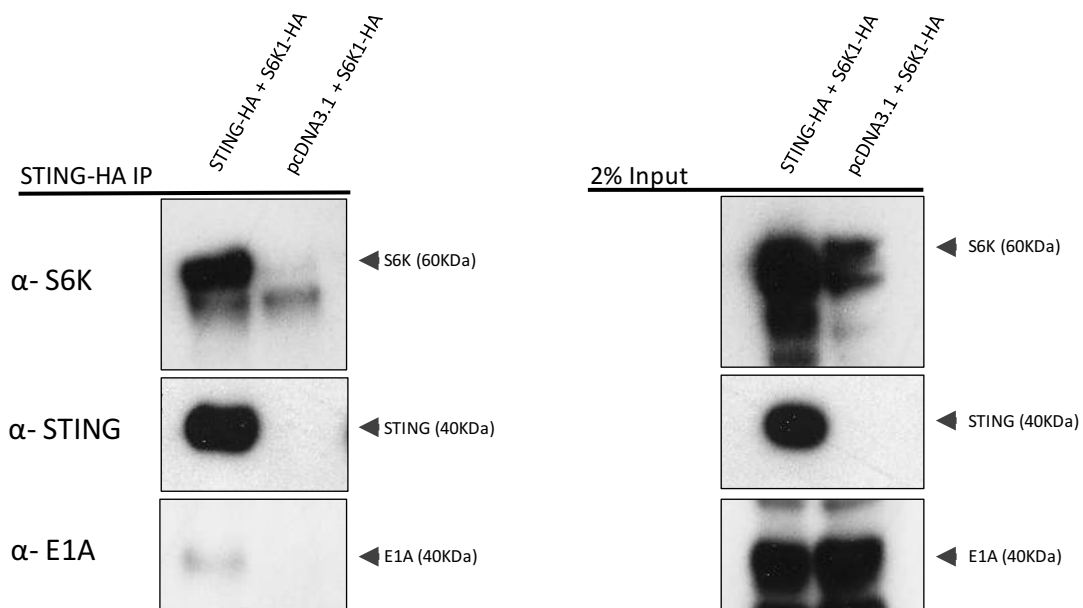
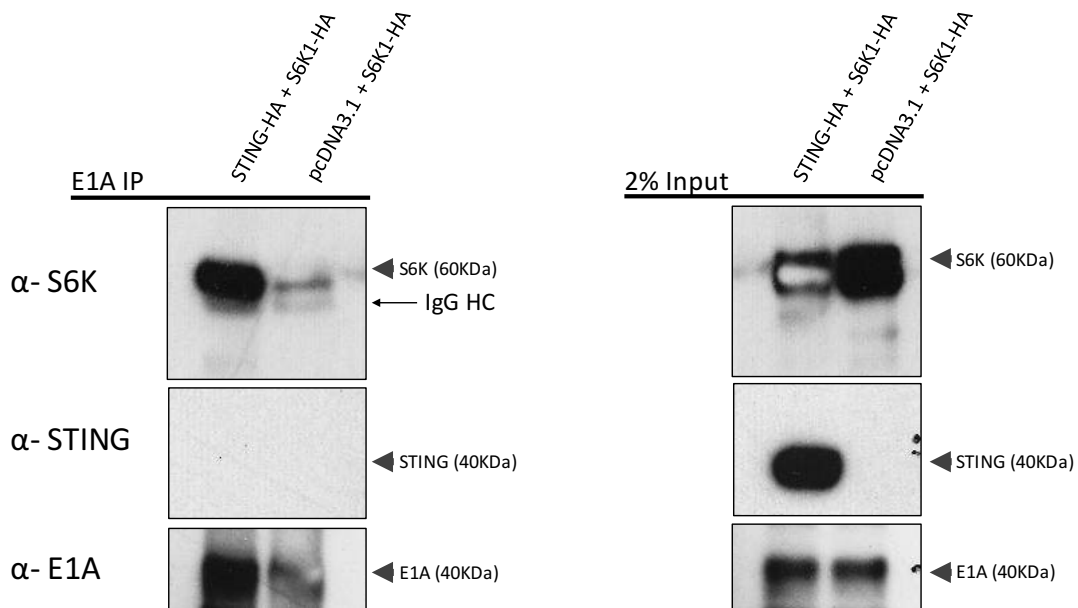


question as to whether E1A was involved in this S6K1-STING-TBK1-IRF3 complex. To date, there has been only one report published investigating induction of p70 S6K by Adenovirus E1A (de Groot *et al.*, 1995). This study reported that the induction was not mediated through protein-protein interactions, but this cannot be verified as the relevant data was not published. I sought to revisit this connection between E1A and S6K, with the aim of demonstrating that E1A can indeed, bind S6K1. Finding ancillary binding partners of E1A that also bind STING, TBK1 and IRF3 could further help to investigate the nature of the E1A-STING interaction. Ancillary binding partners of E1A could bridge the interaction with STING. In addition to S6K1, there are no existing reports analyzing the molecular relationship between E1A and ribosomal protein S6 (RPS6). The RPS6 operates within the mTORC1 signaling pathway to promote protein synthesis and is the most extensively studied S6K substrate. Nevertheless, the biochemical consequences of RPS6 phosphorylation by S6K have yet to be fully determined (Meyuhas, 2008; Meyuhas & Dreazen, 2009). Wang and colleagues (2016) did not investigate whether RPS6 was involved in the S6K1-STING-TBK1-IRF3 complex. Therefore, to extend my exploration of this topic, I also sought to determine if E1A could interact with RPS6. A novel interaction between E1A and RPS6 would also facilitate future exploration into how E1A could potentially modulate known proteins involved in metabolic and innate immune pathways to create a more conducive environment for viral infection.

3.2.1 Verifying the Interaction Between S6K and STING

To expand on Wang and colleagues (2016) finding that S6K binds STING, I assessed if this interaction existed in HEK293 cells. I co-transfected a human STING-HA expression construct with a mouse S6K1-HA expression construct kindly gifted by Wang and colleagues (McMaster University). Co-immunoprecipitations were undertaken using either anti-STING or anti-E1A (anti-M73 + anti-M58) antibodies, followed by western blotting with anti-STING, anti-S6K, and anti-E1A antibodies. As shown in Figure 3.7A, immunoprecipitation with STING verified that mouse S6K binds to human STING. An interaction between S6K and STING was observed, and STING also immunoprecipitated endogenous E1A. The question of whether these three proteins are in complex cannot be determined from this experiment. Interestingly, immunoprecipitation with E1A

Figure 3.7. HAdV-5 E1A interacts with mouse S6K1. (A) HEK293 cells were transfected with 5 μ g of human STING-HA expression vector and 5 μ g of mouse S6K1-HA expression vector. After 24 hr, cells were harvested and lysed, followed by immunoprecipitation of STING and western blotting for endogenous E1A, S6K1-HA, and STING-HA. Inputs shown in right panel. IgG HC denotes the heavy chain. (B) HEK293 cells were transfected with 5 μ g of human STING-HA expression vector and 5 μ g of mouse S6K1-HA expression vector. After 24 hr, cells were harvested and lysed, followed by immunoprecipitation of endogenous E1A and western blotting for E1A, S6K1-HA, and STING-HA. Inputs shown in right panel. IgG HC denotes the heavy chain. Results representative of two independent experiments.

A**B**

(Figure 3.7B) indicated that endogenous E1A was able to co-immunoprecipitate with exogenous mouse S6K1, and produce a strong signal. On the contrary, endogenous E1A did not co-immunoprecipitate with exogenous STING. It is to be assumed that E1A and STING will bind endogenous S6K within the system, but overexpression of mouse S6K1 aids in studying these interactions. When comparing the input signals between STING and S6K1, the inability of endogenous E1A to bind STING through immunoprecipitation with E1A was unexpected.

3.2.2 E1A Binds Endogenous S6K and RPS6

The first indications that E1A could potentially bind human S6K and RPS6 came from co-immunoprecipitation studies in HEK293 cells, which endogenously express HAdV-5 E1A. 13S E1A constructs in pcDNA3.1 were co-transfected with STING-HA or pcDNA3.1 vector. As shown in Figure 3.8, immunoprecipitation with E1A (anti-M73), followed by western blotting for STING-HA, E1A, endogenous S6K, and endogenous RPS6. 13S E1A alone, was found to co-immunoprecipitate with both endogenous S6K and RPS6. The p70 S6K signal was very strong, while the p85 S6K signal was much weaker. The presence of STING did not appear to be a requirement for co-immunoprecipitation of S6K and RPS6 with 13S HAdV-5 E1A. In support of previous results (Figure 3.7), the endogenous E1A present in the control did not co-immunoprecipitate well with STING-HA. In addition, overexpression of 13S E1A was required to co-immunoprecipitate E1A with RPS6. However, a strong p70 S6K signal was detected with E1A in the control co-immunoprecipitation, but not p85 S6K. If E1A does not require STING to bind S6K, then S6K may act as a bridge between E1A and STING.

3.2.3 Characterizing the Interaction Between Mouse S6K1 and HAdV E1A

To verify the interaction of HAdV with mouse S6K1, we overexpressed these proteins with epitope tags in HT1080 cells for co-immunoprecipitation studies. We used mouse S6K1 because it was kindly gifted by Wang and colleagues and has 99% sequence homology to

Figure 3.8. HAdV-5 E1A binds endogenous human S6K and RPS6. HEK293 cells were transfected with 5 μ g of human STING-HA expression vector and 5 μ g of 13S E1A-pcDNA3.1 expression vector (no tag). After 24 hr, cells were harvested and lysed, followed by immunoprecipitation of STING and western blotting for endogenous E1A, endogenous S6K, and endogenous RPS6. Inputs shown in right panel. Results representative of two independent experiments.

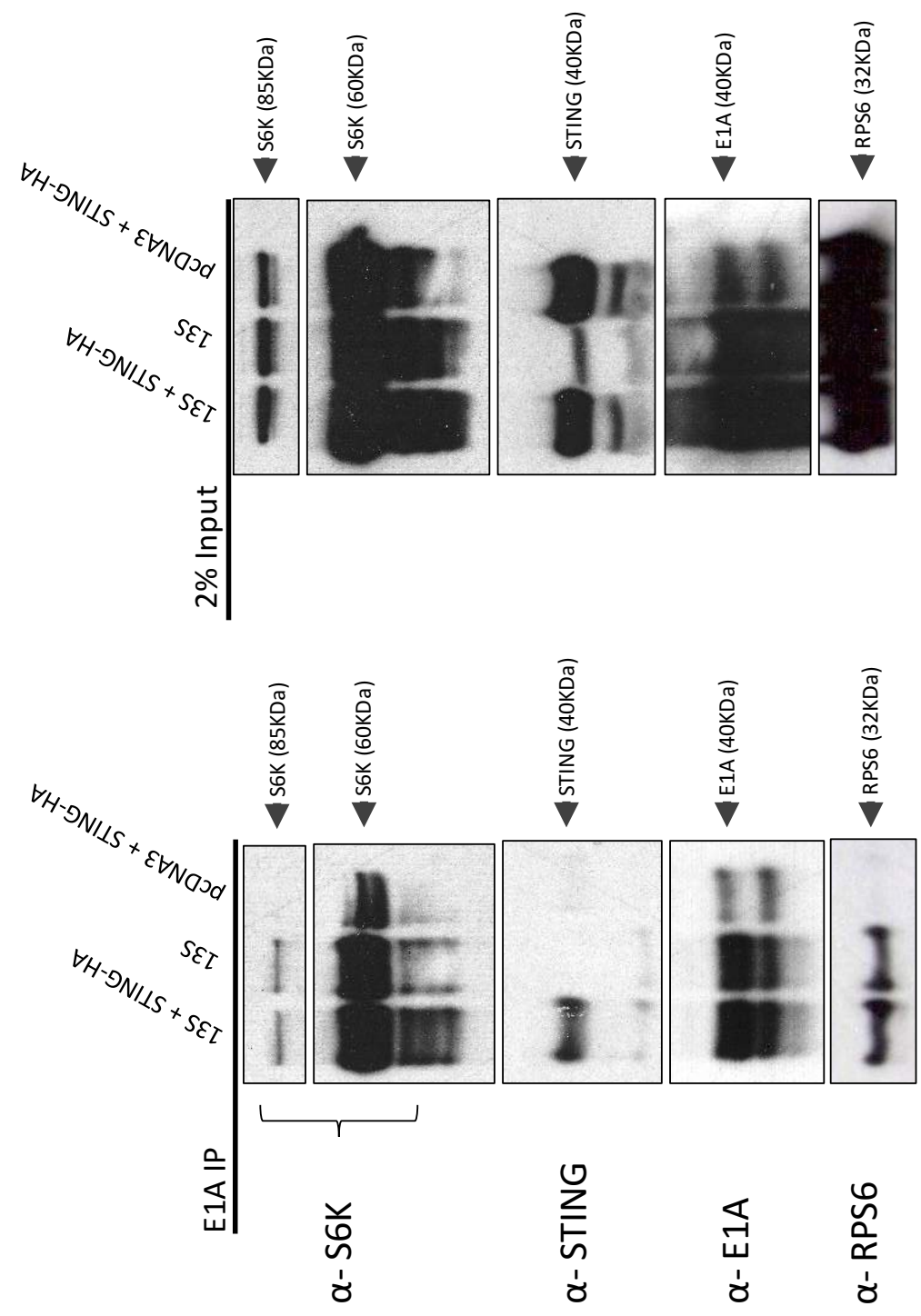
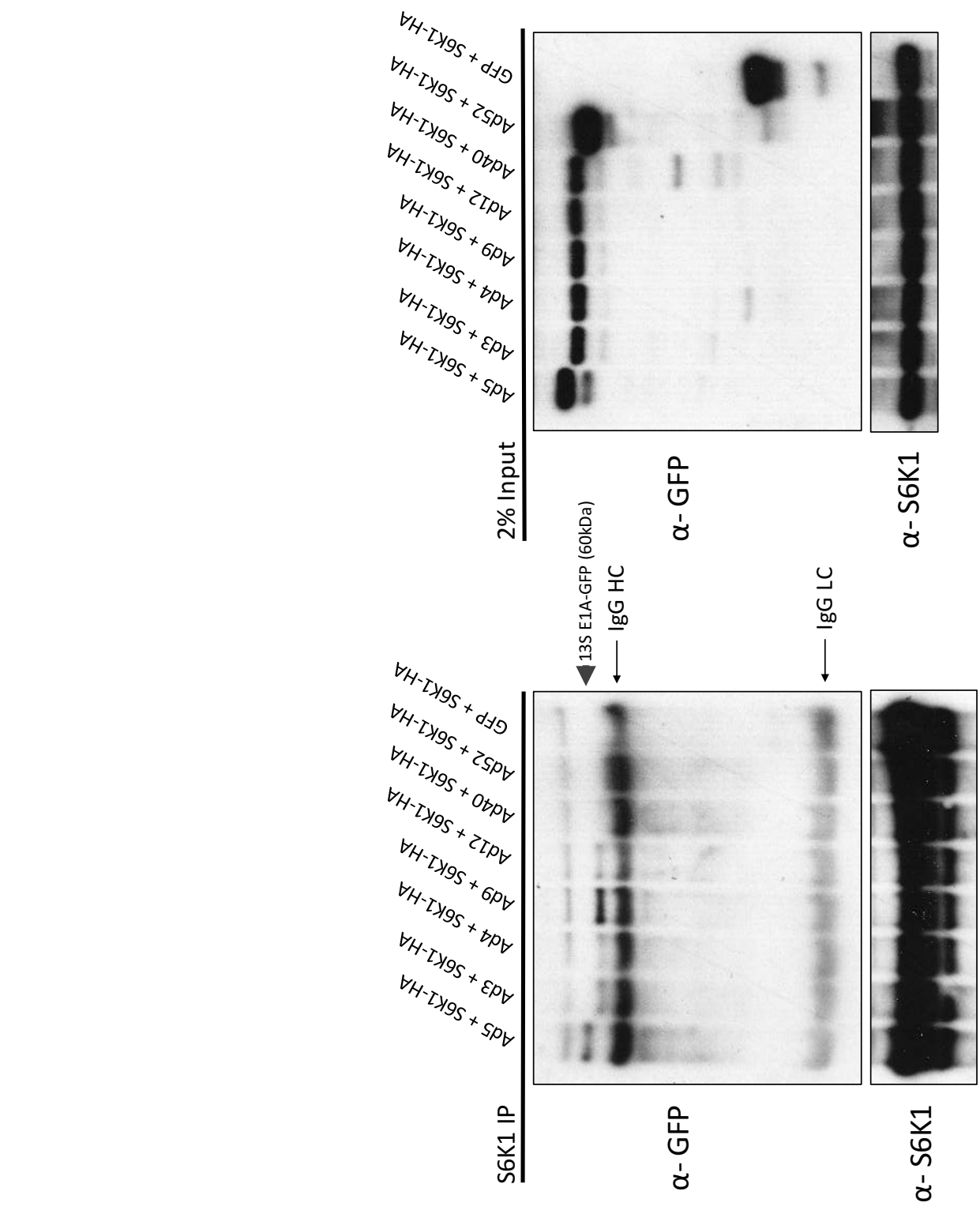


Figure 3.9. HAdV-5 interaction with mouse S6K1 conserved across serotypes. HT1080 cells were transfected with 5 μ g of HAdV 13S-GFP expression vectors representing HAdV-3,-4,-5,-9,-40-and -52, and 5 μ g of mouse S6K1-HA expression vector. After 24 hr, cells were harvested and lysed, followed by immunoprecipitation of S6K and western blotting for E1A-GFP. Inputs shown in right panel. IgG HC denotes the heavy chain. Results representative of three independent experiments.



human S6K1. To assess the conservation of this reaction, GFP-tagged 13S E1A serotypes representing the major Adenoviral families were co-immunoprecipitated with HA-tagged S6K1 using anti-S6K1 antibody. As shown in Figure 3.9, western blotting was undertaken with anti-GFP antibody and the results indicate that HAdV-5,-3,-4,-9, and -12, have relatively strong interactions with mouse S6K1, as compared to HAdV-40 and -52. This indicates that the interacting motif is fairly well conserved but not present within all E1A species.

3.2.4 Assessing the Effect of Ectopically Expressed S6K2 on HAdV-5 E1A-S6K1 and HAdV-5 E1A-RPS6 Interaction

The physiological and cellular roles of S6K1 are well documented (Magnuson *et al.*, 2012), but less is known about S6K2. Over the past few years, researchers have demonstrated that S6K1 and S6K2 have high sequence homology, but S6K2 has additional cellular functions that are independent of S6K1 (Pardo & Seckl, 2013). The predominant form of S6K1, p70, is localized mainly to the cytoplasm, while the p85 isoform, which contains a nuclear localization sequence, is mainly found within the nucleus. S6K2 has two isoforms, a predominant p54 form and a p56 form. Both of these S6K2 isoforms contain nuclear localization signals and reside mainly in the nucleus of resting cells (Karlsson *et al.*, 2015). Within human tissues, S6K2 is expressed at various levels, but expression levels are often inversely correlated with those of S6K1 (Nardella *et al.*, 2011). I wanted to determine if overexpressing S6K2 protein in HT1080 cells effected protein expression levels of S6K1. I also wished to determine if overexpression of RPS6 effected the interaction between RPS6 and 13S E1A, and S6K1 and 13S E1A.

A human S6K2 plasmid, and a human RPS6 plasmid, were constructed for co-transfection into HT1080 cells with 13S E1A. As shown in Figure 3.10, immunoprecipitation with E1A (anti-M73 antibody), was followed by western blotting with anti-S6K antibody and anti-RPS6 antibody. The results suggest that S6K can bind RPS6 and co-immunoprecipitate with E1A. The limitation to this particular experiment was that the anti-S6K antibody used is specific for p70 and p85 S6K1, and not S6K2. Our previous results demonstrated that endogenous E1A in HEK293 cells could immunoprecipitate with endogenous p70 S6K1

Figure 3.10. Overexpression of RPS6 and S6K2 are required for interaction between ectopically expressed HAdV-5 E1A and p70 S6K. HT1080 cells were transfected with 5 μ g of HAdV-5 13S (no tag) expression vector and 5 μ g of human S6K2 expression vector or 5 μ g of human RPS6 expression vector. After 24 hr, cells were harvested and lysed, followed by immunoprecipitation of E1A and western blotting for S6K1 and RPS6. Inputs shown in right panel. IgG HC denotes the heavy chain. Results representative of two independent experiments.

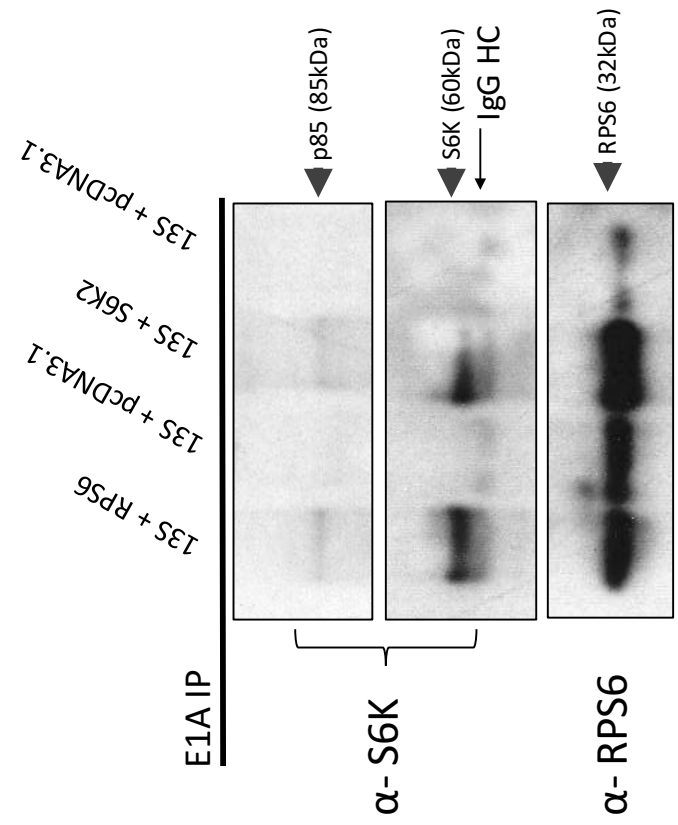
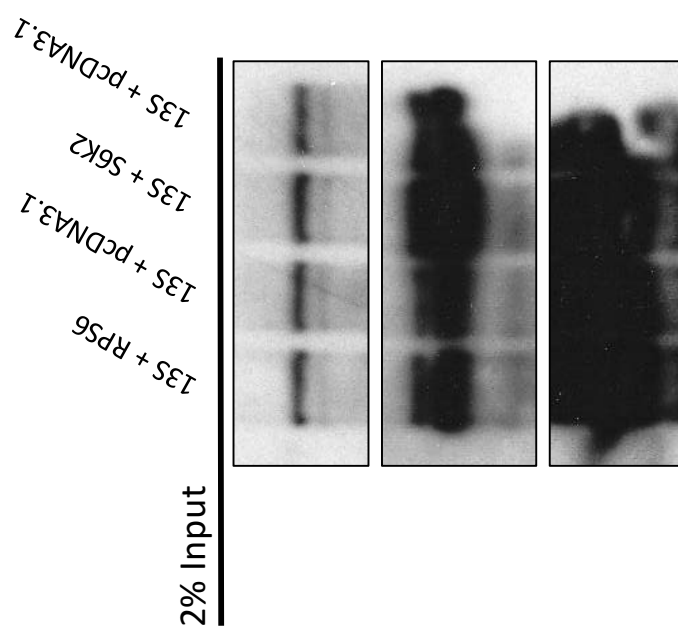


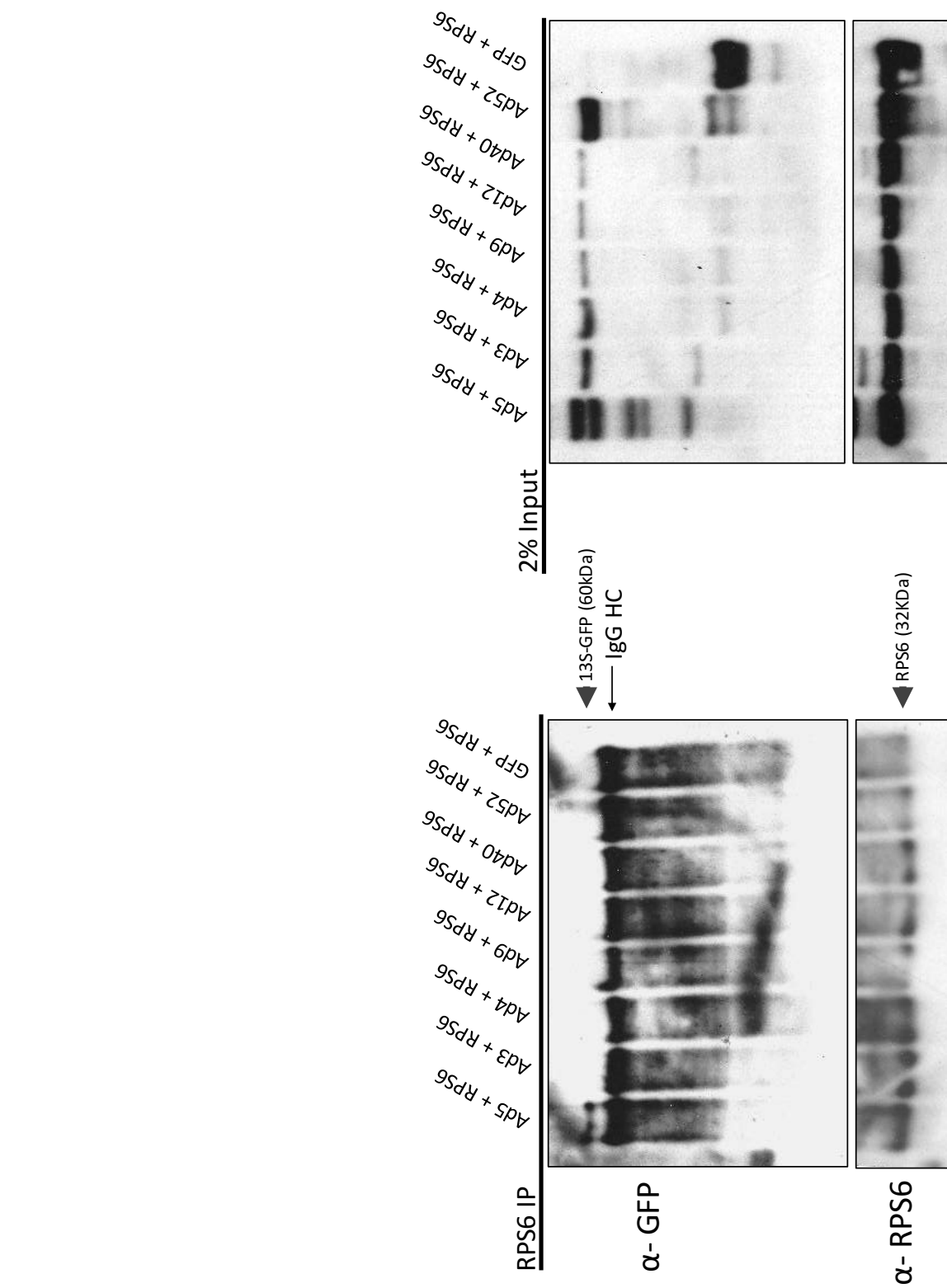
(Figure 3.8). However, in our HT1080 cellular model, transfected 13S E1A construct did not immunoprecipitate with endogenous p70 or p85 S6K1. On the contrary, co-transfection of either S6K2 or RPS6 with 13S E1A did result in the co-immunoprecipitation of p70/p85 S6K1 with E1A. The overexpression of S6K2 and RPS6 would appear to enhance expression of S6K1.

3.2.5 Assessing the Conserved Nature of the E1A and RPS6 Interaction

Since the novel interaction between RPS6 and HAdV-5 E1A was established in my earlier studies, I sought to evaluate if this interaction was conserved across multiple species of adenovirus. Immunoprecipitation experiments with RPS6, were followed by western blotting for GFP and RPS6. The adenovirus E1A species constructs were 13S GFP-tagged isoforms. As shown in Figure 3.11, HAdV-5 E1A was the only E1A species found to interact with RPS6. This verifies earlier E1A-RPS6 interaction experiments that used only the 13S HAdV-5 E1A isoform (Figure 3.10). This result indicates that HAdV-5 E1A is unique in its binding to RPS6, and that the E1A-RPS6 interaction is not conserved across all species of Adenovirus, potentially indicating that the interaction is not mediated through conserved linear motifs.

Ribosomal proteins are not exclusively cytoplasmic, for example the the RPS6 protein has the ability to shuttle across the nuclear membrane and accumulate in the nucleus. To test whether RPS6 binds HAdV-5 in the presence of STING, and therefore potentially in the cytoplasm, we co- transfected 13S E1A-pcDNA, dl1106-pcDNA, and dl1108-pcDNA, with STING-HA into HT1080 cells. Immunoprecipitation with endogenous RPS6 was followed by western blotting for E1A and STING-HA (Figure 3.12). If endogenous RPS6 was able to bind overexpressed STING, then we expected to see a positive signal, but this was not observed. Endogenous RPS6 did however, bind overexpressed 13S E1A and dl1108 deletion mutant, but there was no strong signal observed with dl1106 or dl1107 deletion mutants. The deletion mutant dl1107 and particularly dl1106 abolish stretches of amino acid residues that are not conserved across all HAdV species and are unique to HAdV-5, whereas the dl1108 deletion mutant abolishes a conserved amino acid region.

Figure 3.11. E1A interaction with RPS6 is unique for HAdV-5 serotype. HT1080 cells were transfected with 5 μ g of HAdV 13S-GFP expression vectors representing HAdV-3,-4,-5,-9,-40-and -52, and 5 μ g of RPS6 expression vector. After 24 hr, cells were harvested and lysed, followed by immunoprecipitation of RPS6 and western blotting for E1A-GFP. Inputs shown in right panel. IgG HC denotes the heavy chain. Results representative of two independent experiments.



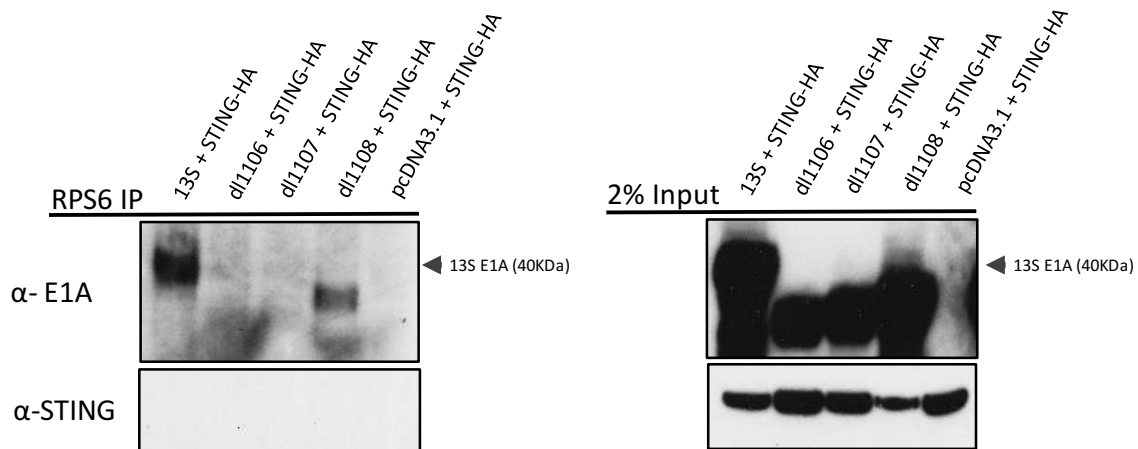


Figure 3.12. HAdV-5 E1A deletion mutants adjacent to or located at the N-terminus of CR2 abolish binding with RPS6. HT0180 cells were transfected with 5 μ g of HAdV-5 13S or deletion mutant expression vectors dl1106, dl1007, and dl1108 (no tag), and 5 μ g of STING-HA expression vector. After 24 hr, cells were harvested and lysed, followed by immunoprecipitation of RPS6 and western blotting for E1A (anti-M73) and STING-HA. Inputs shown in right panel. Results representative of two independent experiments.

Chapter 4

Discussion

4.1 Mapping the interaction between E1A and STING

The ability to evade type I IFN responses is a fundamental aspect of the viral lifecycle. Viruses employ numerous strategies to conceal their presence and disable cellular innate defences. As discussed in the introduction, previous studies have described how human Adenovirus can modulate secondary type I IFN responses, but evasion of the primary type I IFN response is less well understood. The group of Stetson (Lau *et al.*, 2015) discovered that HAdV-5 E1A could antagonize the cGAS-STING pathway in HEK293 cells, but the nature of the protein-protein interaction between HAdV-5 E1A and STING required further investigation.

This study was based on the indication from the group of Stetson that HAdV-5 E1A interacts with STING through the LXCXE motif, and that this antagonism would theoretically prevent the phosphorylation of IRF3 and TBK1, subsequently disabling the release of type I IFN. The involvement of the zinc finger located in CR3 was also postulated, though without validation with data, as potentially being involved in the E1A-STING interaction (Lau *et al.*, 2015). These studies established parameters from which my own experiments initiated.

My data, derived here from co-immunoprecipitation studies, does not support the concept that the LXCXE motif is both necessary and sufficient for binding to STING. As described in section 1.4, the cGAS-STING DNA sensing pathway has several distinct components, but many of these are in complex with each other. Previous studies have demonstrated that cGAS is not expressed in HEK293 cells, therefore, STING is assumed to be the DNA sensor in that pathway. The latest communication from the group of Stetson indicated that the early events of this pathway were intact, suggesting that STING traffics from the endoplasmic reticulum and recruits TBK1. Phosphorylation of IRF3 on serine 386 was

intact, while phosphorylation of serine 396 was impaired (Burleigh & Stetson, 2016). This suggests that E1A was targeting a later step in the pathway and binds STING in complex with other proteins. Indeed, the E1A-STING interaction may not be a direct protein-protein interaction. Wang *et al.* (2016) found that co-transfection of a plasmid encoding STING together with a plasmid encoding S6K1 augmented the STING-dependent phosphorylation of serine 396 of endogenous IRF3 in HEK293T cells. I demonstrated that HAdV-5 E1A binds STING, but we cannot rule out the possibility that HAdV-5 E1A binds STING through S6K1, or binds a surface created by the complex of these two proteins.

I began this study with the expectation that STING would bind HAdV-5 E1A through the LXCXE motif, much in the same way that E1A binds pRb through the LXCXE motif. Previous members of the laboratory have shown that an E1A CR2 deletion mutant, which encodes the LXCXE sequence, can readily co-immunoprecipitate with pRb following co-transfection experiments (unpublished data). I expected to observe a strong interaction between STING and CR2 using co-immunoprecipitation experiments, but this was not seen. Through my own studies, I also could not confirm Stetson's finding that an LXCXE mutant abolished E1A binding with STING in HEK293 cells. When I expanded across an atlas of mutations spanning the CR2 region and conducted my experiments in HT1080 cells, I observed binding between STING and E1A was only slightly diminished. These results indicated that other regions of E1A were likely involved in mediating the interaction with STING.

The N-terminal region of E1A, covering amino acid residues 1-82, consistently bound to STING despite lower overall expression levels in the input cell lysate. Further analysis of the N-terminus led me to construct expression plasmids containing various portions of the E1A N-terminal sequence. Co-immunoprecipitation experiments demonstrated that the first fourteen residues of HAdV-5 E1A were mediating an interaction with STING.

The conserved regions of E1A are largely considered to be disordered, predicted using the online tool PONDR (predictor of natural disordered regions)(Pelka *et al.*, 2013). E1A is well characterized for its ability to interact with proteins through short linear interaction

motifs (Pelka *et al.*, 2013). Linear motifs are also regarded as ‘evolutionary switches’ because subtle amino acid changes can cause short sequences in linear motifs to appear and disappear (Neduva & Russell, 2005). The short lengths of these motifs typically mean that the interactions they mediate are transient and of low affinity. In order to verify that the interaction between STING and the first 14 amino acid residues of E1A are not a laboratory artifact of protein fragmentation, deletion mutants were prepared within the N-terminus that eliminated these amino acid residues. This approach complements earlier experiments because the deletion mutants would not bind STING if the 14 amino acid residues were critical for the interaction. The binding between STING and the E1A N-terminus was greatly diminished in E1A deletion mutants lacking amino acids residues 4 to 25. Thus, the N-terminus of E1A appears necessary and sufficient for mediating the interaction with STING.

Determining the conservation of the interaction between STING and 13S E1A could provide insight into the importance of the interaction from an evolutionary perspective. I demonstrated that the interaction between E1A and STING was fairly conserved across most species of E1A representing the major families of Adenovirus. The conservation of interaction also indicated that conserved motifs within these species may be facilitating the E1A and STING interaction. To further investigate the N-terminal region, I prepared N-terminal constructs spanning the first 15 amino acid residues of various E1A species. I observed that the N-terminus (1-15AA) of HAdV-3,-9,-12, and -40 interacted with STING, while HAdV-52 and 13S Δ N-terminus (Δ 1-80) did not. This suggests that the N-terminus (1-15AA) interaction with STING is likely significant and fundamental across most Adenoviral species for type I IFN evasion strategies. HAdV-52, which did not bind STING, contains considerable differences in the amino acid residues of the extreme N-terminus as compared to other Adenoviral species. Indeed, HAdV-52 is the most divergent species (refer to Figure 1.5). Interestingly, an interaction was detected between STING and the HAdV-9 N-terminus. Beyond the first 8 amino acids, the HAdV-9 N-terminus is divergent from the other representative serotypes, which would indicate that further exploration of the extreme N-terminus, namely amino acids 1-8, should continue.

Past studies have demonstrated that the E1A N-terminus can interact with multiple proteins including the TATA binding domain (TBP), p300 and CREB-binding domain (CBP) (Boyd *et al.*, 2002). Mutation of cysteine at position 6 to alanine abolished the E1A interaction with TBP, p300 and CBP. Following infection, the phosphorylation of IRF3 results in the dimerization and translocation to the nucleus. Upon accumulating in the nucleus, IRF3 binds with CBP and p300. The binding of E1A to p300/CBP through the N-terminus prevents this interaction between IRF3 and CBP/p300, resulting in an inhibition of type I IFN production (Wathelet *et al.*, 1998; Yang *et al.*, 2002, 2004; Yoneyama *et al.*, 1998). Despite reports that p300 can be found in the cytoplasm, the prevailing notion is that the nuclear expression of p300 is predominant (Rotte *et al.*, 2013). This suggests there is a novel binding region within the N-terminus that either binds STING within the cytoplasm, or a protein in complex with STING. As STING is not known to accumulate in the nucleus, future work should remain focused on the discovery of E1A cytoplasmic binding partners.

4.2 Characterizing the interaction between E1A, S6K1 and RPS6

Wang and colleagues (2016) revealed that S6K1 played a new role in the induction of type I IFN responses. Our second aim of this study was to determine whether E1A was involved in the STING-S6K1 interaction, and whether the ribosomal protein S6, which is downstream of S6K1, could also be potentially involved.

A study by de Groot *et al.* (1995) reported that the HAAdV-5 N-terminus (possibly including CR1) was responsible for enhancing expression of p70 S6K. However, they stated (without supporting data) that there was no protein-protein interaction. I revisited this question and showed that E1A can bind both endogenous and exogenous mouse and human p70 S6K through co-immunoprecipitation studies. I used a mouse S6K1 construct because it was donated by Wang and colleagues (McMaster University) and has 99% amino acid sequence homology to human S6K1. I made the novel finding that binding of 13S E1A to p70 S6K1 is fairly conserved across multiple E1A species. I also extended the study of Wang *et al.*

(2016) by demonstrating that human STING could immunoprecipitate with mouse p70 S6K1. The precise binding configuration between p70 S6K1, E1A and STING has yet to be determined, and should be a priority for future investigation. Since E1A binds p70 S6K1 in the absence of STING, it could be postulated that E1A binds p70 S6K1 through a conserved region, and p70 S6K in turn, binds STING. However, we cannot dismiss the possibility that these are separate events and E1A binds p70 S6K1 irrespective of any type I IFN evasion strategies.

Changes in protein expression level of p85 S6K in response to E1A is unclear and further studies should be conducted to determine if E1A may somehow discriminate between the p70 S6K isoform and the p85 S6K isoform. The p85 S6K isoform is less abundant than p70 S6K in most cell types (Reinhard *et al.*, 1992), which explains why we observe stronger interactions between E1A and p70 S6K. The p70 S6K isoform was observed to immunoprecipitate with endogenous E1A in HEK293 cells, whereas the p85 isoform did not. Overexpression of the E1A protein is required to immunoprecipitate p85 S6K1 with E1A. However, like p70 S6K, p85 S6K does not require the presence of STING to bind E1A.

Understanding the biological functions of S6K2 has been largely neglected compared to the number of studies investigating S6K1. In addition, the changes in S6K2 expression upon viral infection is largely undetermined. It would be interesting to determine if HAdV E1A interacts with S6K2, and if HAdV infection alters the protein expression of S6K2.

Indications that E1A could bind RPS6 initially came from positive endogenous RPS6 signals found in co-immunoprecipitation experiments transfecting 13S E1A into HEK293 cells. When I co-transfected RPS6 with multiple HAdV species in HT1080 cells, I initially encountered problems in detecting a signal. However, by increasing the expression of the exogenous RPS6 protein I was able to determine that RPS6 binds HAdV-5, but not the other E1A species. The result demonstrating that dl1106 failed to bind RPS6 may suggest that E1A HAdV-5 has a unique binding region. The absence of RPS6 binding to STING could be due to the fact that STING resides in the cytoplasm, while RPS6 can be found in

the nucleus. E1A primarily localizes to the nucleus (Jiang *et al.*, 2006) and this may be the site of interaction with RPS6, however, E1A may also redistribute RPS6 proteins intracellularly.

4.3 Significance of Findings and Future Directions

My studies have shown that amino acid residues 1-14 of the E1A N-terminus are responsible for mediating the interaction between E1A and STING, and that this interaction is quite conserved across Adenoviral species. This demonstrates a novel binding site within the N-terminus region of E1A, distinct from the putative interaction via the LXCXE motif in CR2. We have also discovered novel E1A binding partners; p70 S6K1, p85 S6K1, and RPS6. The interaction between E1A and S6K1 is fairly conserved, indicating that a conserved motif is likely involved in mediating this interaction, either independently or in conjunction with additional binding sites. The novel interaction between HAdV-5 E1A and RPS6 is not conserved across adenoviral species and does not involve the STING complex. To verify the RPS6-E1A interaction, other serotypes of Adenovirus species C should also be tested for their ability to bind RPS6. Determining the functional significance of this interaction would expand our knowledge of E1A's ability to modulate proteins involved in metabolic pathways. This study provides the first indication that E1A can target a downstream component of the mTOR pathway. The functional significance of the E1A-S6K1 interaction also needs to be fully elucidated. E1A may modulate S6K for several purposes, and may act as both an enhancer and repressor of activity. Enhancing the role of S6K in protein synthesis could provide an environment more conducive to viral replication, whereas repressing an S6K-STING interaction blocks the type I IFN response.

A catalogue of point mutations within the N-terminus region of E1A needs to be constructed to further identify the residues critical for interaction with STING. The region of S6K1 binding on E1A also needs to be mapped, providing specific reagents for future studies that will identify the exact impact of this interaction on the virus replicative cycle. To determine if E1A binds STING through S6K1 or co-binds both proteins, gene knockdown studies could be undertaken whereby E1A and STING are co-transfected into S6K1^{-/-} cells followed by co-immunoprecipitation for STING. As S6K1 was shown by

Wang *et al.* (2016) to augment the STING-dependent phosphorylation of IRF3, theoretically, S6K1 would be an ideal target for E1A to disable the type I IFN response. Further investigation is required to verify the location of the E1A-S6K1 interaction, and the E1A-RPS6 interaction. Immunohistochemical staining of endogenous E1A in HEK293 cells, or transfection of epitope-tagged constructs of E1A, S6K1, STING and RPS6 into HT1080 cells followed by immunofluorescence to track their localization within the cell could be utilized. The ability of E1A to relocalize components of the STING pathway should also be examined.

To complement our previous results, a primary cell line such as mouse embryonic fibroblasts could be transduced with retroviruses encoding mutant E1A with mutations that disrupt binding with S6K. Changes in IFN- β mRNA levels upon stimulation with foreign dsDNA could be evaluated with qPCR. If disruption of binding between E1A and S6K results in rescue of the type I IFN response, then an increase in IFN- β mRNA should be observed. In addition, a screen could be developed in STING and cGAS knockdown cells to verify regions of E1A that block IFN- β . Co-transfection of STING, cGAS, and mutant E1A expression plasmids, together with an IFN- β promoter luciferase reporter construct can identify which mutations rescue IFN- β activation (Ma *et al.*, 2015). To complement our study with an infection model, viruses with deletion mutants in E1A rendering them unable to antagonize the STING-pathway should be constructed and tested in primary cell lines or the HEK293 cell line treated with CRISPR targeting deletion of the E1A loci.

Lau *et al.* identified the Human Papilloma Virus (HPV) E7 protein as an antagonist of the STING pathway because it has an LXCXE motif. However, the HPV E7 protein does not have sequence homology to the HAdV N-terminus region discovered to interact with STING. Therefore, it would be of interest to determine if the E7 LXCXE motif, or a motif that overlaps the LXCXE motif may be inhibiting the phosphorylation of IRF3 at serine 396. I suggest this because the LXCXE motif HPV E7 protein was found to be involved in binding the carboxyl-terminal transactivation domain of IRF1 (Park *et al.*, 2000). Additionally, a PEST domain that overlaps the LXCXE motif in the HPV 16 E7 protein has been found to interact with IRF9 (Antonsson *et al.*, 2006). I would test to see if the

E1A LXCXE motif was involved in abolishing the phosphorylation of IRF3 at serine 396. E1A could be binding STING or S6K1 through the N-terminus and the LXCXE motif may be blocking IRF3 phosphorylation.

I wish to point out the drawbacks of the HEK293 cell model with respect to experiments analyzing the STING-pathway. Many studies analyzing innate immune signaling have been completed in HEK293 cells. In addition to the absence of cGAS, a study published in August 2017 by Wu *et al.* revealed that STING does not undergo the same degradation processes in HEK293 cells as it does in human diploid cells. These processes are vital regulatory mechanisms used to avoid an excessive innate immune response. In human diploid cells, they reported that after stimulation by dsDNA, RIG-1 was found downstream of STING and operated with IL-6 and ULK1 through a negative feedback loop to activate and control STING degradation. Low levels of RIG-1 and IL-6 in HEK293 cells were found to be insufficient for ULK1 activation, resulting in the loss of STING degradation mechanisms (Wu *et al.*, 2017). This leads to the question of whether HEK293 cells are a reliable model to study innate immune responses. HEK293 cells are generated through the transformation of normal HEK cells with sheared HAdV-5 E1A DNA. HEK293 cells have significantly less number of chromosomes than normal human diploid cells and are capable of infinite expansion. It was historically known that stimulation by dsDNA did not produce a type I IFN response in HEK293 cells (Lau *et al.*, 2015). If E1A in HEK293 cells permanently antagonizes the STING-S6K1-TBK1-IRF3 complex, then through the process of passaging, HEK293 cells may no longer require the need for STING regulation. HeLa cells should also be investigated for presence of STING degradation pathways. In addition, future studies investigating viral modulation of metabolic pathways should be cautious about the enhanced expression levels of S6K in HEK293 cells, especially if S6K is used as a marker for protein synthesis.

The present study has added new understanding to the intracellular interactors of E1A, and opened new avenues of research. Substantial studies remain to confirm the functional role of the protein-protein interactions identified.

5 References

- Ablasser, A., Bauernfeind, F., Hartmann, G., Latz, E., Fitzgerald, K. A., & Hornung, V. (2009). RIG-I-dependent sensing of poly(dA:DT) through the induction of an RNA polymerase III-transcribed RNA intermediate. *Nature Immunology*, *10*(10), 1065-1072.
- Ablasser, A., Goldeck, M., Cavlar, T., Deimling, T., Witte, G., Röhl, I., et al. (2013). cGAS produces a 2'-5'-linked cyclic dinucleotide second messenger that activates STING. *Nature*, *498*(7454), 380-384.
- Alexopoulou, L., Holt, A. C., Medzhitov, R., & Flavell, R. A. (2001). Recognition of double-stranded RNA and activation of NF- κ B by toll-like receptor 3. *Nature*, *413*(6857), 732-738.
- Ansieau, S., & Leutz, A. (2001). The conserved mynd domain of BS69 binds cellular and oncoviral proteins through a common PXLXP motif. *Journal of Biological Chemistry*, *277*(7), 4906-4910.
- Antonsson, A., Payne, E., Hengst, K., & McMillan, D. N. A. J. (2006). The human papillomavirus type 16 E7 protein binds human interferon regulatory factor-9 via a novel PEST domain required for transformation. *Journal of Interferon & Cytokine Research*, *26*(7), 455-461.
- Avvakumov, N., Kajon, A. E., Hoeben, R. C., & Mymryk, J. S. (2004). Comprehensive sequence analysis of the E1A proteins of human and simian adenoviruses. *Virology*, *329*(2), 477-492.
- Avvakumov, N., Wheeler, R., D'Halluin, J. C., & Mymryk, J. S. (2002). Comparative sequence analysis of the largest E1A proteins of human and simian adenoviruses. *Journal of Virology*, *76*(16), 7968-7975.
- Bell, J. K., Askins, J., Hall, P. R., Davies, D. R., & Segal, D. M. (2006). The dsRNA binding site of human toll-like receptor 3. *Proceedings of the National Academy of Sciences*, *103*(23), 8792-8797.
- Bell, J. K., Botos, I., Hall, P. R., Askins, J., Shiloach, J., Segal, D. M., et al. (2005). The molecular structure of the toll-like receptor 3 ligand-binding domain. *Proceedings of the National Academy of Sciences*, *102*(31), 10976-10980.
- Bell, J. K., Mullen, G. E. D., Leifer, C. A., Mazzone, A., Davies, D. R., & Segal, D. M. (2003). Leucine-rich repeats and pathogen recognition in toll-like receptors. *Trends in Immunology*, *24*(10), 528-533.
- Berk, A. (1986). Adenovirus promoters and E1A transactivation. *Annual Review of Genetics*, *20*(1), 45-79.

- Bewley, M. C. (1999). Structural analysis of the mechanism of adenovirus binding to its human cellular receptor, CAR. *Science*, 286(5444), 1579-1583.
- Boyd, J. M., Loewenstein, P. M., Tang, Q., Yu, L., & Green, M. (2002). Adenovirus E1A N-terminal amino acid sequence requirements for repression of transcription in vitro and in vivo correlate with those required for E1A interference with TBP-TATA complex formation. *Journal of Virology*, 76(3), 1461-1474.
- Burleigh, K., & Stetson, D. B. (2016). Uncovering the mechanism of E1A antagonism of the cGAS-STING pathway. *The Journal of Immunology*, 196(1), 203.2.
- Chang, S., Lee, C., Lin, P., Huang, H., Chang, L., Ko, W., et al. (2007). A community-derived outbreak of adenovirus type 3 in children in taiwan between 2004 and 2005. *Journal of Medical Virology*, 80(1), 102-112.
- Chen, H., Sun, H., You, F., Sun, W., Zhou, X., Chen, L., et al. (2011). Activation of STAT6 by STING is critical for antiviral innate immunity. *Cell*, 147(2), 436-446.
- Chen, Q., Sun, L., & Chen, Z. J. (2016). Regulation and function of the cGAS-STING pathway of cytosolic DNA sensing. *Nature Immunology*, 17(10), 1142-1149.
- Chiu, Y., MacMillan, J. B., & Chen, Z. J. (2009). RNA polymerase III detects cytosolic DNA and induces type I interferons through the RIG-I pathway. *Cell*, 138(3), 576-591.
- Choi, M. K., Wang, Z., Ban, T., Yanai, H., Lu, Y., Koshiba, R., et al. (2009). A selective contribution of the RIG-I-like receptor pathway to type I interferon responses activated by cytosolic DNA. *Proceedings of the National Academy of Sciences*, 106(42), 17870-17875.
- Civril, F., Deimling, T., de, O. M., Ablasser, A., Moldt, M., Witte, G., et al. (2013). Structural mechanism of cytosolic DNA sensing by cGAS. *Nature*, 498(7454), 332-337.
- Colonna, M. (2007). TLR pathways and IFN-regulatory factors: To each its own. *European Journal of Immunology*, 37(2), 306-309.
- Davey, N. E., Travé, G., & Gibson, T. J. (2011). How viruses hijack cell regulation. *Trends in Biochemical Sciences*, 36(3), 159-169.
- DeCaprio, J. A. (2009). How the rb tumor suppressor structure and function was revealed by the study of adenovirus and SV40. *Virology*, 384(2), 274-284.
- Devarkar, S. C., Wang, C., Miller, M. T., Ramanathan, A., Jiang, F., Khan, A. G., et al. (2016). Structural basis for m7G recognition and 2'-O-methyl discrimination in capped RNAs by the innate immune receptor RIG-I. *Proceedings of the National Academy of*

Sciences, 113(3), 596-601.

Diebold, S. S. (2004). Innate antiviral responses by means of TLR7-mediated recognition of single-stranded RNA. *Science*, 303(5663), 1529-1531.

Diebold, S. S., Montoya, M., Unger, H., Alexopoulou, L., Roy, P., Haswell, L. E., et al. (2003). Viral infection switches non-plasmacytoid dendritic cells into high interferon producers. *Nature*, 424(6946), 324-328.

Diner, E. J., Burdette, D. L., Wilson, S. C., Monroe, K. M., Kellenberger, C. A., Hyodo, M., et al. (2013). The innate immune DNA sensor cGAS produces a noncanonical cyclic dinucleotide that activates human STING. *Cell Reports*, 3(5), 1355-1361.

Dyson, N., Guida, P., McCall, C., Harlow, E. Adenovirus E1A makes two distinct contacts with the retinoblastoma protein. (1992) *J Virol*, 66, 4606-4611.

Fattaey, A., Harlow, E., Helin, K. Independent regions of adenovirus E1A are required for binding to and dissociation of E2F-protein complexes. (1993) *Mol Cell Biol*, 13, 7267-7277.

Ferguson, B., Krippel, B., Andrisani, O., Jones, N., Westphal, H., & Rosenberg, M. (1985). E1A 13S and 12S mRNA products made in escherichia coli both function as nucleus-localized transcription activators but do not directly bind DNA. *Molecular and Cellular Biology*, 5(10), 2653-2661.

Fessler, S. P., & Young, C. S. H. (1999). The role of the L4 33K gene in adenovirus infection. *Virology*, 263(2), 507-516.

Fonseca, G. J., Thillainadesan, G., Yousef, A. F., Ablack, J. N., Mossman, K. L., Torchia, J., et al. (2012). Adenovirus evasion of interferon-mediated innate immunity by direct antagonism of a cellular histone posttranslational modification. *Cell Host & Microbe*, 11(6), 597-606.

Gallimore, P. H. (1972). Tumour production in immunosuppressed rats with cells transformed in vitro by adenovirus type 2. *Journal of General Virology*, 16(1), 99-102.

Gao, P., Ascano, M., Wu, Y., Barchet, W., Gaffney, B. L., Zillinger, T., et al. (2013). Cyclic G(2',5')pA(3',5')p] is the metazoan second messenger produced by DNA-activated cyclic GMP-AMP synthase. *Cell*, 153(5), 1094-1107.

Giordano, A., Whyte, P., Harlow, E., Franza, B. R., Beach, D., & Draetta, G. (1989). A 60 kd cdc2-associated polypeptide complexes with the E1A proteins in adenovirus-infected cells. *Cell*, 58(5), 981-990.

- Green, M., Wold, W. S. M., Brackmann, K., & Cartas, M. A. (1980). Studies on early proteins and transformation proteins of human adenoviruses. *Cold Spring Harbor Symposia on Quantitative Biology*, 44(0), 457-469.
- Guo, F., Han, Y., Zhao, X., Wang, J., Liu, F., Xu, C., et al. (2014). STING agonists induce an innate antiviral immune response against hepatitis B virus. *Antimicrobial Agents and Chemotherapy*, 59(2), 1273-1281.
- Hasan, M., Gonugunta, V. K., Dobbs, N., Ali, A., Palchik, G., Calvaruso, M. A., et al. (2017). Chronic innate immune activation of TBK1 suppresses mTORC1 activity and dysregulates cellular metabolism. *Proceedings of the National Academy of Sciences*, 114(4), 746-751.
- Heil, F. (2004). Species-specific recognition of single-stranded RNA via toll-like receptor 7 and 8. *Science*, 303(5663), 1526-1529.
- Hemmi, H., & Akira, S. (2002). A novel toll-like receptor that recognizes bacterial DNA. In: Raz E (eds) Microbial DNA and Host Immunity. *Humana Press*, Totowa, NJ.
- Hoelzer, K., Shackelton, L. A., & Parrish, C. R. (2008). Presence and role of cytosine methylation in DNA viruses of animals. *Nucleic Acids Research*, 36(9), 2825-2837.
- Krieg, A. M. (2008). Toll-like receptor 9 (TLR9) agonists in the treatment of cancer. *Oncogene*, 27(2), 161-167.
- Hofmann, H., Vanwalscappel, B., Bloch, N., & Landau, N. R. (2016). TLR7/8 agonist induces a post-entry SAMHD1-independent block to HIV-1 infection of monocytes. *Retrovirology*, 13(1)
- Hornung, V., Ellegast, J., Kim, S., Brzozka, K., Jung, A., Kato, H., et al. (2006). 5'-triphosphate RNA is the ligand for RIG-I. *Science*, 314(5801), 994-997.
- Hu, M., Yang, Q., Xie, X., Liao, C., Lin, H., Liu, T., et al. (2016). Sumoylation promotes the stability of the DNA sensor cGAS and the adaptor STING to regulate the kinetics of response to DNA virus. *Immunity*, 45(3), 555-569.
- Ishii, K. J., Coban, C., & Akira, S. (2005). Manifold mechanisms of toll-like receptor-ligand recognition. *Journal of Clinical Immunology*, 25(6), 511-521.
- Ishii, K. J., Coban, C., Kato, H., Takahashi, K., Torii, Y., Takeshita, F., et al. (2005). A toll-like receptor-independent antiviral response induced by double-stranded B-form DNA. *Nature Immunology*, 7(1), 40-48.
- Ishikawa, H., Ma, Z., & Barber, G. N. (2009). STING regulates intracellular DNA-mediated, type I interferon-dependent innate immunity. *Nature*, 461(7265), 788-792.

- Jiang, H., Olson, M. V., Medrano, D. R., Lee, O., Xu, J., Piao, Y., et al. (2006). A novel CRM1-dependent nuclear export signal in adenoviral E1A protein regulated by phosphorylation. *The FASEB Journal*, 20(14), 2603-2605.
- Jiang, X., Kinch, L. N., Brautigam, C. A., Chen, X., Du, F., Grishin, N. V., et al. (2012). Ubiquitin-induced oligomerization of the RNA sensors RIG-I and MDA5 activates antiviral innate immune response. *Immunity*, 36(6), 959-973.
- Jin, L., Waterman, P. M., Jonscher, K. R., Short, C. M., Reisdorph, N. A., & Cambier, J. C. (2008). MPYS, a novel membrane tetraspanner, is associated with major histocompatibility complex class II and mediates transduction of apoptotic signals. *Molecular and Cellular Biology*, 28(16), 5014-5026.
- Jones, M. S., Harrach, B., Ganac, R. D., Gozum, M. M. A., dela Cruz, W. P., Riedel, B., et al. (2007). New adenovirus species found in a patient presenting with gastroenteritis. *Journal of Virology*, 81(11), 5978-5984.
- Jones, N., & Shenk, T. (1979). An adenovirus type 5 early gene function regulates expression of other early viral genes. *Proceedings of the National Academy of Sciences*, 76(8), 3665-3669.
- Joseph, T. D., & Look, D. C. (2001). Specific inhibition of interferon signal transduction pathways by adenoviral infection. *Journal of Biological Chemistry*, 276(50), 47136-47142.
- Kato, H., Takeuchi, O., Mikamo-Satoh, E., Hirai, R., Kawai, T., Matsushita, K., et al. (2008). Length-dependent recognition of double-stranded ribonucleic acids by retinoic acid-inducible gene-I and melanoma differentiation-associated gene 5. *The Journal of Experimental Medicine*, 205(7), 1601-1610.
- Kawai, T., & Akira, S. (2010). The role of pattern-recognition receptors in innate immunity: Update on toll-like receptors. *Nature Immunology*, 11(5), 373-384.
- Kawai, T., & Akira, S. (2011). Toll-like receptors and their crosstalk with other innate receptors in infection and immunity. *Immunity*, 34(5), 637-650.
- Khan, J. A., Brint, E. K., O'Neill, L. A. J., & Tong, L. (2004). Crystal structure of the Toll/Interleukin-1 receptor domain of human IL-1RAPL. *Journal of Biological Chemistry*, 279(30), 31664-31670.
- Kolakofsky, D., Kowalinski, E., & Cusack, S. (2012). A structure-based model of RIG-I activation. *Rna*, 18(12), 2118-2127.
- Konno, H., Konno, K., & Barber, G. N. (2013). Cyclic dinucleotides trigger ULK1 (ATG1) phosphorylation of STING to prevent sustained innate immune signaling. *Cell*, 155(3), 688-698.

- Kowalinski, E., Lunardi, T., McCarthy, A. A., Louber, J., Brunel, J., Grigorov, B., et al. (2011). Structural basis for the activation of innate immune pattern-recognition receptor RIG-I by viral RNA. *Cell*, *147*(2), 423-435.
- Krilov, L. R. (2005). Adenovirus infections in the immunocompromised host. *The Pediatric Infectious Disease Journal*, *24*(6), 555-556.
- Laplante, M., & Sabatini, D. (2012). mTOR Signaling in Growth Control and Disease. *Cell*, *149* (2), 274-293.
- Lau, L., Gray, E. E., Brunette, R. L., & Stetson, D. B. (2015). DNA tumor virus oncogenes antagonize the cGAS-STING DNA-sensing pathway. *Science*, *350*(6260), 568.
- Lewis, P. F., Schmidt, M. A., Lu, X., Erdman, D. D., Campbell, M., Thomas, A., et al. (2009). A Community-Based outbreak of severe respiratory illness caused by human adenovirus serotype 14. *The Journal of Infectious Diseases*, *199*(10), 1427-1434.
- Liu, X., & Marmorstein, R. (2007). Structure of the retinoblastoma protein bound to adenovirus E1A reveals the molecular basis for viral oncoprotein inactivation of a tumor suppressor. *Genes & Development*, *21*(21), 2711-2716.
- Liu, S., Cai, X., Wu, J., Cong, Q., Chen, X., Li, T., et al. (2015). Phosphorylation of innate immune adaptor proteins MAVS, STING, and TRIF induces IRF3 activation. *Science*, *347*(6227), aaa2630-aaa2630.
- Liu, Y., Li, J., Chen, J., Li, Y., Wang, W., Du, X., et al. (2014). Hepatitis B virus polymerase disrupts K63-linked ubiquitination of STING to block innate cytosolic DNA-sensing pathways. *Journal of Virology*, *89*(4), 2287-2300.
- Look, D. C., Roswit, W. T., Frick, A. G., Gris-Alevy, Y., Dickhaus, D. M., Walter, M. J., et al. (1998). Direct suppression of Stat1 function during adenoviral infection. *Immunity*, *9*(6), 871-880.
- Luo, D., Kohlway, A., & Pyle, A. M. (2013). Duplex RNA activated ATPases (DRAs). *RNA Biology*, *10*(1), 111-120.
- Ma, Z., & Damania, B. (2016). The cGAS-STING defense pathway and its counteraction by viruses. *Cell Host & Microbe*, *19*(2), 150-158.
- Ma, Z., Jacobs, S. R., West, J. A., Stopford, C., Zhang, Z., Davis, Z., et al. (2015). Modulation of the cGAS-STING DNA sensing pathway by gammaherpesviruses. *Proceedings of the National Academy of Sciences*, *112*(31), E4306-E4315.
- Mackey, J. K., Rigden, P. M., & Green, M. (1976). Do highly oncogenic group A human adenoviruses cause human cancer? analysis of human tumors for adenovirus 12

- transforming DNA sequences. *Proceedings of the National Academy of Sciences*, 73(12), 4657-4661.
- Magnuson, B., Ekim, B., & Fingar, D. C. (2012). Regulation and function of ribosomal protein S6 kinase (S6K) within mTOR signalling networks. *Biochemical Journal*, 441(1), 1-21.
- Marshall-Clarke, S., Downes, J. E., Haga, I. R., Bowie, A. G., Borrow, P., Pennock, J. L., et al. (2007). Polyinosinic acid is a ligand for toll-like receptor 3. *Journal of Biological Chemistry*, 282(34), 24759-24766.
- McNab, F., Mayer-Barber, K., Sher, A., Wack, A., & O'Garra, A. (2015). Type I interferons in infectious disease. *Nature Reviews Immunology*, 15(2), 87-103.
- Mechnikov, I. (1908). On the Present State of the Question of Immunity in Infectious Diseases. *Nobel Prize Lecture*. December 11, 1908. Stockholm, Sweden.
- Nardella, C., Lunardi, A., Fedele, G., Clohessy, J. G., Alimonti, A., Kozma, S. C., et al. (2011). Differential expression of S6K2 dictates tissue-specific requirement for S6K1 in mediating aberrant mTORC1 signaling and tumorigenesis. *Cancer Research*, 71(10), 3669-3675.
- Neduva, V., & Russell, R. B. (2005). Linear motifs: Evolutionary interaction switches. *FEBS Letters*, 579(15), 3342-3345.
- Negishi, H., Osawa, T., Ogami, K., Ouyang, X., Sakaguchi, S., Koshiba, R., et al. (2008). A critical link between toll-like receptor 3 and type II interferon signaling pathways in antiviral innate immunity. *Proceedings of the National Academy of Sciences*, 105(51), 20446-20451.
- Ogino, T. (2014). Capping of vesicular stomatitis virus pre-mRNA is required for accurate selection of transcription stop-start sites and virus propagation. *Nucleic Acids Research*, 42(19), 12112-12125.
- O'Neill, L. A. J., Golenbock, D., & Bowie, A. G. (2013). The history of toll-like receptors — redefining innate immunity. *Nature Reviews Immunology*, 13(6), 453-460.
- O'Neill, L. A. J. (2009). DNA makes RNA makes innate immunity. *Cell*, 138(3), 428-430.
- O'Neill, L. A. J., Fitzgerald, K. A., & Bowie, A. G. (2003). The Toll-IL-1 receptor adaptor family grows to five members. *Trends in Immunology*, 24(6), 286-289.
- Ouyang, S., Song, X., Wang, Y., Ru, H., Shaw, N., Jiang, Y., et al. (2012). Structural analysis of the STING adaptor protein reveals a hydrophobic dimer interface and mode of cyclic di-GMP binding. *Immunity*, 36(6), 1073-1086.

- Pardo, O. E., & Seckl, M. J. (2013). S6K2: The neglected S6 kinase family member. *Frontiers in Oncology*, 3
- Park, J., Kim, E., Kwon, H., Hwang, E., Namkoong, S., & Um, S. (2000). Inactivation of interferon regulatory factor-1 tumor suppressor protein by HPV E7 oncoprotein. *Journal of Biological Chemistry*, 275(10), 6764-6769.
- Pelka, P., Ablack, J. N. G., Fonseca, G. J., Yousef, A. F., & Mymryk, J. S. (2008). Intrinsic structural disorder in adenovirus E1A: A viral molecular hub linking multiple diverse processes. *Journal of Virology*, 82(15), 7252-7263.
- Perricaudet, M., Akusjärvi, G., Virtanen, A., & Pettersson, U. (1979). Structure of two spliced mRNAs from the transforming region of human subgroup C adenoviruses. *Nature*, 281(5733), 694-696.
- Pichlmair, A., Schulz, O., Tan, C., Rehwinkel, J., Kato, H., Takeuchi, O., et al. (2009). Activation of MDA5 requires higher-order RNA structures generated during virus infection. *Journal of Virology*, 83(20), 10761-10769.
- RIGulation of STING expression: At the crossroads of viral RNA and DNA sensing pathways.(2017). *Inflammation and Cell Signaling*,
- Rotte, A., Bhandaru, M., Cheng, Y., Sjoestroem, C., Martinka, M., & Li, G. (2013). Decreased expression of nuclear p300 is associated with disease progression and worse prognosis of melanoma patients. *Plos One*, 8(9), e75405.
- Sambursky, R. P., Fram, N., & Cohen, E. J. (2007). The prevalence of adenoviral conjunctivitis at the wills eye hospital emergency room. *Optometry - Journal of the American Optometric Association*, 78(5), 236-239.
- Seth, R. B., Sun, L., Ea, C., & Chen, Z. J. (2005). Identification and characterization of MAVS, a mitochondrial antiviral signaling protein that activates NF- κ B and IRF3. *Cell*, 122(5), 669-682.
- Shang, G., Zhu, D., Li, N., Zhang, J., Zhu, C., Lu, D., et al. (2012). Crystal structures of STING protein reveal basis for recognition of cyclic di-GMP. *Nature Structural & Molecular Biology*, 19(7), 725-727.
- Shu, C., Li, X., & Li, P. (2014). The mechanism of double-stranded DNA sensing through the cGAS-STING pathway. *Cytokine & Growth Factor Reviews*, 25(6), 641-648.
- Sun, L., Wu, J., Du, F., Chen, X., & Chen, Z. J. (2012). Cyclic GMP-AMP synthase is a cytosolic DNA sensor that activates the type I interferon pathway. *Science*, 339(6121), 786-791.

- Sun, W., Li, Y., Chen, L., Chen, H., You, F., Zhou, X., et al. (2009). ERIS, an endoplasmic reticulum IFN stimulator, activates innate immune signaling through dimerization. *Proceedings of the National Academy of Sciences*, 106(21), 8653-8658.
- Takeuchi, O., & Akira, S. (2010). Pattern recognition receptors and inflammation. *Cell*, 140(6), 805-820.
- Tanaka, Y., & Chen, Z. J. (2012). STING specifies IRF3 phosphorylation by TBK1 in the cytosolic DNA signaling pathway. *Science Signaling*, 5(214), ra20-ra20.
- Tang, D., Kang, R., Coyne, C., et al. (2012). PAMPs and DAMPs: Signal 0s that Spur Autophagy and Immunity. *Evolutionary Theory*, 249(1), 158-175.
- Tao, X., Xu, Y., Zheng, Y., Beg, A. A., & Tong, L. (2002). *An extensively-associated dimer in the structure of the C713S mutant of the TIR domain of human TLR2* Protein Data Bank, Rutgers University.
- Thomas, P., & Smart, T. G. (2005). HEK293 cell line: A vehicle for the expression of recombinant proteins. *Journal of Pharmacological and Toxicological Methods*, 51(3), 187-200.
- Tollefson, A. E., Ying, B., Doronin, K., Sidor, P. D., & Wold, W. S. M. (2007). Identification of a new human adenovirus protein encoded by a novel late 1-strand transcription unit. *Journal of Virology*, 81(23), 12918-12926.
- Tong, L., Xu, Y., Tao, X., Shen, B., Horng, T., Medzhitov, R., et al. (2000). *Nature*, 408(6808), 111-115.
- Trentin, J. J., Yabe, Y., & Taylor, G. (1962). The quest for human cancer viruses: A new approach to an old problem reveals cancer induction in hamsters by human adenovirus. *Science*, 137(3533), 835-841.
- Tsuchida, T., Zou, J., Saitoh, T., Kumar, H., Abe, T., Matsuura, Y., et al. (2010). The ubiquitin ligase TRIM56 regulates innate immune responses to intracellular double-stranded DNA. *Immunity*, 33(5), 765-776.
- Van Valen Leigh. (1973). A new evolutionary law. *Evolutionary Theory*. 1, 1-30.
- Van Roey, K., Uyar, B., Weatheritt, R. J., Dinkel, H., Seiler, M., Budd, A., et al. (2014). Short linear motifs: Ubiquitous and functionally diverse protein interaction modules directing cell regulation. *Chemical Reviews*, 114(13), 6733-6778.
- Walls, T., Shankar, A. G., & Shingadia, D. (2003). Adenovirus: An increasingly important pathogen in paediatric bone marrow transplant patients. *The Lancet Infectious Diseases*, 3(2), 79-86.

- Walsh, M. P., Seto, J., Liu, E. B., Dehghan, S., Hudson, N. R., Lukashev, A. N., et al. (2011). Computational analysis of two species C human adenoviruses provides evidence of a novel virus. *Journal of Clinical Microbiology*, *49*(10), 3482-3490.
- Wang, Y., Lian, Q., Yang, B., Yan, S., Zhou, H., He, L., et al. (2015). TRIM30 α is a negative-feedback regulator of the intracellular DNA and DNA virus-triggered response by targeting STING. *PLOS Pathogens*, *11*(6), e1005012.
- Wang, F., Alain, T., Szretter, K. J., Stephenson, K., Pol, J. G., Atherton, M. J., et al. (2016). S6K-STING interaction regulates cytosolic DNA-mediated activation of the transcription factor IRF3. *Nature Immunology*, *17*(5), 514-522.
- Warner, M. J., Bridge, K. S., Hewitson, J. P., Hodgkinson, M. R., Heyam, A., Massa, B. C., et al. (2016). S6K2-mediated regulation of TRBP as a determinant of miRNA expression in human primary lymphatic endothelial cells. *Nucleic Acids Research*, *63*1.
- Wathelet, M. G., Lin, C. H., Parekh, B. S., Ronco, L. V., Howley, P. M., & Maniatis, T. (1998). Virus infection induces the assembly of coordinately activated transcription factors on the IFN- β enhancer in vivo. *Molecular Cell*, *1*(4), 507-518.
- Wickham, T. J., Mathias, P., Cheresch, D. A., & Nemerow, G. R. (1993). Integrins $\alpha\beta$ 3 and $\alpha\beta$ 5 promote adenovirus internalization but not virus attachment. *Cell*, *73*(2), 309-319.
- Wu, J., Sun, L., Chen, X., Du, F., Shi, H., Chen, C., et al. (2012). Cyclic GMP-AMP is an endogenous second messenger in innate immune signaling by cytosolic DNA. *Science*, *339*(6121), 826-830.
- Wu, J., & Chen, Z. J. (2014). Innate immune sensing and signaling of cytosolic nucleic acids. *Annual Review of Immunology*, *32*(1), 461-488.
- Wu, J., Li, W., Shao, Y., Avey, D., Fu, B., Gillen, J., et al. (2015). Inhibition of cGAS DNA sensing by a herpesvirus virion protein. *Cell Host & Microbe*, *18*(3), 333-344.
- Wu, X., Yang, J., Na, T., Zhang, K., Davidoff, A. M., Yuan, B., et al. (2017). RIG-I and IL-6 are negative-feedback regulators of STING induced by double-stranded DNA. *Plos One*, *12*(8), e0182961.
- Yang, H., Lin, C. H., Ma, G., Orr, M., Baffi, M. O., & Wathelet, M. G. (2002). Transcriptional activity of interferon regulatory factor (IRF)-3 depends on multiple protein-protein interactions. *European Journal of Biochemistry*, *269*(24), 6142-6151.
- Yoneyama, M. (1998). Direct triggering of the type I interferon system by virus infection: Activation of a transcription factor complex containing IRF-3 and CBP/p300. *The EMBO Journal*, *17*(4), 1087-1095.

- Yoneyama, M., Kikuchi, M., Matsumoto, K., Imaizumi, T., Miyagishi, M., Taira, K., et al. (2005). Shared and unique functions of the DExD/H-box helicases RIG-I, MDA5, and LGP2 in antiviral innate immunity. *The Journal of Immunology*, 175(5), 2851-2858.
- Yoneyama, M., Kikuchi, M., Natsukawa, T., Shinobu, N., Imaizumi, T., Miyagishi, M., et al. (2004). The RNA helicase RIG-I has an essential function in double-stranded RNA-induced innate antiviral responses. *Nature Immunology*, 5(7), 730-737.
- Yousef, A. F., Fonseca, G. J., Pelka, P., Ablack, J. N. G., Walsh, C., Dick, F. A., et al. (2010). Identification of a molecular recognition feature in the E1A oncoprotein that binds the SUMO conjugase UBC9 and likely interferes with polySUMOylation. *Oncogene*, 29(33), 4693-4704.
- Zhang, G., Chan, B., Samarina, N., Abere, B., Weidner-Glunde, M., Buch, A., et al. (2016). Cytoplasmic isoforms of kaposi sarcoma herpesvirus LANA recruit and antagonize the innate immune DNA sensor cGAS. *Proceedings of the National Academy of Sciences*, 113(8), E1034-E1043.
- Zhang, J., Hu, M., Wang, Y., & Shu, H. (2012). TRIM32 protein modulates type I interferon induction and cellular antiviral response by targeting MITA/STING protein for K63-linked ubiquitination. *Journal of Biological Chemistry*, 287(34), 28646-28655.
- Zhang, X., Shi, H., Wu, J., Zhang, X., Sun, L., Chen, C., et al. (2013). Cyclic GMP-AMP containing mixed phosphodiester linkages is an endogenous high-affinity ligand for STING. *Molecular Cell*, 51(2), 226-235.
- Zhang, Y., Yeruva, L., Marinov, A., Prantner, D., Wyrick, P. B., Lupashin, V., et al. (2014). The DNA sensor, cyclic GMP-AMP synthase, is essential for induction of IFN- β during Chlamydia trachomatis infection. *The Journal of Immunology*, 193(5), 2394-2404.
- Zhong, B., Yang, Y., Li, S., Wang, Y., Li, Y., Diao, F., et al. (2008). The adaptor protein MITA links virus-sensing receptors to IRF3 transcription factor activation. *Immunity*, 29(4), 538-550.
- Zhong, B., Zhang, L., Lei, C., Li, Y., Mao, A., Yang, Y., et al. (2009). The ubiquitin ligase RNF5 regulates antiviral responses by mediating degradation of the adaptor protein MITA. *Immunity*, 30(3), 397-407.

Curriculum Vitae

Name: Jessica Hill

**Post-secondary
Education and
Degrees:**

Western University
MSc. Candidate. 2015-2017

The University of Toronto, Toronto, Canada
University College London, London, UK
Hons. BSc. 2009-2014

Presentations:

Poster 2017 London Health Research Da